Environment Canada Environnement Canada

Hydrogeochemical Processes Affecting the Migration of Radionuclides in a Fluvial Sand Aquifer at the Chalk River Nuclear Laboratories

R.E. Jackson and K.J. Inch

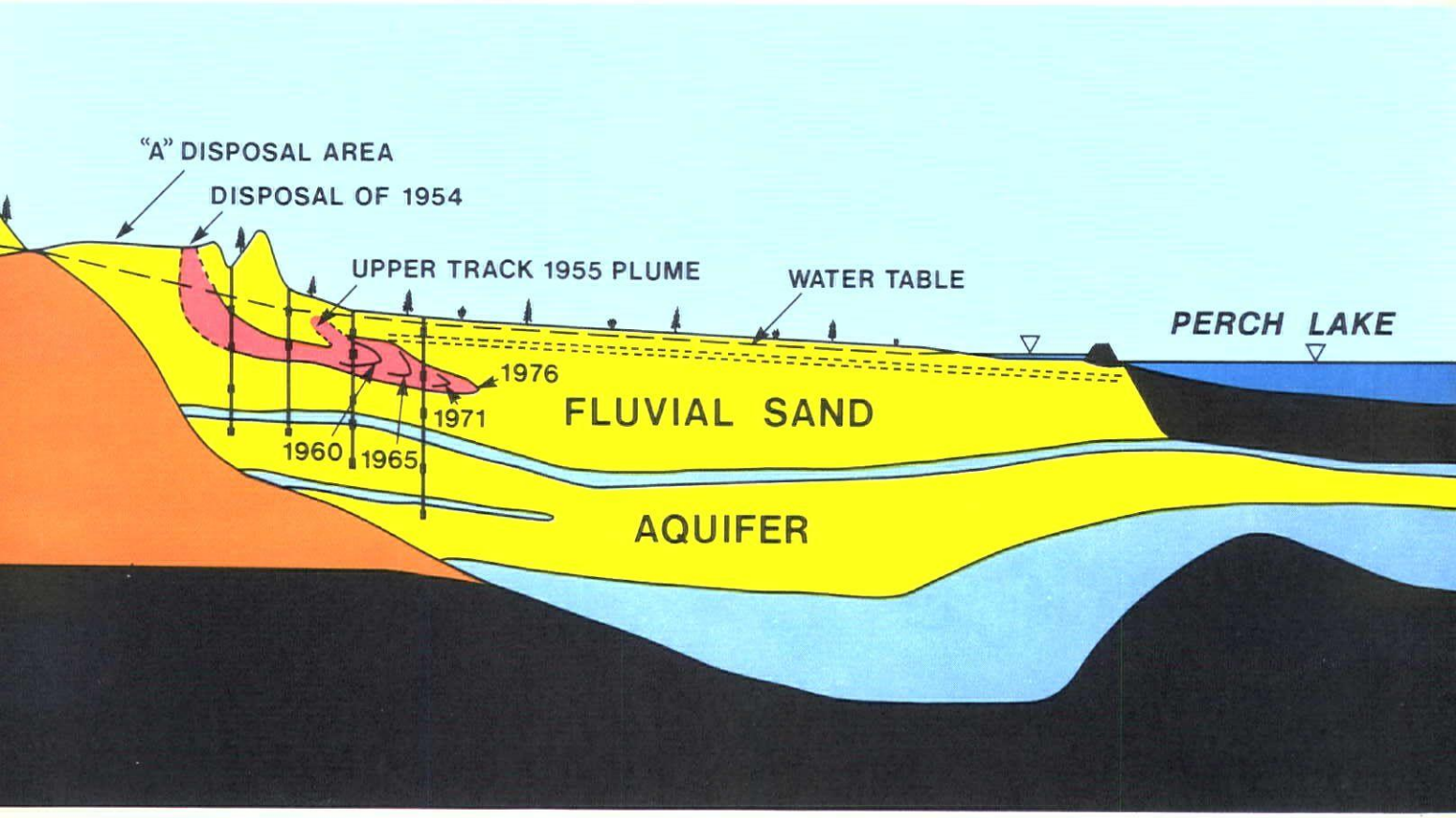

NHRI PAPER NO. 7
SCIENTIFIC SERIES NO. 104

NHRI

NATIONAL HYDROLOGY RESEARCH INSTITUTE
INLAND WATERS DIRECTORATE
OTTAWA, CANADA, 1980

Environment Canada
Environnement Canada

Hydrogeochemical Processes Affecting the Migration of Radionuclides in a Fluvial Sand Aquifer at the Chalk River Nuclear Laboratories

R.E. Jackson and K.J. Inch

NHRI PAPER NO. 7
SCIENTIFIC SERIES NO. 104

NHRI

NATIONAL HYDROLOGY RESEARCH INSTITUTE
INLAND WATERS DIRECTORATE
OTTAWA, CANADA, 1980

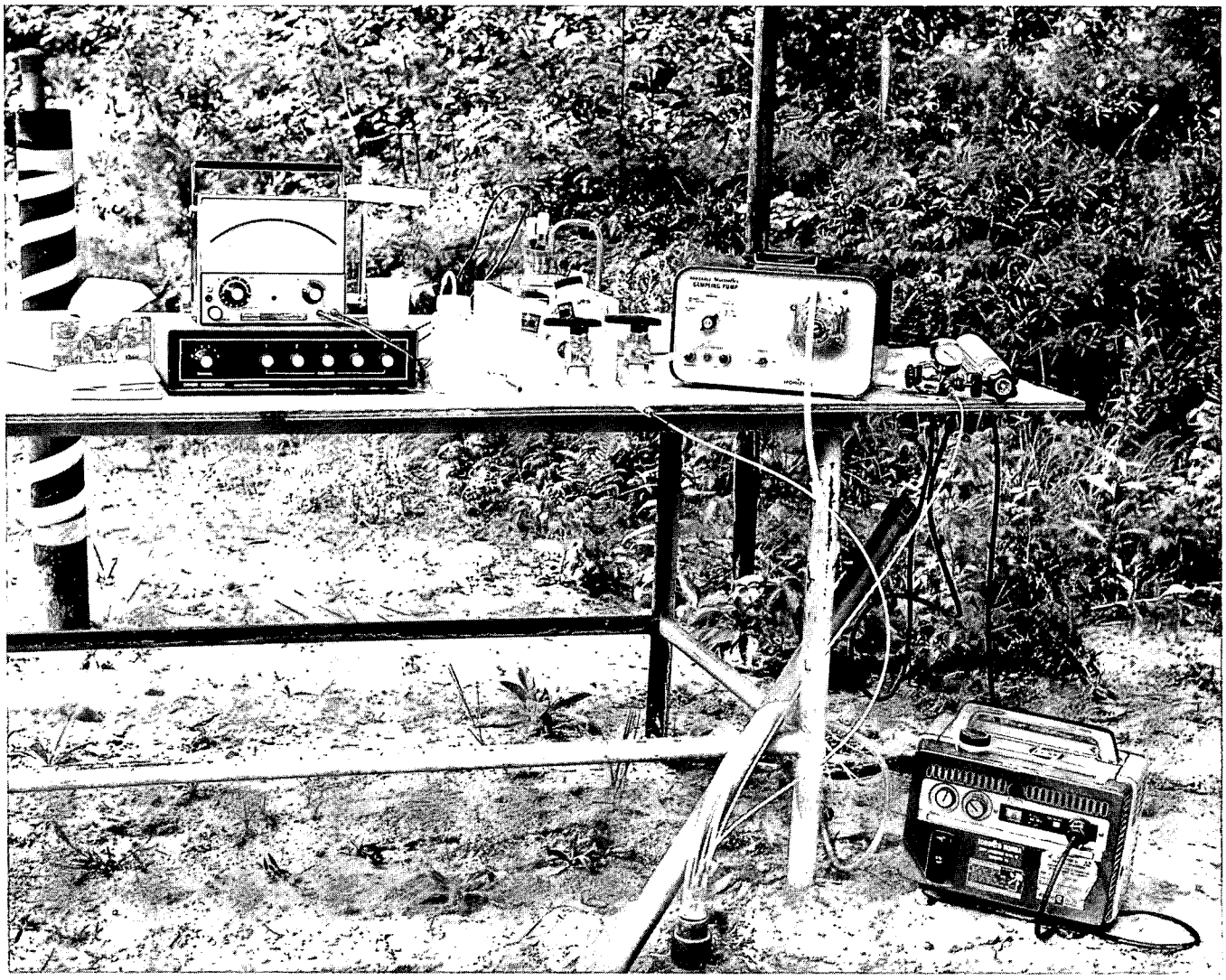

Measurement of pH and E_H at multilevel piezometer MA, October 1978. (Photo courtesy of Atomic Energy of Canada Limited.)

Cat. No. En 36-502/104

ISBN 0-662-10871-X

Contents

Contents (Cont.)

Tables

Tables (Cont.)

Illustrations

Abstract

In the mid-1950s, two experimental disposals of liquid radioactive waste containing approximately 700 curies (Ci) of ^{90}Sr and ^{137}Cs were made into shallow pits dug into the sandy ground of one of the disposal areas at the Chalk River Nuclear Laboratories (CRNL), 200 km northwest of Ottawa, Ontario. The disposal area is part of the recharge area of a shallow groundwater flow system of approximately 1 km in length containing two aquifers—the Middle and Lower Sands units. In the past 25 years, the radioactive wastes have migrated into both aquifers and have chromatographically separated into ^{90}Sr and ^{137}Cs plumes. These plumes are moving at characteristic velocities much less than the velocity of the transporting groundwater ($V_{GW} \sim 10^{-4}$ cm/s). For ^{90}Sr, this characteristic velocity is 3% of that of groundwater; for ^{137}Cs, it is about 0.3%.

The objectives of this study are (1) to investigate the hydrogeochemical controls on the migration of the radionuclides and (2) to develop methods of sampling, preservation and analysis of contaminated groundwaters and aquifer sediments.

Approximately 80% of all grains in the Middle and Lower Sands units are quartz or feldspar; minor amounts of mica, chlorite and hornblende are also present. Although present in only trace amounts (i.e., <1%), carbonates, sulphides, organic matter, vermiculite, and iron and manganese oxyhydroxides play important roles in the hydrogeochemical evolution of the groundwaters and/or the migration of the radionuclides. The sand units themselves are fine grained and well sorted, containing only a small percentage of silt and clay.

Groundwaters were sampled, using piezometers distributed throughout the aquifer, and analyzed in the field (pH, E_H, O_2, S_T^{2-} and alkalinity) and at CRNL (major ions). The pH, alkalinity and calcium values are consistent with those derived from a closed-system model of calcite dissolution with initial conditions of pH = 5.2 to 6.0 and $P_{CO_2} = 10^{-1.5}$ to $10^{-2.0}$. The E_H, oxygen, nitrate, iron, manganese and sulphate values are consistent with those derived from a closed-system model of organic matter oxidation. The alumino-silicate aquifer matrix of quartz and feldspar seems to be relatively insoluble compared with such minor or trace components as biotite, hornblende and calcite.

For studies of groundwater quality or pollution it is concluded that E_H measurements should be complemented with measurements of dissolved oxygen and sulphide, since these can give an independent assessment of the redox level of a groundwater. Three distinct redox zones seem to exist in the groundwater flow system—oxygen, iron-manganese and sulphide. The mobility of multivalent transition metals and nonmetals varies in these zones.

Radioactively contaminated aquifer sediments were obtained at a depth from 5 to 12 m by means of a cohesionless sediment sampler modified for the purpose. The aluminum core tubes were sectioned and the interstitial waters and the associated sediments were separated by centrifuge extraction and immiscible fluid displacement techniques. Interstitial waters were oxygenated and slightly acidic (pH ~ 6). Most of the ^{90}Sr ($K_d \sim 10$ mL/g) is exchangeably adsorbed, primarily to feldspars and layer silicates (in particular biotite); the rest is either specifically adsorbed to Fe(III) [and perhaps Mn(IV)] oxyhydroxides or fixed to unknown sinks. Less than one half of adsorbed ^{137}Cs is exchangeable with 0.5 *M* $CaCl_2$; the high levels of ^{137}Cs adsorption and fixation ($K_d \sim 10^2$ mL/g) are believed to be due to its reaction with micaceous minerals. Complexation of ^{90}Sr and ^{137}Cs does not appear to be an important factor in affecting their transport or adsorption. In some parts of the aquifer where the contaminated sediments were not studied, the retardation of ^{90}Sr may be occurring due to the precipitation of $SrCO_3$. Since these sediments are the products of the weathering of granitic rocks, this information may be relevant to adsorption of radionuclides in fractured granite.

Résumé

Vers le milieu des années 50, on a effectué le déversement expérimental de déchets radioactifs liquides contenant environ 700 curies de Sr^{90} et Cs^{137}, dans des puits peu profonds: ces derniers étaient creusés dans le sol sableux de l'une des zones de rejet des déchets, sur le site des laboratoires nucléaires de Chalk River (CRNL), à 200 km au nord-ouest d'Ottawa en Ontario. Ce secteur fait partie de l'aire d'alimentation d'un réseau d'écoulement souterrain peu profond, d'environ 1 km de longueur, contenant deux formations aquifères — l'unité sableuse moyenne et l'unité sableuse inférieure. Au cours des 25 dernières années, les déchets radioactifs ont migré dans ces deux aquifères et se sont subdivisés suivant un processus chromatographique, en traînées de Sr^{90} et Cs^{137}. Celles-ci se déplacent à des vitesses caractéristiques, bien inférieures à la vitesse des eaux souterraines qui les transportent ($V_{GW} \sim 10^{-4}$ cm/s). En ce qui concerne le Sr^{90}, cette vitesse caractéristique correspond à 3 % de la vitesse des eaux souterraines; pour le Cs^{137}, à environ 0,3 %.

Les objectifs de cette étude étaient (1) d'examiner les facteurs hydrogéochimiques qui régissent la migration des radionuclides et (2) de mettre au point des méthodes d'échantillonnage, de conservation et d'analyse des eaux souterraines et des sédiments aquifères contaminés.

Environ 80 % de toutes les particules des unités sableuses inférieure et moyenne sont constituées de quartz ou de feldspath; on rencontre aussi des quantités accessoires de mica, de chlorite et de hornblende. Quoique seulement présents à l'état de traces (p. ex. <1 %), les carbonates, les sulfures, les matières organiques, la vermiculite et les oxyhydroxides de fer et de manganèse jouent un rôle important dans l'évolution hydrogéochimique des eaux souterraines et la migration des radionuclides. Les unités sableuses elles-mêmes sont caractérisées par une granulométrie fine et sont bien triées; elles ne contiennent qu'un faible pourcentage de silt et d'argile.

On a effectué l'échantillonnage des eaux souterraines à l'aide de piézomètres répartis dans tout l'aquifère; on a analysé ces échantillons *in situ* (dosage du pH, E_H, O_2, S_T^{2-} et de l'alcalinité), et aux laboratoires CRNL (dosage des principaux ions). Les valeurs de pH, de l'alcalinité et du calcium concordent avec les valeurs déterminées pour un modèle en cycle fermé du processus de dissolution de la calcite, dans des conditions initiales de pH = 5,2 à 6,0 et $P_{CO_2} = 10^{-1,5}$ à $10^{-2,0}$. Les valeurs du E_H, de l'oxygène, des nitrates, du fer, du manganèse et des sulfates concordent avec les valeurs déterminées pour un modèle en cycle fermé de l'oxydation des matières organiques. La matrice alumino-silicatée des aquifères, composée de quartz et de feldspath, semble relativement insoluble par rapport aux constituants accessoires ou présents en traces, comme la biotite, la hornblende et la calcite.

Dans les études de qualité ou de contamination des eaux souterraines, on a conclu que la détermination du E_H doit être complétée par celle des concentrations en oxygène dissous et en sulfures, qui permettraient d'obtenir de façon indépendante une mesure du potentiel redox des eaux souterraines. Il semble exister trois zones distinctes de potentiel redox dans le réseau d'écoulement souterrain — oxygène, manganèse-fer et sulfures. La mobilité des métaux de transition plurivalents et des éléments non métalliques varie dans ces zones.

On a obtenu sur une épaisseur de 5 m à 12 m des sédiments aquifères contaminés à l'aide d'un échantillonneur modifié pour prélever les sédiments dépourvus de cohésion. On a sectionné les tubes carottiers en aluminium et séparé l'eau interstitielle et les sédiments associés, par centrifugation et une technique de déplacement des fluides non miscibles. Les eaux interstitielles, qui ont subi un certain degré d'oxygénation, étaient légèrement acides (pH ~6). La plupart du Sr^{90} ($K_d \sim 10$ mL/g) a été adsorbé par échange ionique, principalement sur les feldspaths et les phyllosilicates (en particulier la biotite); le reste a été soit spécifiquement adsorbé sur les oxyhydroxides de Fe(III) et peut-être de Mn(IV), ou fixé sur des sites récepteurs inconnus. Moins de la moitié du Cs^{137} adsorbé est échangeable vis-à-vis du $CaCl_2$ à 0,5 M; les niveaux les plus élevés d'adsorption et de fixation du Cs^{137} ($K_d \sim 10^2$ mL/g) résultent sans doute de la réaction de celui-ci avec les minéraux micacés. Il ne semble pas que la complexation du Sr^{90} et du Cs^{137} contribue beaucoup à modifier leur transport ou leur adsorption. Dans certaines parties de l'aquifère dont on n'a pas étudié les sédiments contaminés, il peut y avoir ralentissement du mouvement du Sr^{90}, en raison de la précipitation de $SrCO_3$. Puisque ces sédiments sont le produit de l'altération de roches granitiques, cette information peut présenter un intérêt quant à l'adsorption des radionuclides dans les terrains granitiques fracturés.

Acknowledgments

The following people are gratefully acknowledged: Janis Gulens, Eric Reardon, Doug Champ, D.L. Suarez, D. Maynes, D. Lawson, B. Kaye and R.N. Farvolden for their comments and suggestions on earlier versions of this manuscript; Bill Merritt, Doug Champ, Ron Patterson and Janis Gulens for their interest, cooperation and, most of all, instruction; Ivan Ophel and A.M. Marko for providing laboratory facilities at CRNL; Don Lennox and Gerry Grisak for their support of the project; Ron Patterson, Ken Lyon, Norm Catto, John Pickens, Laura Johnston and Tessa Spoel for their camaraderie in the field; Bert Risto, Christy Ryan and Pius Durepeau for patiently recovering the contaminated sediments and suggesting modifications to the techniques; Jim Young, Jim Judd and Bert Risto for their help in the laboratory; and Peter Barry for his guidance.

This report is the Ph.D. Thesis of the senior author, as presented to the University of Waterloo, Department of Earth Sciences (R.N. Farvolden, Supervisor).

Introduction

OBJECTIVES

The fate of radioactive wastes in the environment has received scientific attention for at least 25 years; in the 1970s, however, it has become a major issue in the public debate on the environmental impact of nuclear power. In this study, the geochemical controls on the migration of liquid radioactive wastes in a fluvial sand aquifer system are described; the radionuclides under consideration are ^{90}Sr and ^{137}Cs. These wastes were disposed of in shallow trenches in the recharge area of the aquifer at the Chalk River Nuclear Laboratories (200 km northwest of Ottawa, Ontario) during the mid-1950s in experiments to determine the consequences of the escape of such radionuclides from waste management facilities.

The objectives of this study are:

(1) To summarize the basic geochemical theory relevant to the contaminant hydrogeology of ^{90}Sr and ^{137}Cs (considered in Chapter 2).

(2) To collect new information and to collate existing background data relating to the hydrostratigraphy, sedimentary mineralogy and groundwater hydrology of and radionuclide migration in the aquifer (Chapter 3).

(3) To develop (i.e., adopt and modify) techniques for the sampling, preservation and analysis of (i) shallow contaminated groundwaters and (ii) cohesionless contaminated aquifer sediments (Chapters 4 and 5).

(4) To collect and analyze data concerning the geochemistry of groundwater as it relates to the migration of radionuclides within the aquifer (Chapter 4).

(5) To determine the degree of partitioning of the radionuclides between solution and solid phases and to identify the sinks (i.e., adsorbents or precipitates) responsible for removing the radionuclides from solution in groundwater (Chapter 5).

HYDROGEOLOGICAL CONTEXT OF THE PRESENT STUDY

Until quite recently Canadian hydrogeologists considered that groundwater pollution and quality matters presented a growing problem but not one as important as that of groundwater supply development [see for example Meyboom (1968)] . By 1975 groundwater quality had become "the major area of concern" among those hydrogeologists polled by Lennox and Parsons (1975). In that year Cherry *et al.* (1975a) used the term "contaminant hydrogeology" to describe the physical and chemical processes controlling contaminant migration in the subsurface.

Somewhat earlier Freeze (1972) had pointed out that the mechanism of subsurface pollution is amenable to analysis by "mathematical prediction models based on the equation of subsurface flow and solved numerically with the aid of a digital computer." Furthermore, he noted that

> Hydrogeochemical interaction between fluid and soil is probably the most important retarding influence on pollutant transport. . . .When the hydrogeochemical mechanisms are quantitatively understood, it would be reasonable to use retardation coefficients to obtain more accurate estimates of pollution buildup rates.

The purpose of this study is to quantify the hydrogeochemical mechanisms retarding the migration of radionuclides at Chalk River and to show how retardation coefficients (or in this case distribution coefficients) may be obtained by hydrogeologists from the analysis of contaminated groundwaters and aquifer materials.

HYDROGEOCHEMICAL RETARDATION OF SOLUTES DURING TRANSPORT IN POROUS MEDIA

The origin of the retardation coefficients referred to by Freeze is the dispersion-convection (i.e., solute-transport) equation. The theoretical development of this equation follows that of Ogata (1970) and makes the founding

assumption that Fick's laws of diffusion apply to the problems of solute transport in porous media.

The derivation of the dispersion-convection equation describing hydrodynamic dispersion of a solute in a solvent of similar density and viscosity is based on a mass balance analysis of transport by convection and dispersion through a cubic element in space (Fig. 1). For the flow parallel to the x-axis only, the two terms can be written:

$$\text{Convective transport} = \theta V_x C_A dydz$$

$$\text{Dispersive transport} = -\theta D'_x \frac{\partial C_A}{\partial x} dydz$$

where θ is the porosity, V_x is the average interstitial velocity in the x direction, C_A is the concentration of the solute A, dydz is the elemental cross-sectional area of the cubic element, and D'_x, the *coefficient of hydrodynamic dispersion* in the x direction, is a measure of the rate at which the concentration gradient $\frac{\partial C_A}{\partial x}$ is dissipated. The negative sign is used to indicate that the direction of flux is positive in the direction of decreasing concentration. The units of the two transport terms are in solute mass per unit time.

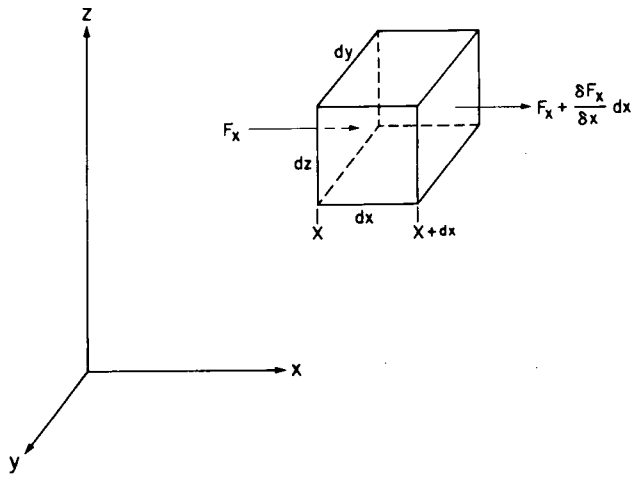

Figure 1. Mass balance of solute flux in a cubic element in space.

If it is assumed that these two components are linearly additive and if F_x represents the mass flux per unit cross-sectional area transported in the x direction in unit time, then

$$F_x = \theta V_x C_A - \theta D'_x \frac{\partial C_A}{\partial x} \quad (1)$$

If the flux of solute A is affected not only by convection and dispersion but also be geochemical reaction (i.e., adsorption or precipitation) within the unit cube, then the mass balance equation being sought must express the following condition:

Net change of solute flux between inflow and outflow	=	Rate of change of solute concentration inside of cubic elements	+	Rate of change of solute owing to geochemical reactions	(2)

The two rate terms on the right-hand side of Equation 2 are given by $\partial C_A/\partial t$ and $\partial q_A/\partial t$ where q_A is the amount of solute A *adsorbed or precipitated* per unit mass of the porous medium. Equation 2 can now be written:

$$(dydz)\left\{(-\theta D'_x \frac{\partial C_A}{\partial x} + \theta V_x C_A)_x - (-\theta D'_x \frac{\partial C_A}{\partial x} + \theta V_x C_A)_{x+dx}\right\} = (dxdydz\,\theta)\frac{\partial C_A}{\partial t} + (dxdydz\,\rho_b)\frac{\partial q_A}{\partial t} \quad (3)$$

where ρ_b is the bulk density (mass/volume). The subscripts x and x+dx refer to the flux into the cubic element at plane x and out of the element at plane x+dx. Dividing both sides by (dxdydz θ), i.e., assuming porosity is constant,

$$\frac{(D'_x \frac{\partial C_A}{\partial x} - V_x C_A)_{x+dx} - (D'_x \frac{\partial C_A}{\partial x} - V_x C_A)_x}{dx} = \frac{\partial C_A}{\partial t} + \frac{\rho_b}{\theta}\frac{\partial q_A}{\partial t} \quad (4)$$

which is the partial differential equation

$$\frac{\partial}{\partial x}(D'_x \frac{\partial C_A}{\partial x} - V_x C_A) = \frac{\partial C_A}{\partial t} + \frac{\rho_b}{\theta}\frac{\partial q_A}{\partial t} \quad (5)$$

If we assume that D'_x is independent of position in the x direction and that the average interstitial velocity, V_x, is constant, we can write

$$D'_x \frac{\partial^2 C_A}{\partial x^2} - V_x \frac{\partial C_A}{\partial x} = \frac{\partial C_A}{\partial t} + \frac{\rho_b}{\theta}\frac{\partial q_A}{\partial t} \quad (6)$$

Rearranging terms,

$$\frac{\partial C_A}{\partial t} = D'_x \frac{\partial^2 C_A}{\partial x^2} - V_x \frac{\partial C_A}{\partial x} - \frac{\rho_b}{\theta} \frac{\partial q_A}{\partial t} \qquad (7)$$

When the ionic species in question is a radionuclide, there is the added effect of radioactive decay to consider and Equation 7 then becomes:

$$\frac{\partial C_A}{\partial t} = D'_x \frac{\partial^2 C_A}{\partial x^2} - V_x \frac{\partial C_A}{\partial x} - \frac{\rho_b}{\theta} \frac{\partial q_A}{\partial t}$$

$$- \lambda C_A - \frac{\lambda \rho_b q_A}{\theta} \qquad (8)$$

where λ is the first-order rate constant or disintegration constant for the radionuclide in question. Therefore the rate of change with time of the concentration of ionic species A in solution is equal to the sum of its rates of change owing to dispersion minus its rates of change owing to convection, geochemical reaction and radioactive decay.

Equation 8 is a satisfactory description of a solute transport process affected by geochemical retardation, such as adsorption or precipitation, provided that the geochemical reactions which occur do not affect the ratio ρ_b/θ. Should large amounts of a mineral species be precipitating out of solution in a groundwater flow system, it is conceivable that the bulk density and the porosity of the porous medium could be materially affected. In such an extreme case, Equation 8 would be unsuitable as a description of the mass transport process. The case with which the present study is concerned, however, is a traditional one in radioactive waste management in which a radionuclide has accidentally escaped from a waste management area and is in solution in trace amounts relative to the major groundwater cations. For such a case the adsorption or precipitation of the radionuclide will not affect the ratio ρ_b/θ.

For the special case of hydrogeochemical retardation owing to adsorption on an ion exchanger R^-, such as:

$$A^+ + B^+R^- \rightleftarrows A^+R^- + B^+ \qquad (9)$$

it is desirable to transform Equation 8 into a form such that the dependent variables, C_A and q_A, are reduced to dimensionless values between 0.0 and 1.0. In doing this it is possible to establish relationships between the independent variables in Equation 8 (Lai and Jurinak, 1972).

For the adsorption reaction being considered,

$C = C_A + C_B$ = total competing cation concentration in solution (meq/mass)

$Q = q_A + q_B$ = total cation-exchange capacity (meq/mass)

let $C_A = CX_A$ and $q_A = QY_A$

where X_A is the reduced concentration of A^+ in solution varying from 0 to 1, and where Y_A is the reduced concentration of A^+ adsorbed on R^-.

For a cation-exchange reaction of constant total competing cation concentration in solution and a constant exchange capacity, C and Q are constant. Therefore, it is possible to obtain the following expressions in terms of the reduced variables, X_A and Y_A, for the terms in Equation 8:

$$\frac{\partial C_A}{\partial t} = C \frac{\partial X_A}{\partial t}$$

$$\frac{\partial C_A}{\partial x} = Q \frac{\partial X_A}{\partial x}$$

$$\frac{\partial^2 C_A}{\partial x^2} = C \frac{\partial^2 X_A}{\partial x^2} \qquad (10)$$

$$\frac{\partial q_A}{\partial t} = Q \frac{\partial Y_A}{\partial t}$$

$$\lambda C_A = \lambda C X_A$$

$$\frac{\lambda \rho_b q_A}{\theta} = \frac{\lambda \rho_b Q Y_A}{\theta}$$

Substituting Equation 10 into 8 and rearranging terms, the following form for the material balance equation is obtained:

$$D'_x \frac{\partial^2 X_A}{\partial x^2} - V_x \frac{\partial X_A}{\partial x} - \lambda C X_A - \frac{\lambda \rho_b Q Y_A}{\theta}$$

$$= \frac{\partial X_A}{\partial t} + \frac{\rho_b Q}{\theta C} \frac{\partial Y_A}{\partial t} \qquad (11)$$

Assuming that the ion-exchange reaction between A^+ and B^+ is instantaneous, there is a unique function relating X_A and Y_A, which is called the exchange isotherm:

$$Y_A = f(X_A) \tag{12}$$

By using the chain rule of differentiation we can write:

$$\frac{\partial Y_A}{\partial t} = f' \frac{\partial X_A}{\partial t} \tag{13}$$

where f' is the slope of the exchange isotherm (Fig. 2).

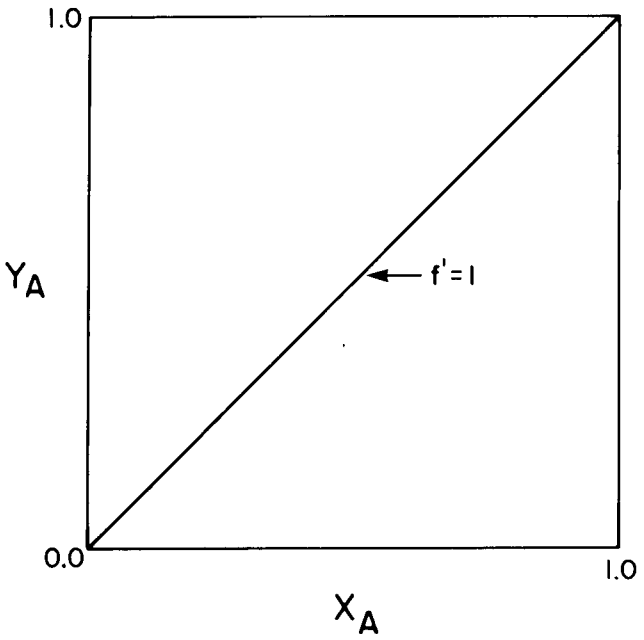

Figure 2. Linear exchange isotherm.

Substituting Equation 13 into 11, we can write:

$$D'_x \frac{\partial^2 X_A}{\partial x^2} - V_x \frac{\partial X_A}{\partial x} - \lambda C X_A - \frac{\lambda \rho_b Q Y_A}{\theta}$$

$$= \frac{\partial X_A}{\partial t} + \frac{\rho_b Q}{\theta C} f' \frac{\partial X_A}{\partial t} \tag{14}$$

or

$$D_A \frac{\partial^2 X_A}{\partial x^2} - V_A \frac{\partial X_A}{\partial x} - \frac{\lambda (C X_A + \frac{\rho_b}{\theta} Q Y_A)}{1 + \frac{\rho_b}{\theta} \frac{Q}{C} f'} = \frac{\partial X_A}{\partial t}$$

where

$$D_A = \frac{D'_x}{1 + \frac{\rho_b}{\theta} \frac{Q}{C} f'} \tag{15}$$

and

$$V_A = \frac{V_x}{1 + \frac{\rho_b}{\theta} \frac{Q}{C} f'} \tag{16}$$

Equations 15 and 16 will be referred to as the retardation equations, since they predict the reduction in the dispersion coefficient and average interstitial velocity of cation A^+ relative to the dispersion coefficient, D'_x, and velocity, V_x, of a conservative tracer. The term $\rho_b Q$ expresses the total cation-exchange capacity per unit volume of porous medium, whereas the term θC expresses the amount of all competing cations (in this case A^+ and B^+) in solution per unit volume of the porous medium. The parameter f' is called a selectivity quotient (Amphlett, 1964) for the case in which A^+ is present only in trace quantities. For a linear adsorption isotherm (Fig. 2) in which A^+ is the trace ion, the term $Qf'/C = K_d^A$, the distribution coefficient of A^+. The denominator in Equations 15 and 16 (i.e., $1 + \rho_b K_d^A/\theta$) may be thought of as a retardation coefficient using the terminology of Freeze (1972).

Geochemical Theory

CHEMICAL EQUILIBRIA IN GROUNDWATERS

The methods of calculating the equilibrium distribution of inorganic aqueous species are described in this section and follow principles outlined by Garrels and Christ (1965), Stumm and Morgan (1970) and Truesdell and Jones (1974). It is assumed that a chemical analysis of the groundwater in question and field measurements of temperature, pH and redox level are available. On the basis of these methods and the knowledge of the thermodynamic equilibrium constants of the major aqueous species, minerals and gases, it is possible to compute the state of reaction of the groundwater with respect to solid and gaseous phases. The results of such computations, using the computer program WATEQ [Truesdell and Jones (1974)], are discussed in Chapter 4.

Mass-Action Equilibria

At equilibrium aqueous species related by a reaction of the form

$$aA + bB = cC + dD \qquad (17)$$

in which a moles of species A and b moles of B react to produce c moles of C and d moles of D, have a mass-action or thermodynamic equilibrium constant given by

$$K = \frac{\{C\}^c \{D\}^d}{\{A\}^a \{B\}^b} \qquad (18)$$

where $\{C\}$ represents the activity (to be defined later) of substance C.

The equilibrium constant is related to the standard free energy change of reaction, ΔG_r^0, by the expression

$$\Delta G_r^0 = -2.303\ RT \log K \qquad (19)$$

or

$$\log K = -\Delta G_r^0 / 2.303\ RT \qquad (20)$$

where R is the gas constant and T is the absolute temperature. The standard free energy change of reaction may be considered as a measure of the tendency of the reaction (17) to occur (Krauskopf, 1967, p. 216). At equilibrium $\Delta G_r^0 = 0$ and there is no net change in the distribution of the aqueous species in (17); negative values of ΔG_r^0 indicate a tendency for reaction (17) to proceed to the right and vice versa.

The equilibrium constant varies with temperature. Its value at the temperature of the groundwater sample may be expressed by the Van't Hoff relationship

$$\log K = \log K_{Tr} - \frac{\Delta H_{Tr}}{2.3\ R}\left(\frac{1}{T} - \frac{1}{T_r}\right) \qquad (21)$$

where ΔH_{Tr} is the enthalpy change of the reaction at some specified reference temperature, Tr (298.15°K or 25°C in the present study).

Ion Activities and Activity Coefficients

The chemical potential, μ_i, of component i in an aqueous solution such as groundwater may be written as

$$\mu_i = \mu_i^0 + RT\ 1n\ \{i\} \qquad (22)$$

where μ_i^0 is a constant under specified conditions of temperature and pressure and $\{i\}$ is the activity of component i, which may be considered "an idealized concentration" (Stumm and Morgan, 1970, p. 29). For an individual ion in a mixed electrolyte solution, such as groundwater, Equation 22 may be rewritten

$$\mu_i = \mu_i^0 + RT\ 1n\ \gamma_i m_i \qquad (23)$$

in which m_i is the molal (i.e., moles of solute per 1000 g of water) concentration of i and γ_i is its activity coefficient. By the infinite dilution convention

$$\gamma_i \rightarrow 1 \text{ as } I \rightarrow 0 \qquad (24)$$

where the ionic strength $I = \frac{1}{2} \Sigma Z_i^2 C_i \sim \frac{1}{2} \Sigma Z_i^2 m_i$, C_i is the molar (i.e., moles of solute per 1000 mL of solution) concentration and Z_i is the charge of each ion i, the summation being taken over all ions in solution.

The identity $\{i\} = \gamma_i m_i$ established in Equation 23 requires that μ_i^0, γ_i and the concentration scale be defined consistently with respect to one another. Truesdell and Jones (1974) noted "the convention that activities are dimensionless requires that single-ion activity coefficients have dimensions of molality^{-1}." To estimate these coefficients use is made of the Debye-Hückel equation from which single-ion activity coefficients for dilute solutions may be calculated:

$$\log \gamma = - \frac{A Z_i^2 \sqrt{I}}{1 + Ba\sqrt{I}} \qquad (25)$$

where A and B are constants dependent only on the dielectric constant, density and temperature (Truesdell and Jones, 1974, p. 241); Z_i and I are as defined; and a "may be regarded as the effective diameter of the hydrated ion" (Kielland, 1937).

Distribution of Anionic Weak Acid Species

The speciation of weak acids (e.g., H_2CO_3, H_4SiO_4, H_2S) may be calculated from the total analytical concentrations (i.e., mC_T, mSi_T, mS_T^{2-}), the pH, the activity coefficients of individual species and the relevant equilibrium constants. For equilibria involving dissolved CO_2, the distribution of species is as follows:

$$H_2CO_3 = H^+ + HCO_3^- \qquad (26)$$

$$HCO_3^- = H^+ + CO_3^{2-} \qquad (27)$$

The concentration of each of these species is calculated as follows:

$$K_1 = \frac{10^{-pH}\, m_{HCO_3^-}\, \gamma_{HCO_3^-}}{m_{H_2CO_3}\, \gamma_{H_2CO_3}} \qquad (28)$$

$$K_2 = \frac{10^{-pH}\, m_{CO_3^{2-}}\, \gamma_{CO_3^{2-}}}{m_{HCO_3^-}\, \gamma_{HCO_3^-}} \qquad (29)$$

(N.B. $pi = -\log\{i\}$.)

The mass balance equation for total carbon is

$$m_{C_T} = m_{H_2CO_3} + m_{HCO_3^-} + m_{CO_3^{2-}} \qquad (30)$$

The mass-action Equations 28 and 29 may be combined with the mass balance Equation 30 to solve for, as an example, the bicarbonate molality:

$$m_{HCO_3^-} = \frac{m_{C_T}}{1 + \left(\frac{\gamma_{HCO_3^-}}{10^{pH}\, K_1\, \gamma_{H_2CO_3}} + \frac{K_2\, 10^{pH}\, \gamma_{HCO_3^-}}{\gamma_{CO_3^{2-}}} \right)} \qquad (31)$$

By substitution into the mass-action equations the other species may be determined.

Complexes

The concentrations of complex ions are evaluated by a similar procedure. In this case the analytical concentrations of the relevant cations and anions must be known as well as the formation constants for the complexes in question. For the case of the strontium species $SrSO_4^0$ and $SrHCO_3^+$, the reactions are:

$$Sr^{2+} + HCO_3^- = SrHCO_3^+ \qquad (32)$$

$$Sr^{2+} + SO_4^{2-} = SrSO_4^0 \qquad (33)$$

for which the formation constants are (Langmuir, 1979, p. 359):

$$K_1 = \frac{\{SrHCO_3^+\}}{\{Sr^{2+}\}\{HCO_3^-\}} \sim 10^{-1.2} \qquad (34)$$

$$K_2 = \frac{\{SrSO_4^0\}}{\{Sr^{2+}\}\{SO_4^{2-}\}} \sim 10^{-2.5} \qquad (35)$$

From these equations the expressions

$$m_{SrHCO_3^+} = \frac{K_1\, m_{Sr^{2+}}\, \gamma_{Sr^{2+}} \{HCO_3^-\}}{\gamma_{SrHCO_3^+}} \qquad (36)$$

$$m_{SrSO_4^0} = \frac{K_2\, m_{Sr^{2+}}\, \gamma_{Sr^{2+}} \{SO_4^{2-}\}}{\gamma_{SrSO_4^0}} \qquad (37)$$

may be substituted in the mass balance equation for strontium as follows:

$$m_{Sr_T} = m_{Sr^{2+}} + m_{SrHCO_3^+} + m_{SrSO_4^0} \qquad (38)$$

to obtain an expression for the free (uncomplexed) Sr^{2+} ion:

$$m_{Sr^{2+}} = \frac{m_{Sr_T}}{1 + \gamma_{Sr^{2+}}\left(\frac{K_1\{HCO_3^-\}}{\gamma_{SrHCO_3^+}} + \frac{K_2\{SO_4^{2-}\}}{\gamma_{SrSO_4^0}}\right)} \quad (39)$$

The computed concentration of free strontium, $m_{Sr^{2+}}$, may then be substituted back into the mass-action expressions (34) and (35) to solve for the concentration of the complexes. The concentrations assigned to complex ions and weak acid species reduce the concentrations of the free ions and change the ionic strength and therefore the activities and activity coefficients of these ions. Corrected values of all these quantities may be calculated iteratively using computer programs such as WATEQ (Truesdell and Jones, 1974, p. 243).

Saturation Index

It is possible to deduce from a chemical analysis of a groundwater sample whether precipitation or dissolution of particular mineral species is likely to be occurring. This is accomplished by comparing the measured ion activity product of the dissolved constituents of a mineral species with its solubility product, yielding the saturation index, SI,

$$SI = \log_{10}(IAP/K_{SO}) \quad (40)$$

where IAP is the ion activity product $\{A\}^x\{B\}^y$ and K_{SO} is the solubility product of the mineral $[A_x B_y]$. If $SI < 0$, the groundwater is undersaturated with respect to $[A_x B_y]$ and a net dissolution of the mineral should occur; at $SI = 0$, the groundwater is at equilibrium with the mineral; when $SI > 0$, the groundwater is supersaturated with the mineral's constituent ions and net precipitation should occur.

Oxidation-Reduction Reactions

The oxidation-reduction state of an aqueous solution may be defined by the Nernst equation (Stumm and Morgan, 1970, p. 316):

$$E_H = E_H^0 + \frac{2.3RT}{nF}\log\frac{\{ox\}}{\{red\}} \quad (41)$$

where E_H is the equilibrium or redox potential in volts, E_H^0 is the standard reduction potential of the reaction (ox + ne = red) at 25°C and unit activity, R is the gas constant, T is the absolute temperature (°K), n is the number of moles of electrons (e) transferred in the reaction, F is the Faraday constant (at 25°C, 2.3RT/F = 0.059 volts), and $\{ox\}$ and $\{red\}$ are the activities at equilibrium of the oxidized and reduced species, respectively, involved in the reaction.

The E_H may be converted to the negative logarithm of the conventional activity of the electron (i.e., pE) by the relation

$$pE = \frac{E_H}{2.3RT/F} = \frac{E_H}{0.059} \quad \text{at } 25°C \quad (42)$$

where

$$\{e\} = 10^{-pE} \quad (43)$$

that is,

$$pE = -\log\{e\} \quad (44)$$

By doing this it is possible to compute the speciation of "redox active" elements by a conventional equilibrium constant. Consider, the example, the equilibrium

$$Fe^{3+} + e^- = Fe^{2+} \quad (45)$$

for which the equilibrium constant is

$$K = \frac{\{Fe^{2+}\}}{\{Fe^{3+}\}\{e\}} \quad (46)$$

Individual activities may be calculated from this expression and knowledge of m_{Fe_T} or $m_{Fe^{2+}}$ or $m_{Fe^{3+}}$ by successive approximations.

Alternatively, the redox level of groundwaters may be estimated by computing an equilibrium or redox potential for a particular redox reaction such as the SO_4^{2-} - HS^- system (Stumm and Morgan, 1970, p. 310):

$$SO_4^{2-} + 9H^+ + 8e = HS^- + 4H_2O \quad (47)$$

for which

$$pE = 4.25 - 1.125\,pH - 0.125\,pSO_4 + 0.125\,pHS \quad (48)$$

Gas Partial Pressures

The partial pressure of CO_2 in a groundwater may be estimated by (Truesdell and Jones, 1974, p. 246):

$$\log P_{CO_2} = pH_2O - pH - pHCO_3 - pK \quad (49)$$

for which the activity of water is defined by (Garrels and Christ, 1965, p. 66):

$$\{H_2O\} = 1 - 0.017 \Sigma m_i \quad (50)$$

where Σm_i is the sum of molalities of all dissolved species.

GEOCHEMICAL FACTORS AFFECTING THE MOBILITY OF CONTAMINANTS IN GROUNDWATER

The migration of dissolved contaminants in groundwater flow systems is due to their transport by groundwater. The transport rates or migration velocities are moderated by a variety of geochemical and biochemical processes, which have been summarized by Langmuir (1972) as:

(1) complex formation,
(2) acid-base reactions,
(3) oxidation-reduction processes,
(4) precipitation-dissolution reactions,
(5) adsorption-desorption reactions, and
(6) microbial reactions.

Of these six processes, only (4), (5) and (6) can lead to the removal of contaminants from solution, i.e., adsorption or precipitation from solution and certain microbial reactions. The other processes, however, play an important role by affecting the availability of the contaminant for adsorption or precipitation.

Complexation

The significance of complex-ion formation in the study of groundwater pollution is that the concentration of potential contaminants and their mobility are governed to varying extents by the concentration and nature of the complexes they form. For example, chloride and hydroxide complexes may significantly affect the mobility of heavy metals (e.g., Pb^{2+}, Cd^{2+}, Zn^{2+}) in groundwaters contaminated by leachates from sanitary landfills and other waste disposal sites. When complexed by inorganic or organic ligands (e.g., Cl^-, EDTA) the contaminants may not immediately be available for adsorption or precipitation, and consequently the mobility of heavy metal contaminants may be increased in the groundwater flow system.

On the other hand, contaminants may become associated with adsorbed complexing ligands (e.g., humic compounds) associated with hydrous metal oxides (Davis and Leckie, 1978), in which case the mobility of such contaminants will be reduced in the aquifer system. Therefore adsorbing and nonadsorbing ligands may compete for contaminant ions and thus determine, on the basis of the relevant formation constants, the distribution of complexed contaminants between adsorbed and solution states.

Acid-Base Reactions

It has been pointed out (Stumm and Morgan, 1979, p. 383) that the natural waters of this planet have evolved through a gigantic acid-base titration involving acids that are transported through the hydrologic cycle (e.g., H_2CO_3) and bases or amphoteric substances which are released by the weathering of rocks (e.g., OH^-). The acidity or basicity of the resulting waters may be identified by the pH, which is defined as $pH = -\log_{10}\{H^+\}$.

The pH and alkalinity of many groundwaters are controlled by the dissolved carbonate system arising from the dissolution of calcite ($CaCO_3$) and soil-zone CO_2 to form the various species of dissolved carbon dioxide, i.e., H_2CO_3, HCO_3^- and CO_3^{2-}. While $CaCO_3$ is an efficient pH buffer in the neutral and acid pH range, the incongruent dissolution of alumino-silicate minerals provides a greater buffer capacity when $pH < 9$ (Stumm and Morgan, 1970, pp. 418–421), although the kinetics of such reactions may be quite slow.

Knowledge of the pH of groundwater and its buffering agents is important, since the solubility of many minerals and therefore of potential contaminant sources and sinks is dependent on the pH. Furthermore, the surface charge of many adsorbents is determined by the adsorption of H^+ and OH^- from solution.

Oxidation-Reduction Processes

Oxidation-reduction processes are of major importance in governing the geochemistry of those elements that may gain or lose electrons in groundwaters, e.g., Fe, Mn, C, N, O, S, As and U. Oxidation is the removal of electrons from an atom or group of atoms (e.g., $Fe^{2+} = Fe^{3+} + e^-$); reduction is the addition of electrons to an atom or group of atoms (e.g., $Fe^{3+} + e^- = Fe^{2+}$). Earlier, the redox potential, E_H, was introduced to describe the redox state of groundwater. In Table 1, redox potentials adjusted to pH = 7 (E_H^*) are reported for some redox processes that may occur in groundwater.

By combining the equations in Table 2 it is possible to create two sequences of redox reactions. The first of these sequences (Table 2) shows the order of reduction reactions that should occur on the basis of thermodynamic predictions (Stumm and Morgan, 1970) in a system closed to the introduction of dissolved oxidants and with an

Table 1. Reaction Constants of Some Reduction Processes per Mole of Electrons (modified after Stumm and Morgan, 1970, p. 318)

Reaction	E_H^* (mV)
(1) $1/4\ O_2\ (g) + H^+ + e^- = 1/2\ H_2O$	+813
(2) $1/5\ NO_3^- + 6/5\ H^+ + e^- = 1/10\ N_2\ (g) + 3/5\ H_2O$	+746
(3) $1/2\ MnO_2\ (s) + 2\ H^+ + e^- = 1/2\ Mn^{2+} + H_2O$	+396
(4) $1/8\ NO_3^- + 5/4\ H^+ + e^- = 1/8\ NH_4^+ + 3/8\ H_2O$	+363
(5) $Fe(OH)_3 + 3\ H^+ + e^- = Fe^{2+} + 3\ H_2O$	-185
(6) $1/8\ SO_4^{2-} + 9/8\ H^+ + e^- = 1/8\ HS^- + 1/2\ H_2O$	-214
(7) $1/8\ CO_2\ (g) + H^+ + e^- = 1/8\ CH_4\ (g) + 1/4\ H_2O$	-244
(8) $1/6\ N_2\ (g) + 4/3\ H^+ + e^- = 1/3\ NH_4^+$	-277
(9) $1/4\ CO_2\ (g) + H^+ + e^- = 1/4\ CH_2O + 1/4\ H_2O$	-484

$$E_H^* = E_H^\circ + \frac{RT}{nF} \ln \{H^+\}^p$$

$$[H^+] = 1.0 \times 10^{-7}\ M$$

p—Stoichiometric coefficient for H^+.
g—Gas.
s—Solid.

Table 2. Redox Processes in a Closed System (modified after Stumm and Morgan, 1970, p. 337)

Reaction	Equation
(1) Aerobic respiration	$CH_2O + O_2\ (g) = CO_2\ (g) + H_2O$
(2) Denitrification	$CH_2O + 4/5\ NO_3^- + 4/5\ H^+ = CO_2\ (g) + 2/5\ N_2\ (g) + 7/5\ H_2O$
(3) Mn(IV) reduction	$CH_2O + 2\ MnO_2\ (s) + 4\ H^+ = 2\ Mn^{2+} + 3\ H_2O + CO_2\ (g)$
(4) Fe(III) reduction	$CH_2O + 8\ H^+ + 4\ Fe(OH)_3 = 4\ Fe^{2+} + 11\ H_2O + CO_2\ (g)$
(5) Sulphate reduction	$CH_2O + 1/2\ SO_4^{2-} + 1/2\ H^+ = 1/2\ HS^- + H_2O + CO_2\ (g)$
(6) Methane fermentation	$CH_2O + 1/2\ CO_2\ (g) = 1/2\ CH_4 + CO_2\ (g)$
(7) Nitrogen fixation	$CH_2O + H_2O + 2/3\ N_2\ (g) + 4/3\ H^+ = 4/3\ NH_4^+ + CO_2\ (g)$

g—Gas.
s—Solid.

excess of organic material; the organic material is written as the simple carbohydrate CH_2O. The hydrogeological analog of this geochemical model is the recharge of rainwater, saturated with dissolved oxygen, through the soil zone during which time HCO_3^-, SO_4^{2-} and NO_3^- become dissolved in it and then into a confined aquifer containing MnO_2, $Fe(OH)_3$ and excess organic material. It also occurs in groundwater contaminated with organic-rich leachate which rapidly uses up the available oxygen in the groundwater (Matthess, 1972). Consequently in such hydrogeological systems, the following sequence of redox processes should occur (Stumm and Morgan, 1970, p. 337; Champ *et al.*, 1979):

(1) the reduction of O_2 and its disappearance from the groundwater,

(2) the denitrification of the groundwater,
(3) the appearance in the groundwater of Mn^{2+} and Fe^{2+}, and
(4) the reduction of sulphate to sulphide, carbon dioxide to methane, and nitrogen to ammonia.

Elements of such a sequence have been described by Edmunds (1977) for the Lincolnshire Limestone of England, by Schwille (1976) for contaminated groundwaters in West Germany and by Champ *et al.* (1979) for the groundwaters at Chalk River.

A second redox model may be created to account for the sequence of reactions which should occur, according to thermodynamic predictions, in reduced groundwaters in contact with dissolved oxygen (Table 3). Hydrogeological examples of such redox processes include the purification of leachate by oxygenated groundwaters (Matthess, 1972), the oxidation of spring waters, and the oxidation of sulphide minerals in a confined aquifer being recharged with oxygenated water (Ragone *et al.*, 1973).

In such environments the following sequence of redox processes should occur (Stumm and Morgan, 1970, p. 337; Champ *et al.*, 1979):

(1) the oxidation of the organics,
(2) the oxidation of sulphide to sulphate,
(3) the oxidation of ferrous iron and the precipitation of $Fe(OH)_3$,
(4) the oxidation of the ammonium ion to nitrate,
(5) the oxidation of dissolved manganese and the precipitation of MnO_2 or some similar hydrous oxide.

An understanding of the redox environment is crucial in predicting the mobility of those elements that have variable valances or charges and the solubility of transition metal oxides which may function as adsorbents in aquifer systems. For instance, the thermodynamically stable forms of oxidized iron and manganese are highly insoluble and adsorbent oxides, i.e., $Fe(OH)_3$ and MnO_2; following reduction, however, Fe^{2+} and Mn^{2+} ions move with the groundwater and may cause serious deterioration in groundwater quality. In comparison, those elements which form oxyanions, such as $HCrO_4^-$, NO_3^-, $H_2AsO_4^-$, are extremely mobile in oxidized groundwaters but may be less so in reduced environments.

Precipitation-Dissolution Reactions

In addition to their adsorption from solution, contaminants may be removed from solution either by direct precipitation or by isomorphous substitution with an ion of similar size in a crystal that is forming (coprecipitation) or that has formed (replacement). Of particular importance in the removal of contaminants from solution in groundwater is the formation of metal carbonates (e.g., $SrCO_3$, $CdCO_3$), phosphates ($FePO_4 \cdot 2H_2O$), sulphides (ZnS, PbS), hydroxides [$Fe(OH)_3$] and oxides (MnO_2). Saturation index calculations may be employed to determine whether dissolution or precipitation of the mineral species is likely to be occurring.

In carbonate aquifers groundwater saturation with respect to $CaCO_3$ is not always readily attained (e.g., Back and Hanshaw, 1971), although "in the absence of inhibition, relatively short times should be sufficient to establish equilibrium" (Plummer and Wigley, 1976, p. 199). Furthermore, there are several reports of supersaturation of $CaCO_3$ in aquifers [e.g., the Chalk and Triassic sandstones in England (Edmunds, 1977)]. At present it seems that this departure from equilibrium may be best explained by the effects of inhibiting ions and molecules at centres of dissolution and precipitation of $CaCO_3$ particles (Plummer and Wigley, 1976; Berner *et al.*, 1978).

Table 3. Redox Processes in an Open System (modified after Stumm and Morgan, 1970, p. 337)

Reaction	Equation
(1) Aerobic respiration	$O_2\ (g) + CH_2O = CO_2\ (g) + H_2O$
(2) Sulphide oxidation	$O_2\ (g) + 1/2\ HS^- = 1/2\ SO_4^{2-} + 1/2\ H^+$
(3) Fe(II) oxidation	$O_2\ (g) + 4\ Fe^{2+} + 10\ H_2O = 4\ Fe(OH)_3 + 8\ H^+$
(4) Nitrification	$O_2\ (g) + 1/2\ NH_4^+ = 1/2\ NO_3^- + H^+ + 1/2\ H_2O$
(5) Mn(II) oxidation	$O_2\ (g) + 2\ Mn^{2+} + 2\ H_2O = 2\ MnO_2\ (s) + 4\ H^+$

g—Gas.
s—Solid.

The replacement of one element in a crystal lattice by another is common in mineral formation. It has been pointed out by Krauskopf (1967) that those elements that replace one another tend to be of similar ionic radii, covalent character and valence. The significant feature of replacement and coprecipitation processes is that the new solid phase is more stable in the final solution than the original solid phase, although the new phase may be a poorly crystalline and metastable phase (Jenne, 1977). This implies that the new solid phase is more insoluble than the original solid phase and that the propensity of a contaminant ion to be absorbed into a mineral lattice can be expressed by solubility arguments.

Adsorption-Desorption Reactions

In natural porous media contaminants are adsorbed onto inorganic and organic adsorbents, of which those particles having a size range of 10^{-3} to 10^{-6} mm—colloids—are particularly important. Sennett and Olivier (1965) described colloids as being large when compared with small molecules but sufficiently small so that interfacial forces, as well as inertial forces, are significant in controlling their behaviour.

The adsorption capacity of colloids and other particles in solution is due to their ability to generate or sustain a charged solid-solution interface, creating an *electrical double layer* (EDL). Parks (1975) has described several models of the EDL, of which three are shown in Figure 3.

In the simplest of models of the EDL, adsorption is due solely to the electrostatic (i.e., coulombic or physical) attraction of oppositely charged adsorbent and adsorbate phases. "Electrostatic adsorption...is rapid and readily reversible, and electrostatically adsorbed ions undergo equilibrium exchange" (Parks, 1975, p. 242). Figure 3, case I, shows a negatively charged solid in contact with a layer of cations (the Stern layer) beyond which is a diffuse layer of ions in solution (the Gouy layer). The oppositely charged ions in the Gouy layer (counterions) are fully hydrated and can approach the charged surface no closer than their hydrated radii, d; the plane through the centres of the hydrated counterions is known as the Stern plane.

The surface charge may be due to (1) imperfections or substitutions within the crystal lattice of a particle and/or (2) chemical reactions at the solid-solution interface involving certain potential-determining ions in solution, e.g., H^+ or OH^- (Stumm and Morgan, 1970, pp. 454-456). In the second case, the groundwater pH will directly affect the adsorption behaviour of adsorbents and is itself a reflection of this behaviour. The point at which the solid surface charge is zero is called the point of zero charge and the pH at this point is denoted by pH_{pzc}. The surface charge will become positive at higher concentrations of positive potential-determining ions and, as such, will be an anion exchanger. Should an excess of negative determining ions be introduced into this heterogeneous solution, these anions may be adsorbed and the surface charge reversed.

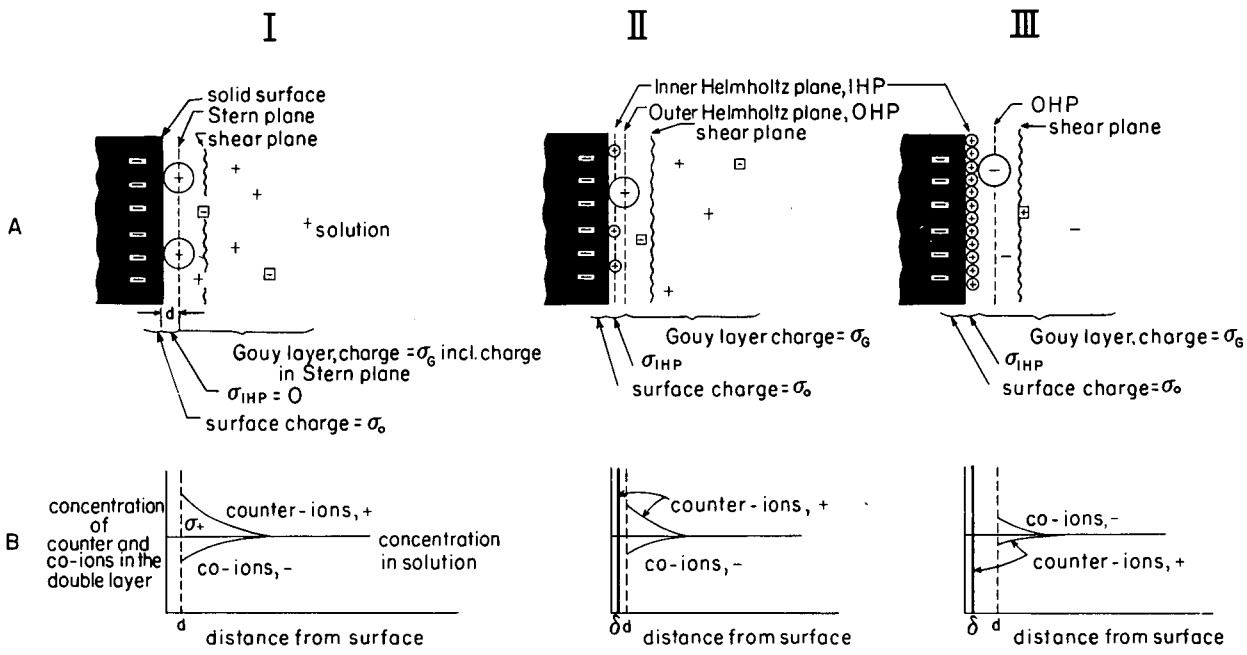

Figure 3. Electrical double layers. Positive and negative ions are denoted by (+) and (-), respectively (after Parks, 1975).

In contrast with this physical or electrostatic adsorption, chemisorption, or specific adsorption, is the result of much stronger binding forces leading to the formation of a sort of surface compound (Moore, 1964, p. 744). "Unlike electrostatic adsorption, specific adsorption may be slow and is less readily reversible in the sense that equilibrium is not achieved in a reasonable time" (Parks, 1975, p. 243). In the case of specific adsorption, the EDL is assumed to be composed of three zones of charge: the surface charge, the specifically adsorbed charge and the Gouy-layer (electrostatically adsorbed) charge. The locus of the centres of specifically adsorbed ions [at a distance δ from the surface (Fig. 3, case II)] is called the inner Helmholtz plane (IHP). The IHP and the outer Helmholtz plane (OHP), the locus of centres of the Gouy layer ions closest to the charged surface, replace the Stern plane of case I. In case II, the surface charge (σ_0) is balanced by the charges in the other two zones of charge, i.e., $\sigma_0 = -(\sigma_{IHP} + \sigma_G)$. If specific adsorption is sufficiently strong so that $\sigma_{IHP} > \sigma_0$, adsorption is said to be superequivalent (case III, Fig. 3). In this case an adsorbent may adsorb a like-charged adsorbate.

It is now possible to define the cation-exchange capacity (CEC) of a negatively charged particle as the excess of counterions in the EDL which can be exchanged for other cations in the bulk of the solution (i.e., the area under the curve in Figure 3 marked σ_+). Cation-exchange capacities are usually reported in units of milliequivalents (meq) of an index cation adsorbed per unit mass of porous medium. Table 4 shows typical exchange capacities for various kinds of inorganic and organic materials. For the clay minerals, the larger exchange capacities are exhibited by such three-layer minerals as vermiculite and montmorillonite, which are capable of swelling in solutions of polar molecules (e.g., water). Hydrous metal oxides, such as those of iron and manganese, may form as coatings on sediments in oxidizing environments and can play a major role in the sorption of heavy metal ions from waters in contact with such sediments (Jenne, 1968 and 1977). The extremely high exchange capacities of humic acid, an organic colloid, are due primarily to its high content of ionizable functional groups, e.g., -COOH.

Table 4. Cation-Exchange Capacities of Various Aquifer Materials

Colloid	CEC (meq/g)	Source
Kaolinite	0.03–0.05	Carroll (1959)
Montmorillonite	0.70–1.0	Carroll (1959)
Illite	0.1–0.4	Carroll (1959)
Vermiculite	1.0–1.5	Carroll (1959)
Chlorite	0.1–0.4	Carroll (1959)
Humic acid		Marshall (1964)
(a) Chernozem	4.3	
(b) Podzol	4.1	

Since such ion exchangers only comprise a part of the bulk weight of rocks and sediments, the cation-exchange capacities of these materials are lower than the exchange capacities of the materials shown in Table 4. For example, the exchange capacities of the surficial tills and glaciolacustrine clays in Ontario are generally of the order of 0.1–0.3 meq/g (Grisak and Jackson, 1978).

So far it has been assumed that all ions of equal valence have an equal probability of being adsorbed by a colloid; yet this is not the case. There is a well-defined selectivity or affinity series which is discussed in terms of clay minerals by Stumm and Morgan (1970, pp. 492–493). If cation-exchange equilibria are dominated by electrical dipole interactions between the counterions and water molecules and are unaffected by specific ion affinities of certain types of ion-exchange sites (e.g., interlayer mica sites for cesium), then the affinity series for the alkali and alkaline earth metals can be written:

$$Cs^+ > K^+ > Na^+ > Li^+$$

and

$$Ba^{2+} > Sr^{2+} > Ca^{2+} > Mg^{2+} > Be^{2+}$$

that is, Cs has a greater affinity for being sorbed than K^+ which, in turn, has a greater affinity than either Na^+ or Li^+. Electrical double layer theory "predicts correctly that the affinity of the exchanger for bivalent ions is much larger than that for monovalent ions, and that the selectivity for higher-valent ions decreases with increasing ionic strength of the solution" (Stumm and Morgan, 1970, p. 488). An inspection of the periodic table of elements will show that affinity for adsorption increases with ionic radius in elements of both Groups I and II. It should be noted that pure electrostatic adsorption is "relatively non-selective" (Parks, 1975, p. 247).

Geochemical measures of the mobility or adsorption of contaminants are useful parameters in predicting the migration of contaminants in groundwater flow systems. One such geochemical measure is the distribution coefficient (K_d) which has been used in radioactive waste management studies to describe the partitioning of a radioactive contaminant between solid (rock or sediment) and aqueous solution (groundwater) phases. As such, it offers the hydrogeologist a parameter with which to measure either the relative affinity of the aquifer matrix for a particular contaminant

or the mobility of the contaminant in the aquifer or groundwater flow system.

The distribution coefficient, K_d, has been defined as "the number of milliequivalents of an ion adsorbed per gram of exchanger divided by the number of milliequivalents of that ion per millilitre remaining in solution at equilibrium" (Amphlett, 1964). In the hydrogeological context, the exchanger is the grains of the aquifer and the solution is the groundwater. It should be noted that reactions other than adsorption may affect the K_d. It may be derived as follows.

For the simple chemical equilibrium representing an ion exchange process (Amphlett, 1964):

$$A^+ + B^+R^- \rightleftarrows A^+R^- + B^+ \tag{51}$$

where A^+ and B^+ are the competing cations for R^-, the cation exchanger (e.g., aquifer material such as a clay particle), a selectivity coefficient may be written:

$$K_{AB} = \frac{\{AR\}\{B^+\}}{\{A^+\}\{BR\}} \tag{52}$$

that is, K_{AB} is a mass-action equilibrium constant, $\{A^+\}$ and $\{B^+\}$ are the activities of the counterions in solution, and $\{AR\}$ and $\{BR\}$ are the activities of the adsorbed phases. Rearranging terms,

$$\frac{\{B^+\}}{\{A^+\}} = K_{AB}\frac{\{BR\}}{\{AR\}} \tag{53}$$

If the exchanger is considered to be a binary solid solution with components AR and BR as pure end members, then (Garrels and Christ, 1965, p. 28)

$$\{BR\} = \lambda_{BR}\, N_{BR} \text{ and } \{AR\} = \lambda_{AR}\, N_{AR} \tag{54}$$

where λ_{BR} and λ_{AR} are the rational activity coefficients, and N_{BR} and N_{AR} are the mole fractions, i.e.,

$$N_{BR} = \frac{(BR)}{(BR) + (AR)} \tag{55}$$

Substituting Equation 54 into Equation 53,

$$\frac{\{B^+\}}{\{A^+\}} = K_{AB}\frac{\lambda_{BR}\, N_{BR}}{\lambda_{AR}\, N_{AR}} \tag{56}$$

If the exchanger forms a regular solution it can be shown that (Garrels and Christ, 1965, p. 273-274):

$$\frac{\{B^+\}}{\{A^+\}} = K_{AB}\left(\frac{N_{BR}}{N_{AR}}\right)^{1-(B/2RT)} \tag{57}$$

where B is a constant, independent of composition.

Garrels and Christ (1965, p. 274) point out that expression (57) is strictly valid only when $N_{BR} \sim N_{AR}$. For the case in which A^+ is present in trace quantities relative to B^+, this condition is clearly not satisfied. Other problems occur in natural water-sediment systems which result in the measured adsorption parameters such as K_d being of little or no thermodynamic value. In cases involving the specific adsorption of ions, the reactions may be slow and therefore chemical equilibrium is not necessarily attained (Parks, 1975). Similarly, if the adsorption reaction rate is slow and the interstitial water velocity is fast, then reaction kinetics control the adsorption process and local chemical equilibrium cannot be assumed (James and Rubin, 1979). Furthermore, secondary reactions, such as precipitation, isomorphous substitution of the radionuclide or its fixation due to lattice collapse, may prevent the attainment of true equilibrium (Jenne and Wahlberg, 1968).

In practice, therefore, experimentally determined selectivity quotients involving concentrations rather than activities are used (e.g., Amphlett, 1964, p. 2; Jenne and Wahlberg, 1968):

$$K_B^A = \frac{(A^+R^-)(B^+)}{(A^+)(B^+R^-)} = \frac{(A^+R^-)/(A^+)}{(B^+R^-)/(B^+)} \tag{58}$$

where (A^+) and (B^+) are the concentrations of these ions in solution and (A^+R^-) and (B^+R^-) are their concentrations in the adsorbed phase.

The selectivity quotient can be related to the distribution coefficient if the cation-exchange capacity, Q, of the exchanger, R^-, and the total competing cation concentration in solution, C, are known (Amphlett, 1964). By definition:

$$(A^+) + (B^+) = C \tag{59}$$

$$(A^+R^-) + (B^+R^-) = Q \tag{60}$$

When the system under consideration (Equation 51) is at equilibrium, then by definition

$$K_d^A = (A^+R^-)/(A^+) \tag{61}$$

and the selectivity quotient may be rewritten, using Equations 59 and 60, as

$$K_B^A = K_d^A \frac{[C - (A^+)]}{[Q - (A^+R^-)]} \quad (62)$$

For the case in which the contaminant, A^+, is present in amounts much less than B^+, $(A^+) \ll C$ and $(A^+R^-) \ll Q$, the distribution coefficient may be rewritten as

$$K_d^A \sim \frac{K_B^A Q}{C} \quad (63)$$

Therefore the distribution coefficient is directly proportional to the cation-exchange capacity and the selectivity quotient, and inversely proportional to the total competing cation concentration. For this case in which (A^+) and (A^+R^-) are assumed to be very small, $(B^+) \simeq C$ and therefore K_d^A is proportional to $(B^+)^{-1}$.

For the more general case of the trace ion A^{n+}:

$$A^{n+} + nB^+R^- = A^{n+}R_n^- + nB^+ \quad (64)$$

$$K_d^A \sim \frac{K_B^A Q^n}{C^n} \quad (65)$$

Therefore, if the law of mass action is obeyed, a plot of log K_d^A versus log (B^+) will be a straight line of slope -n, the charge of the exchanging ion (Amphlett, 1964).

If it is assumed, following the work of Gillham *et al.* (1978), that the principal competing cations for ^{90}Sr and ^{137}Cs are their respective stable ions, then assuming no selectivity between stable and radioactive ions, $K_B^A = 1.0$ and the distribution coefficient for each of these radionuclides is a linear function of cation-exchange capacity and stable-ion concentration as in Equation 63. Therefore K_d is sensitive to variations in the abundance of highly adsorbent minerals and organics (Table 4) and to factors controlling the abundance of dissolved stable Sr^{2+} and Cs^+.

Since Q is usually expressed in milliequivalents of cations per gram of exchanger and C in terms of milliequivalents per millilitre, the units of the distribution coefficient are milligrams per gram. Those working in the field of radioactive waste management have tended to measure K_d by radiochemical analysis such that the distribution coefficient is determined as the ratio:

$$K_d = \frac{\text{dps/g}}{\text{dps/mL}} \quad (66)$$

where dps stands for disintegrations per second.

The distribution coefficient affects the mobility of a contaminant in an aquifer system. By the retardation Equation 16:

$$V_A = \frac{V_{GW}}{1 + \frac{\rho_b}{\theta} K_d^A} \quad (67)$$

where $Qf'/C = K_d^A$ for $f' = 1$ (i.e., no selectivity). This expression is known as the retardation equation, since nonzero values of K_d dictate that $V_A < V_{GW}$, and hence the contaminant ion is retarded in its flow through the aquifer. If V_A, V_{GW}, ρ_b and θ are known for a particular aquifer system contaminated by ionic species A^+, then K_d may be determined. This method of solution is known as field mapping, since V_A can then obviously be determined from field mapping contaminant migration over time.

Microbial Reactions

Bacteria are unicellular microbes with rigid cell walls and a variety of shapes (e.g., rods, spheres, etc.). They vary in size between 0.5 μm and 10 μm, roughly the size of small silt and large clay particles. The microbes that cause the decomposition of organic wastes are called heterotrophic bacteria ("feeding on others"), since they require complex organic molecules, such as carbohydrates, as nutrition. Consequently they use C, H, O, P, N and S plus much smaller amounts of the major inorganic cations present in groundwater to build protoplasm.

For bacteria to function and proliferate it is not only necessary that a favourable nutritional environment exist but also suitable temperature and pH conditions must occur. While most bacteria exhibit optimum growth rates at 30°C to 40°C, a large class, the psychrophiles, grow well at near zero temperatures. Furthermore, families of bacteria have adapted themselves to pH environments outside the optimum range of 6.5 to 7.5.

Hutchinson (1974) has indicated that biochemical processes initiated by bacteria may have either beneficial or detrimental consequences on particular pollutants, depending on the type of organism present and the environment within which it exists. The beneficial effects include:

(1) The purification of contaminated water by which organic pollutants are broken down to relatively innocuous products such as CO_2, H_2O, NO_3^- and SO_4^{2-} in aerobic environments.

(2) The cycling of N, S, C and P, which are essential in cell synthesis and which therefore may be removed from the groundwater.

Among the detrimental consequences of pronounced microbial activity listed by Hutchinson (1974) are the aftereffects of the utilization of all existing free oxygen. Thereafter bound oxygen in the form of NO_3^- and SO_4^{2-} is necessarily used as an electron sink (oxidizing agent) and reduced species are produced such as CH_4, H_2, NH_3 and H_2S. Furthermore, in such anaerobic environments various heavy metals may become relatively more soluble (e.g., Fe^{2+}, Mn^{2+}).

These beneficial and detrimental consequences are directly related to the redox processes discussed earlier in this Chapter (Tables 2 and 3). In aerobic environments the innocuous products are a result of the redox processes occurring in an open system—open that is to dissolved oxygen (DO). Should all the available DO be reduced before all the dissolved organic carbon (DOC) contaminating a groundwater is oxidized, then the sequence of redox processes of a closed system would occur. Langmuir (1972) has stated that approximately 4 mg/L DOC is sufficient to produce an anaerobic environment in groundwater contaminated by sanitary landfill leachate. The redox reactions shown in Tables 2 and 3 should occur spontaneously; in the absence of catalysts, however, the reactions may be very slow. The role of the bacteria is to catalyze these reactions so that the reactions proceed more quickly.

GEOCHEMICAL FACTORS AFFECTING THE MOBILITY OF ^{90}Sr AND ^{137}Cs IN GROUNDWATER

^{90}Sr

The retardation of radiostrontium (see Table 5 for general chemical data) relative to the mean groundwater velocity may be due to either precipitation or adsorption processes. Irrespective of the mechanism, however, it is the rule that ^{90}Sr is retarded in its transport through aquifers. Table 6 summarizes the mobility of this isotope in terms of the relative ionic velocity, V_A/V_{GW}, which may be defined by rearranging the terms in Equation 67:

$$V_A/V_{GW} = \frac{1}{1 + \frac{\rho_b}{n} K_d^A} \qquad (68)$$

Wahlberg and his colleagues studied the exchange adsorption of strontium in pure clay mineral–aqueous systems and concluded that mass-action equilibria reactions adequately described the uptake of strontium onto the clays (Wahlberg and Dewar, 1965; Wahlberg *et al.*, 1965). Values of the selectivity quotients are shown in Table 7. They further concluded that "if the concentration of stable plus radioactive strontium is below 10^{-4} *N* (4.4 mg/L), the presence of stable strontium will have no effect on the adsorption of the radioactive strontium by sediments" and that the K_d value for Sr exchange is constant (Wahlberg

Table 5. General Chemical Data for ^{90}Sr and ^{137}Cs

Radionuclide	Predominant form in aqueous solution	Half-life* (yr)	Ionic radii (Å)†	
			Crystal	Hydrated
^{90}Sr	Sr^{2+}	28.5	1.13	4.12
^{137}Cs	Cs^+	30.1	1.69	3.29

*Seelmann-Eggebert *et al.* (1974).
†Nightingale (1959).

Table 6. Relative Ionic Velocities of ^{90}Sr in Porous Media

Relative ionic velocity	Porous medium	Cation-exchange capacity (meq/g)	Source
0.011	Sand and gravel	0.077	Ewing (1959)
0.03	Fluvial sands	0.01	Parsons (1961) and Jackson *et al.* (1977)
0.004	Sandstone	0.025	Tamura (1972)
0.35	Sands and gravels	?	Baetslé (1969)

et al., 1965, p. C9). Yet Gillham *et al.* (1978) have shown "measured K_d values to be related to the concentration of naturally-occurring stable cesium and strontium."

Table 7. Selectivity Quotients for the Reactions $MR_2 + Sr^{2+} \rightleftarrows Sr\ R_2 + M^{2+}$ or $2MR + Sr^{2+} \rightleftarrows Sr\ R_2 + 2M^+$ [using tracer-level strontium in the presence of a single competing cation (M^+ or M^{2+})]

Cation-saturated clay	K_M^{Sr}
Na^+-montmorillonite	1.1
Ca^{2+}-montmorillonite	1.1
Na^+-illite	3.0
Ca^{2+}-illite	1.1
Na^+-kaolinite	9.0
Ca^{2+}-kaolinite	1.2

Source: Wahlberg *et al.* (1965).

Tamura (1972), however, takes a pessimistic view of predicting the migration of radioisotopes in groundwater flow systems solely from the results of laboratory studies of pure clay systems such as that of Wahlberg and his associates:

> However, because most natural formations contain hydrous iron and aluminum oxides, whose properties are not well characterized, it is not yet possible to predict reliably the K_d of strontium even for formations whose clay mineralogy is known.

Tamura (1964) showed that deviations between the observed K_d and that calculated from mass-action equilibria expressions for strontium adsorption on an illitic shale were due to increased strontium adsorption by hydrous iron oxide particles on the shale. Furthermore, "tests with iron oxide which was coated on quartz sand particles show that strontium sorption was increased by three to four times over the pure sand" (Tamura, 1964). Kinniburgh *et al.* (1975) showed that ^{90}Sr was specifically adsorbed to amorphous hydrous iron oxides (pH_{pzc} = 8.1) from solutions containing 250 000 times more Na than Sr; approximately 10% of ^{90}Sr was adsorbed at pH = 6.2 and 50%, at pH = 7.1. Egorov and Lyubimov (1969) showed that MnO_2 sorbed Sr^{2+} and released H^+, K^+ and Mn^{2+} to solution; yet the work of Murray *et al.* (1968) implies that Sr adsorption on MnO_2 is not specific.

Table 8 shows the distribution coefficients given by Tamura (1972) for various minerals relative to radiostrontium in natural waters at pH = 7.5 and pH = 10.0. The increase in K_d with pH is probably due to the increased number of negatively charged potential-determining ions (i.e., OH^-) that are adsorbed at the increased pH level. This necessitates the sorption of an increased number of positive counterions (e.g., Sr^{2+}) to maintain the electrical neutrality of the double layer.

Table 8. Distribution Coefficients of Selected Minerals for ^{90}Sr at pH 7.5 and 10

Material	Size or area*	K_d (mL/g)†	
		pH = 7.5	pH = 10
Montmorillonite	<2 μm	506	–
Illite	<2 μm	117	760
Kaolinite	<2 μm	55	257
Alumina	230 m^2/g	2100	34 000
Muscovite	<50 μm	82	–
Biotite	<50 μm	48	–
Quartz	<50 μm	0	–

*Size in micrometre diameter, area in square metres per gram.
†Aqueous solution: 7.5×10^{-4} *M* $Ca(HCO_3)_2$, 4.1×10^{-4} *M* $Mg(HCO_3)_2$ and <1 mg/L Na^+.

Note: Initial form of exchange sites not stated.
Source: Tamura (1972).

Two ions that satisfy the rules governing replacement and coprecipitation are Sr^{2+} and Ca^{2+}. They are of similar ionic radius—1.13 Å for Sr^{2+} and 0.99 Å for Ca^{2+}—and their electronegativity differences vis-à-vis a carbon atom, as in $CaCO_3$ or $SrCO_3$, are identical. Consequently, it is not surprising to find that the replacement of ^{90}Sr for Ca in $CaCO_3$ is an effective method of radiostrontium retardation. Halevy and Tzur (1964) noticed that considerably more radiostrontium was being adsorbed by a soil column than the cation-exchange capacity of the calcareous soil would predict. They concluded that the Sr solution passing through the column was dissolving $CaCO_3$ and precipitating $SrCO_3$. Jenne and Wahlberg (1968) concluded that ^{90}Sr in a Tennessee stream was being retarded by the isomorphous substitution of ^{90}Sr for Ca in *in situ* precipitated $CaCO_3$. Routson (1973) reported that phosphate-rich wastes disposed of in the calcareous glaciofluvial sediments at Hanford, Washington, caused the replacement of calcite with apatite in the alkaline pH range. Then ^{90}Sr replaced Ca in the apatite by isomorphous substitution. It is this same reaction, the entry of ^{90}Sr into apatite, by which radiostrontium is incorporated into human bone.

^{137}Cs

It is generally accepted (Tamura, 1972; Routson, 1973) that the mobility of trace concentrations of radiocesium (see Table 5 for general chemical data) in aquifer systems is controlled by the presence or absence of micaceous minerals such as illite, muscovite and biotite. This selective sorption of cesium by micaceous minerals is such that it is often referred to as "fixation" (i.e., irreversible adsorption), whereas, as Routson (1973) has pointed out, it is probable that the adsorption rate is simply much faster than the desorption rate. An early interpretation of this reaction was that microconcentrations of radiocesium were fixed to the micas by their precipitation on the mica surface (Schulz *et al.*, 1960). This conceptual model is now in disfavour, since it is unlikely that the saturation of cesium salts occurs in most shallow groundwater flow systems and a better conceptual model is now available.

This improved paradigm was developed by Tamura and Jacobs at Oak Ridge (Tamura, 1972). They showed that the highly selective response of illite for ^{137}Cs was due to the 10-Å c-axis spacing of the mica unit cell. To demonstrate the importance of this spacing they saturated a hydrobiotite (i.e., an interlayered biotite vermiculite) with potassium, therefore reducing its c-axis spacing from 12.5 Å to 10 Å, and then observed increased radiocesium adsorption despite having reduced the cation-exchange capacity from 0.7 to 0.1 meq/g (Tamura, 1964). They concluded that the selectivity for ^{137}Cs was due to the limited access of other ions into the interlayer positions near the edges of the illite crystallites. Francis and Brinkley (1976), who demonstrated the preferential adsorption of ^{137}Cs by micaceous minerals under environmental conditions for the first time, report that the fixation is due to "the trapping of Cs ions in either the interlayer regions of vermiculite, a partially expanded mineral, or at the frayed edges of illites and micas."

In Table 9, values of K_d are listed for vermiculite, illite and kaolinite in distilled water and in 0.1 *N* NaCl.

Table 9. Distribution Coefficients for ^{137}Cs and Selected Clay Minerals

Clay mineral (<2-μm fraction)	Cation-exchange capacity (meq/g)	K_d (mL/g)	
		Distilled water	0.1 *N* NaCl
Vermiculite	1.27	52 000	2 700
Illite	0.20	26 000	28 600
Kaolinite	0.11	2 500	94

Note: Initial form of exchange sites not stated.
Source: Tamura (1972).

The competition between Na^+ and Cs^+ for ion-exchange sites is particularly obvious for vermiculite and kaolinite; the decrease in adsorption in 0.1 *N* NaCl is explainable by referring to Equation 63. Tamura (1972, p. 321) noted that the relatively constant K_d for illite can only be explained by the "molecular sieve" mechanism of the illite crystallites. Wahlberg and Fishman (1962) noted that K^+ (3.31 Å) was more effective than Na^+ in competing with Cs^+ for exchange sites on illite, presumably due to the similarity in the sizes of the hydrated ionic radii of K^+ and Cs^+. The recent work of Gillham *et al.* (1978), however, suggests that stable Cs is the chief competitor with radiocesium for such exchange sites.

Amphlett (1964, p. 87) noted that cesium adsorption on hydrous $MnO(OH_2)$ obeys the normal affinity series

$$Cs^+ > NH_4^+ > K^+ > Na^+ > Li^+$$

and that "saturation was reached at 10^{-2} mg Cs/mg $MnO(OH)_2$, corresponding to a capacity of 0.73 meq/g." Jenne and Wahlberg (1968) and Evans and Dekker (1966), however, suggested that hydrous metal oxide coatings inhibit ^{137}Cs adsorption.

The Lower Perch Lake Basin

The location of the study area is the Chalk River Nuclear Laboratories, 200 km northwest of Ottawa, Ontario (Fig. 4). A variety of hydrological and geochemical research studies are being undertaken in the Perch Lake basin (Fig. 5) under the auspices of Atomic Energy of Canada Limited.

PHYSIOGRAPHY AND CLIMATE

The lower Perch Lake basin (Fig. 6) at Chalk River is the southern part of a watershed, the sides of which are formed by bedrock ridges that rise approximately 30 m above the swampland which forms the flood plain of the mainstream draining the upper basin. The ridges are covered with aspen, birch, maple, jack pine, and oak. The low-lying bogs are populated predominantly by ash, alder, balsam and spruce. The climate of the Chalk River area is that of a cold snow forest (Köppen's classification) with a warm summer and no distinct dry season. The mean air temperature ranges from a January low of -12°C to a July high of +19°C. Annual precipitation is of the order of 840 mm, of which approximately 60% is lost by evapotranspiration (Barry, 1975, p. 102).

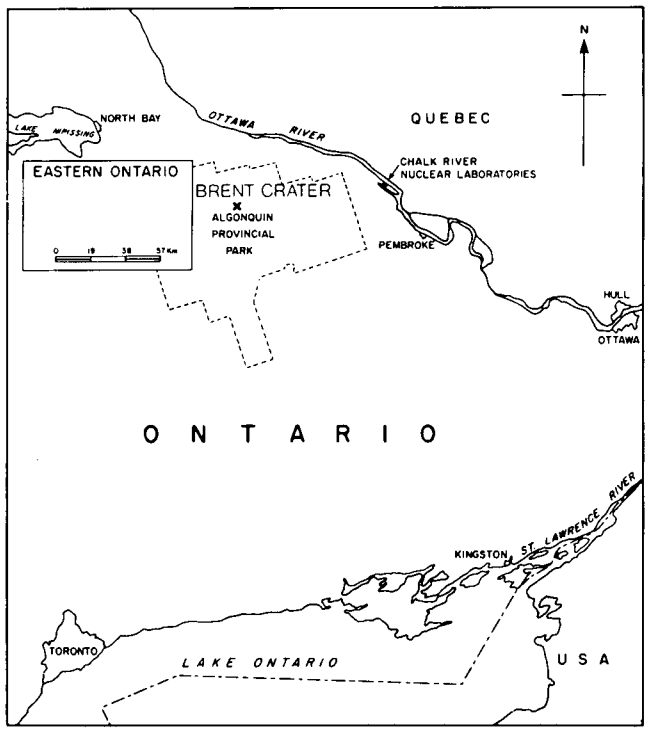

Figure 4. Location of Chalk River Nuclear Laboratories.

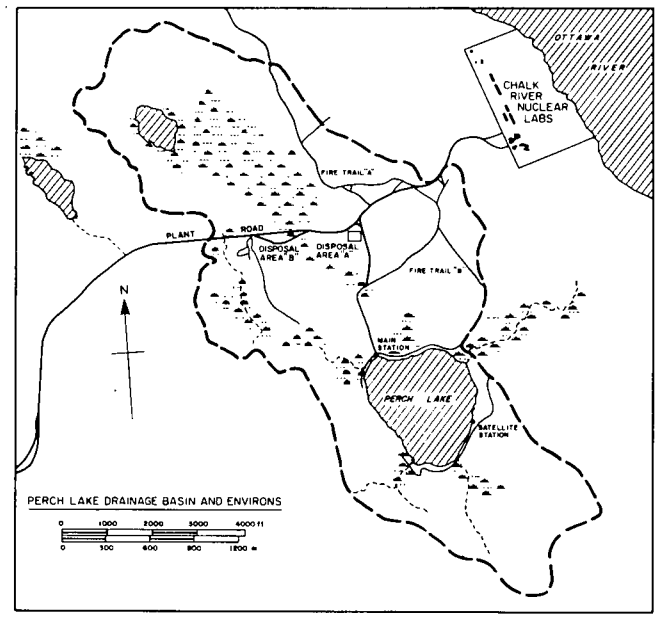

Figure 5. Perch Lake basin and Chalk River Nuclear Laboratories.

BEDROCK GEOLOGY

The bedrock in the basin is mainly pink and grey granitic gneiss of the Grenville Province (Precambrian) of the Canadian Shield (Gadd, 1962). The gneiss is predominantly granitic with abundant biotite and garnet. Gadd (1958, 1959, 1962) observed that the bedrock was much faulted and fractured. These faults trend northwest and are probably connected by cross fractures. Diamond-drill cores taken during the installation of piezometer nest KNEW (Fig. 6) revealed considerable horizontal and vertical fracturing, although sections as long as 0.3 m were

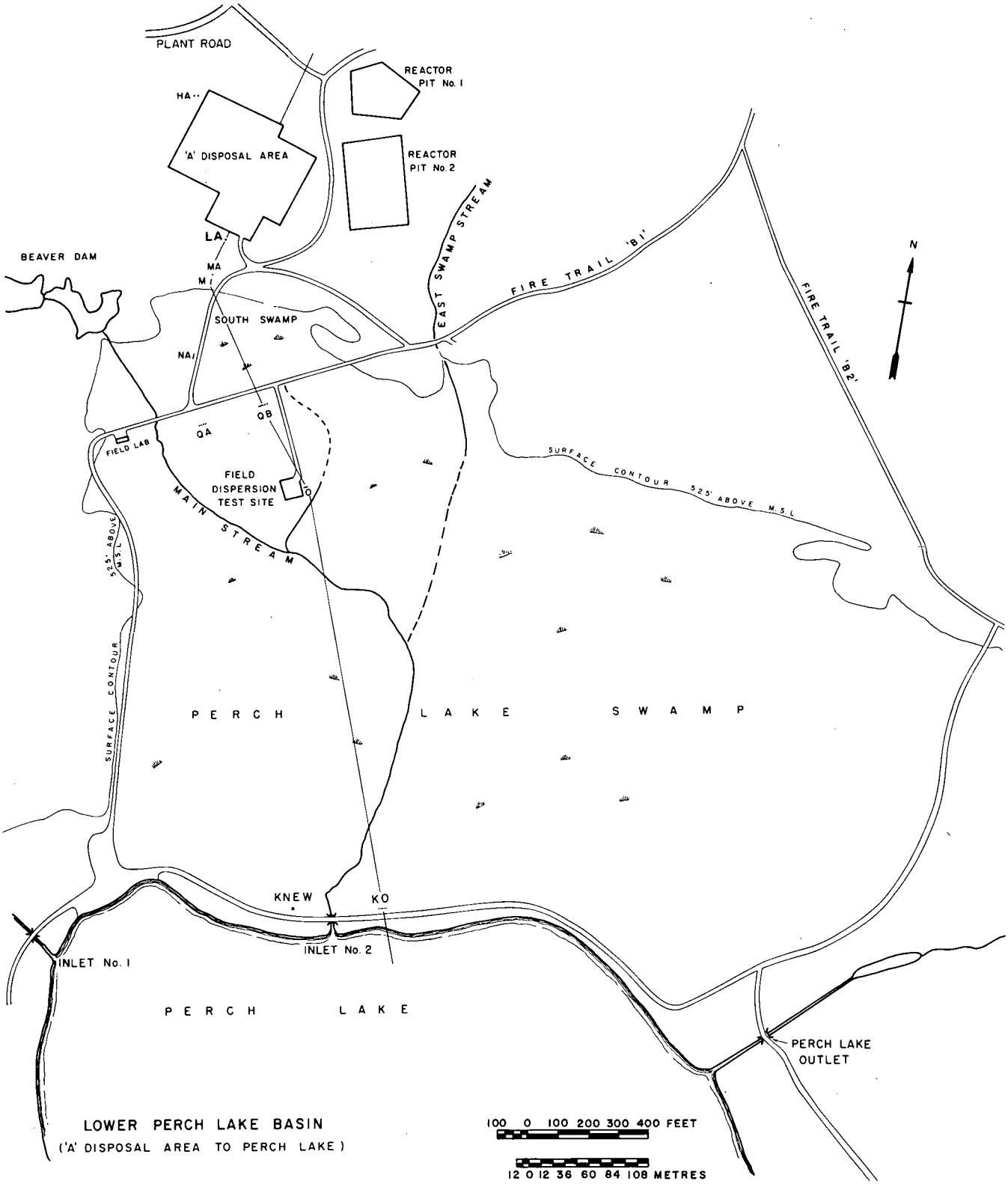

Figure 6. Lower Perch Lake basin with piezometer nests and cross-sectional profile indicated.

unfractured. The cored material was granitic gneiss with carbonate veins and some pyrite and hematite. The upper sections of the core showed signs of significant chemical weathering, and carbonate and chlorite were observed in the fractures.

There is no local evidence of the Paleozoic sedimentary rocks that have been observed in the Brent crater (Lozej and Beales, 1975) and south of Pembroke (Fig. 4).

QUATERNARY GEOLOGY

Between the Precambrian and the Pleistocene, erosion removed most if not all sediment deposited during this time interval and, at the same time, carved deep valleys into the bedrock along northwesterly directions. During the Pleistocene these valleys provided pathways for the glaciers which were generally moving southeastwards. Valleys oriented parallel to this regional movement, such as the Ottawa Valley, received thick deposits of till which were laid down over the Precambrian bedrock between about 12 000 and 60 000 years B.P. (Gadd, personal communication). The till is generally sandy "like a fine gravel with some admixed silt" (Gadd, 1958).

Catto (1978) has correlated this basal till with the Guildwood (Ontario) and Gentilly (Quebec) tills. Later it was submerged by the Champlain Sea, whose intrusion is recorded by a sequence of marine clays and sands at 140 m above the present sea level. Deposited above these marine sediments are a loess and a second till, which Catto has correlated with the Saint-Narcisse readvance in Quebec (11 000 years B.P.) and which was associated with an ice sheet moving in a southwesterly direction. Subsequently large volumes of fluvial sands were deposited in the Chalk River area by the Ottawa River, which was draining the upper Great Lakes through North Bay and northern Quebec. Some of this sand has been reworked into aeolian deposits. These fluvial and aeolian sediments are composed predominantly of fine-grained sands, which today form a groundwater flow system in the lower Perch Lake basin, and in which are dispersed thin beds of silts and clays (Fig. 7).

Parsons (1960) classified these fluvial and aeolian sediments into four hydrostratigraphic units:

(1) the Upper Sands layer of up to 12 m thick;
(2) a middle layer of interlayered silts and clays of up to 1 m thick;
(3) the Lower Sands layer of up to 10 m thick; and
(4) a basal deposit of silts and clays of up to 10 m thick.

These sediments are shown in Figure 7 along with recent revisions of the stratigraphy based on drilling, seismic and mathematical modelling studies (Cherry *et al.*, 1975b; J.F. Pickens, personal communication). The most significant of these revisions is the separation of the Upper Sands unit into three units—the shallow Upper Sands unit of approximately 2 m thickness and the Middle Sands unit of approximately 10 m thickness, which are separated by the Upper Silt and Clay unit. Grain size curves for some of these units are shown in Figure 8.

SEDIMENTARY MINERALOGY

Mineralogical examinations of the sand fraction (Wentworth classification) of the Middle Sands, Middle Silt and Clay, and Lower Sands units have been conducted. Figure 9 shows that approximately 70% of all grains are either quartz or plagioclase. Measurement of extinction angles suggests that the plagioclase falls in the Ab_{90} to Ab_{50} range (oligoclase to andesine). Minor amounts (i.e., <20%) of sericite, mica, chlorite, K-feldspar and hornblende are also present.

The silt and clay fractions of these units have been analyzed by X-ray diffractometry. Figure 10 shows the diffractograms of untreated, glycolated and heat-treated samples of the clay fraction from the Middle Silt and Clay unit at O piezometer nest. A semiquantitative analysis of the peak height ratios suggests the following quantities of minerals: 35% mica-vermiculite, 25% chlorite, 15% hornblende, 15% quartz and 10% plagioclase. The vermiculite is indicated by the inflation of the (001) mica peak upon heating. X-Ray analyses of the silt and clay fraction (i.e., <75 μm) dispersed within the Middle and Lower Sands (at O piezometer nest) suggest that plagioclase and quartz are the predominant minerals present and that minor amounts of amphibole, K-feldspar, mica, and interstratified mica-vermiculite are also present (N. Miles, Soil Research Institute, Ottawa, personal communication).

The extent of *in situ* weathering of the sediments is of considerable importance. Significant amounts of sericite, a secondary fine-grained muscovite derived from feldspar, have been observed which are probably of detrital origin. No unequivocal observations of kaolinite have been made either by optical microscopy or by X-ray diffractometry. As the sharpness of the diffraction peaks in Figure 10 and the presence of hornblende suggest, little geochemical weathering seems to have occurred.

The presence of calcite in the sediments of the lower Perch Lake basin has been indicated by electron microscopy

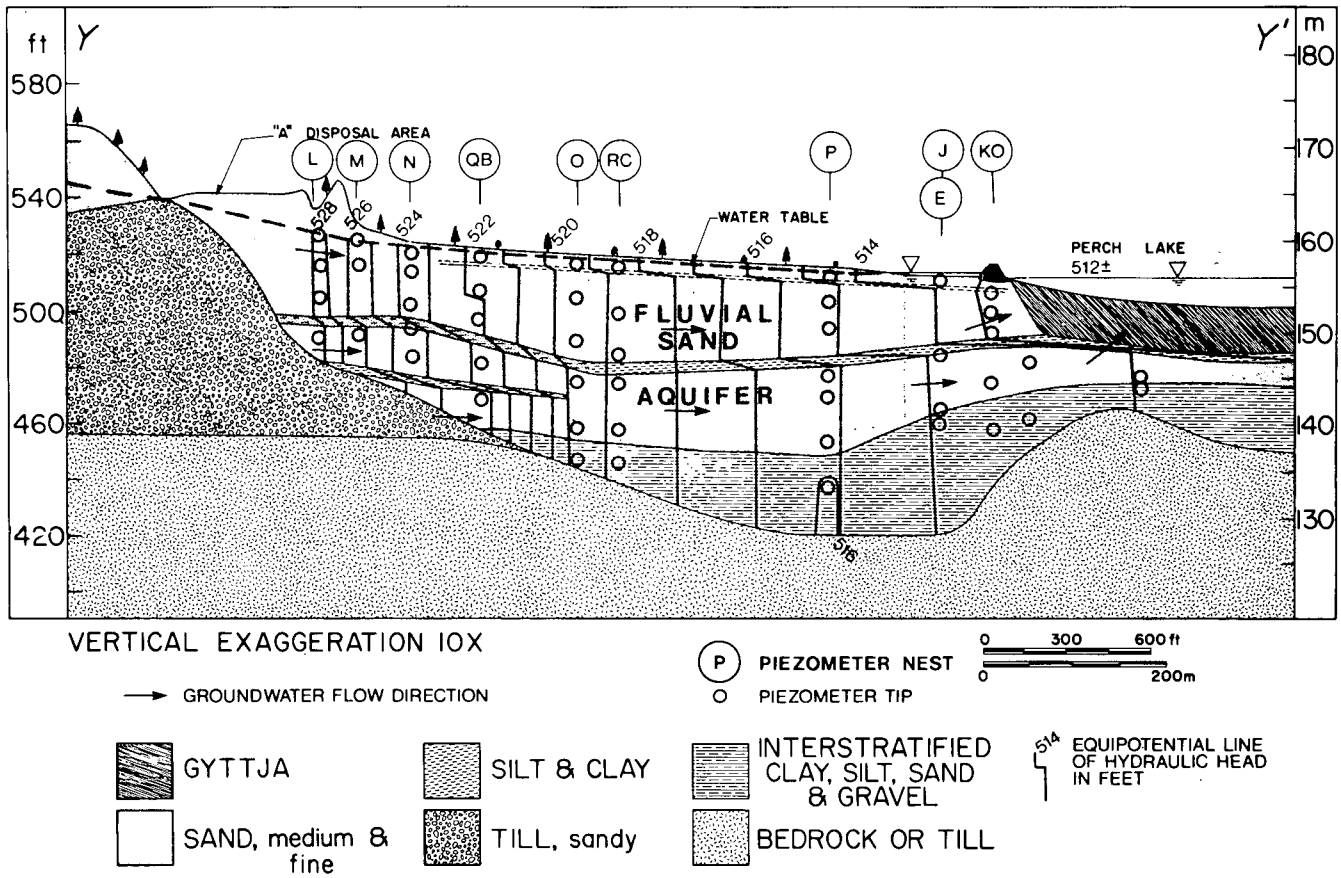

Figure 7. Equipotential lines of hydraulic head, lower Perch Lake basin. Hydraulic head measurements averaged over period 1973–75 (from Cherry *et al.*, 1975b).

Figure 8. Grain size distribution curves.

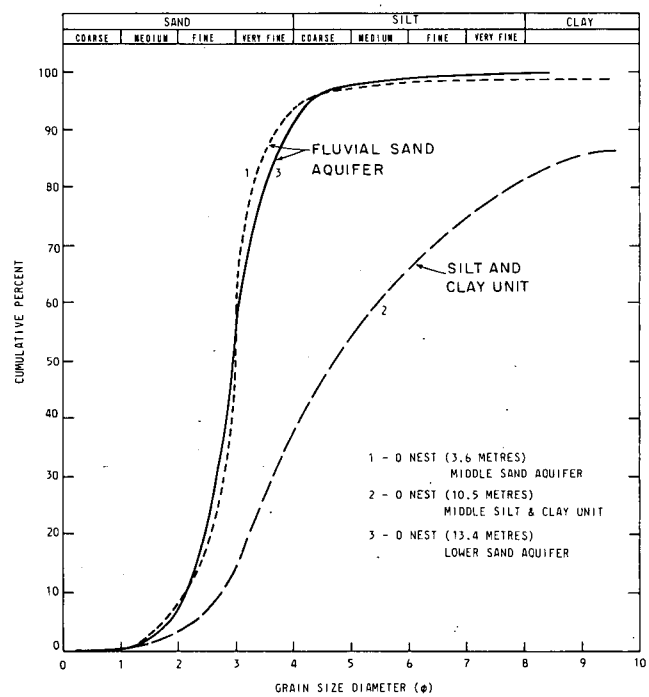

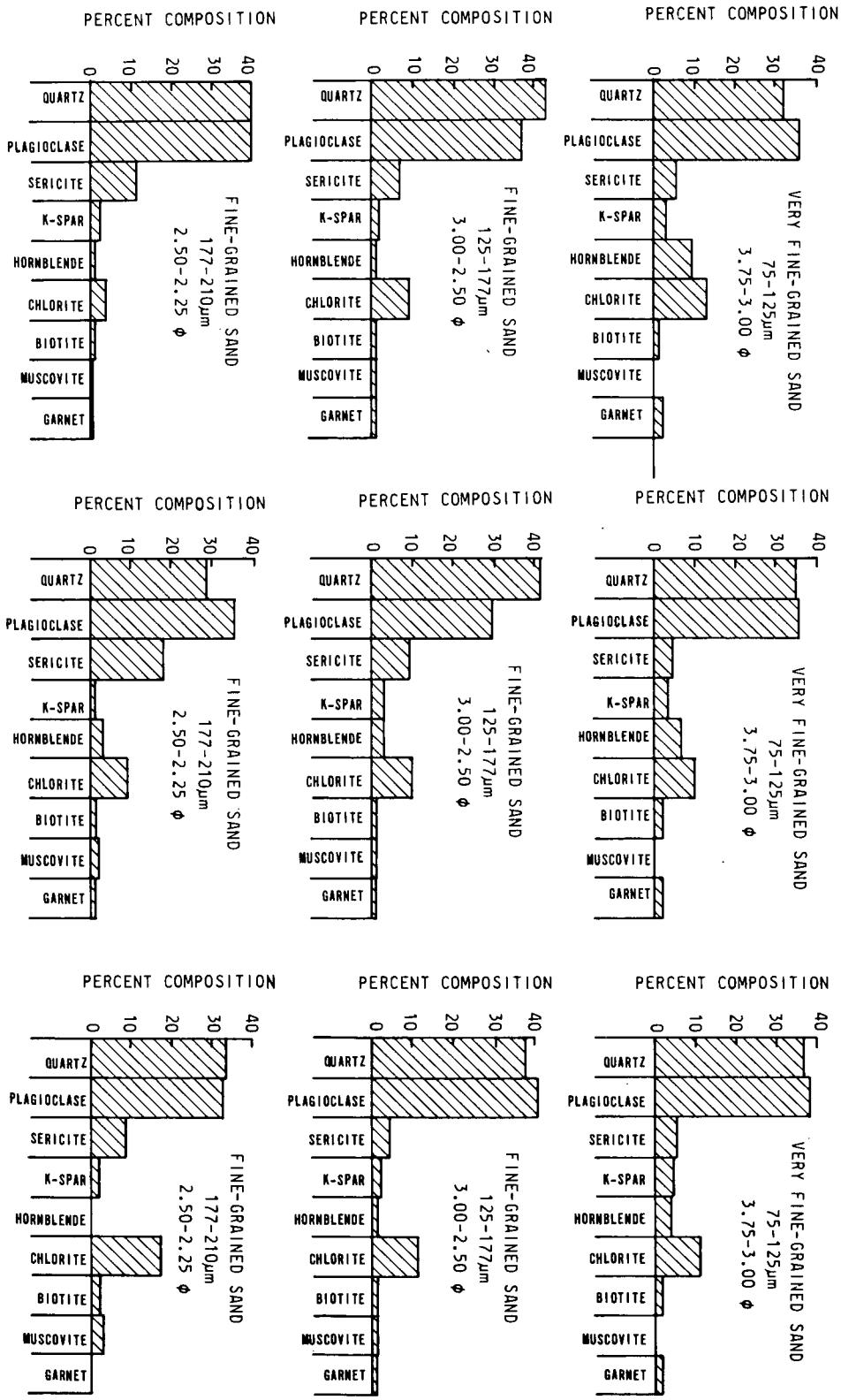

Figure 9. Histograms of major mineral phases as identified by optical microscopy.

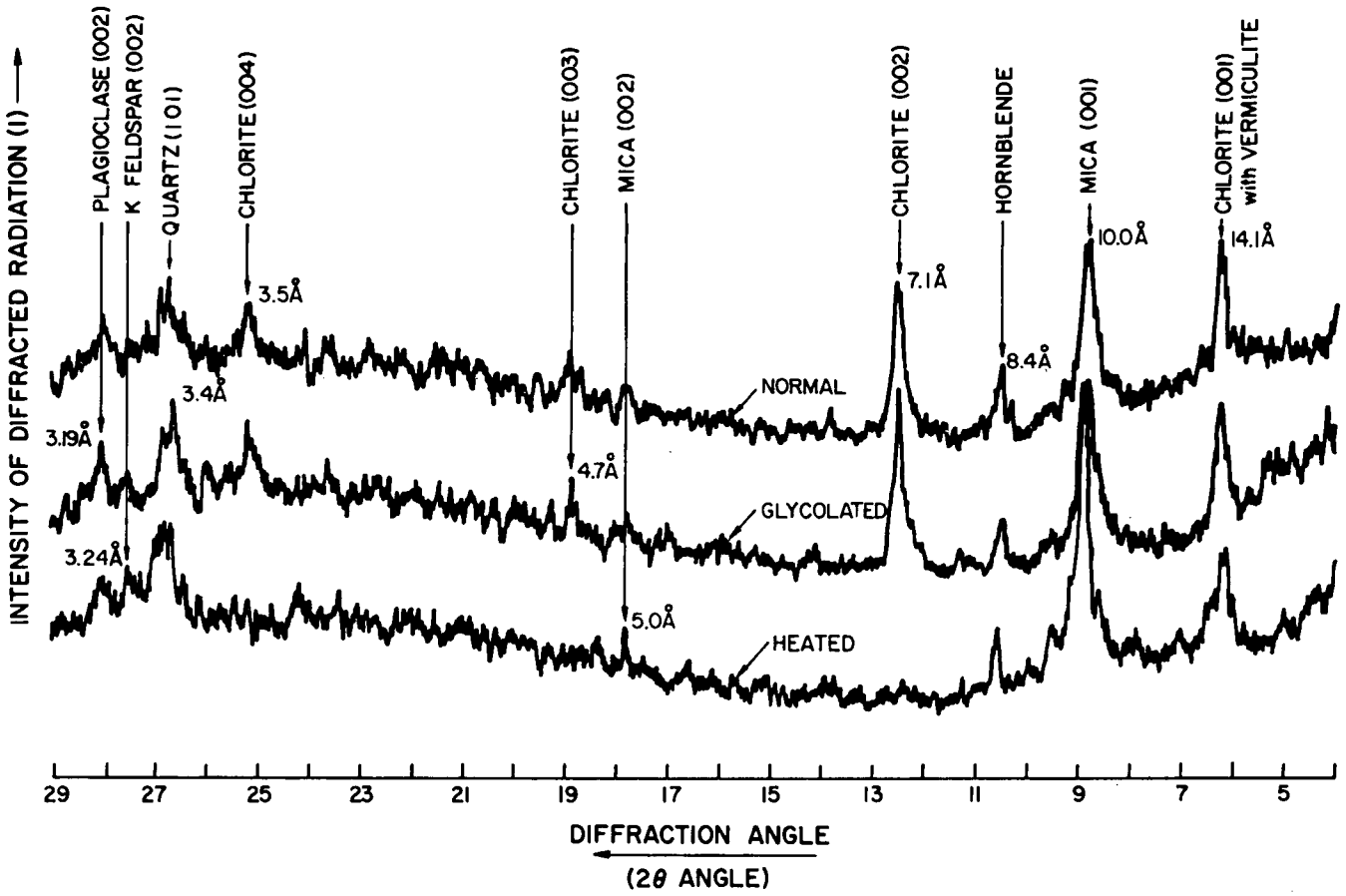

Figure 10. X-Ray diffractograms of the clay-sized fraction from O nest.

and differential thermal analysis (Buchanan, 1958) and by gasometric (Chittick) measurements (3% to 5%) of KNEW sediments (Jackson and Cherry, 1974, Fig. 4b). The amount of calcite present in most parts of the groundwater flow system, however, is evidently not enough to cause its identification by optical microscopy or X-ray diffraction (i.e., <2%). Buchanan (1958) described the calcite as pure and well crystallized, having angular or subangular grains of up to 15 μm in size; most calcite particles that he observed, however, were in the <0.08-μm fraction. Unfortunately, records have not been kept which state exactly from where in the waste management area the sample analyzed by Buchanan was taken.

Scanning electron microscopic analysis of aquifer sediments taken from a 3-m depth showed the presence of two diagenetic materials on the surface of the quartz grains. X-Ray analysis showed that one of these materials was an iron-sulphur compound, probably pyrite; the other was an unknown substance containing Na, Mg, Al, Si, S, Ca and Fe (Davidson, 1978).

GROUNDWATER HYDROLOGY

The hydraulic conductivity of the sand units has been estimated by a variety of methods including pumping test analysis, falling head and constant head tests of piezometers, and field permeameter tests. If all methods of analysis are considered a hydraulic conductivity value of the order of 1×10^{-3} to 5×10^{-3} cm/s is indicated (Cherry *et al.*, 1975b). Porosity measurements on over 100 samples yielded a mean value of 0.38 (Parsons, 1960). When this value is used together with a specific gravity of 2.73 g/cm^3 for the sands, one obtains a bulk density value of 1.7 g/cm^3.

The groundwater flow pattern is shown in plan view in Figure 11 and in cross section in Figure 7 (from Cherry *et al.*, 1975b). The upland area near disposal area "A" forms the recharge area of the basin, and the swamp near Perch Lake and the lake itself form the groundwater discharge area. Cherry *et al.* (1975b) reported that the flow patterns are "strongly affected by the silt and clay beds in the sandy stratigraphic sequences." The groundwater

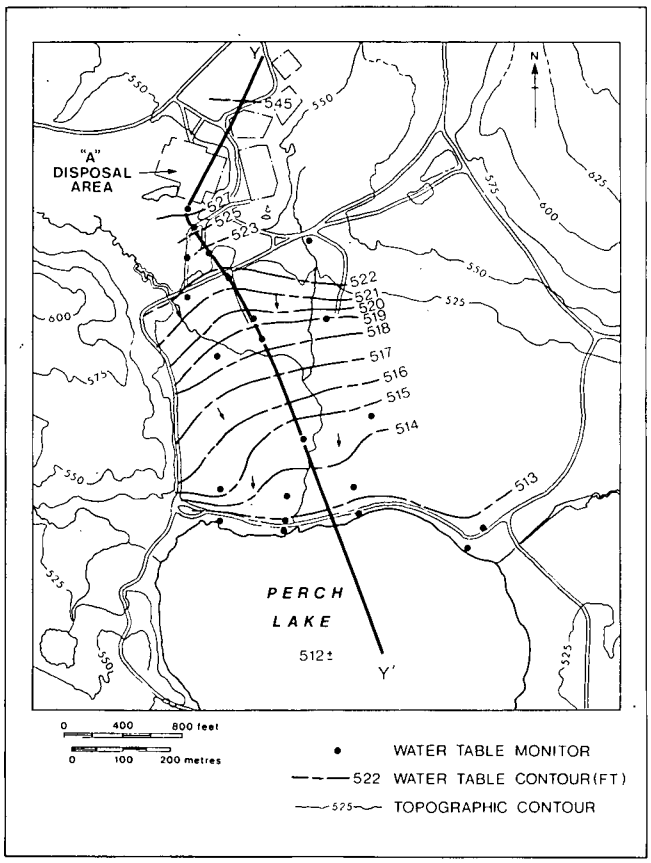

Figure 11. Water table contours in the lower Perch Lake basin. Hydraulic head measurements taken November 1973 (from Cherry *et al.*, 1975b).

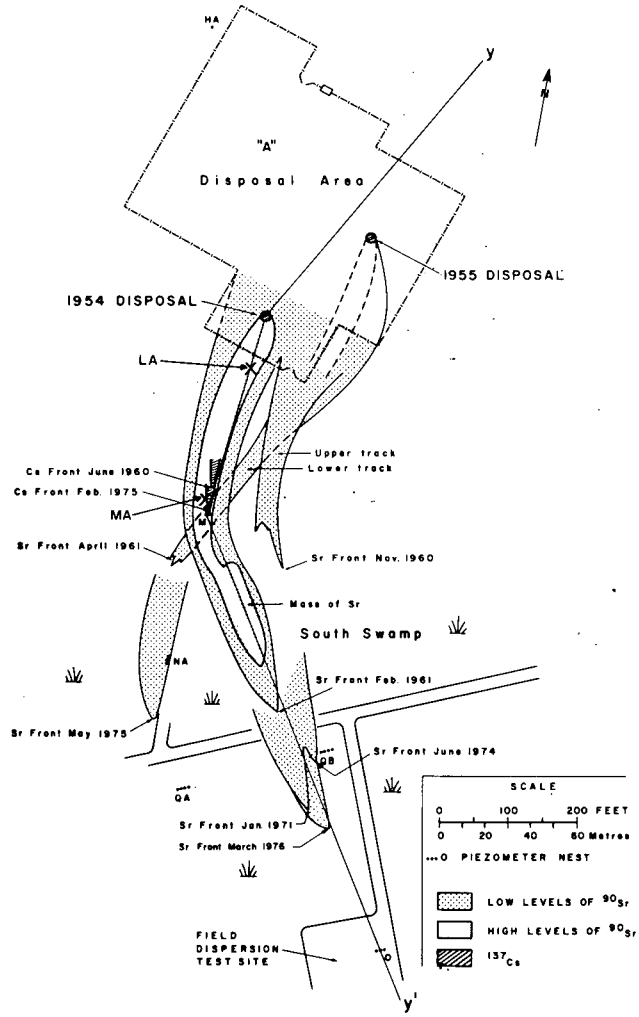

Figure 12. Plan view of radioactive waste migration paths from the 1954 and 1955 disposals.

flow directions in the till unit beneath disposal area "A" are uncertain; the migration of the 1954 and 1955 radioactive liquid wastes (Figs. 12, 13, 14 and 15), however, indicates that the general direction is that indicated in Figure 7.

Cherry *et al.* (1975b) estimated that the groundwater discharge to Perch Lake from the lower Perch Lake basin is of the order of 0.2 to 0.9 mm/day over the area of the lake.

The residence time of groundwater in the flow system between disposal area "A" and Perch Lake has been estimated "to be at least, in round figures, 10 years" by Barry and Entwistle (1975). Parsons (1960) estimated that the travel time of groundwater along two flow paths with "a high rate of seepage" from N piezometer nest to Perch Lake (Fig. 7) is between 10 and 20 years. A similar period for the whole flow system (approximately 1 km) is obtained using a mean groundwater velocity of 15 to 20 cm/day (from Figure 4 of Pickens *et al.*, 1977).

RADIONUCLIDE MIGRATION AND ADSORPTION

In 1954, about 7 m^3 of medium-level liquid radioactive waste containing about 60 Ci of ^{90}Sr and 70 Ci of ^{137}Cs was released into a pit lined with lime and dolomite at disposal area "A". An experimental disposal in 1955 contained 300 Ci of ^{90}Sr and 250 Ci of ^{137}Cs; no attempt, however, was made to neutralize it with lime or dolomite as in the previous disposal (Merritt and Mawson, 1967).

Since that time these wastes have chromatographically separated (Evans, 1958; Parsons, 1961) into ^{90}Sr and ^{137}Cs plumes (Figs. 12, 13, 14 and 15), which are migrating through the sandy aquifer at characteristic velocities much less than the velocity of the transporting groundwater ($V_{GW} \sim 2 \times 10^{-6}$ m/s). For ^{90}Sr, this characteristic

Figure 13

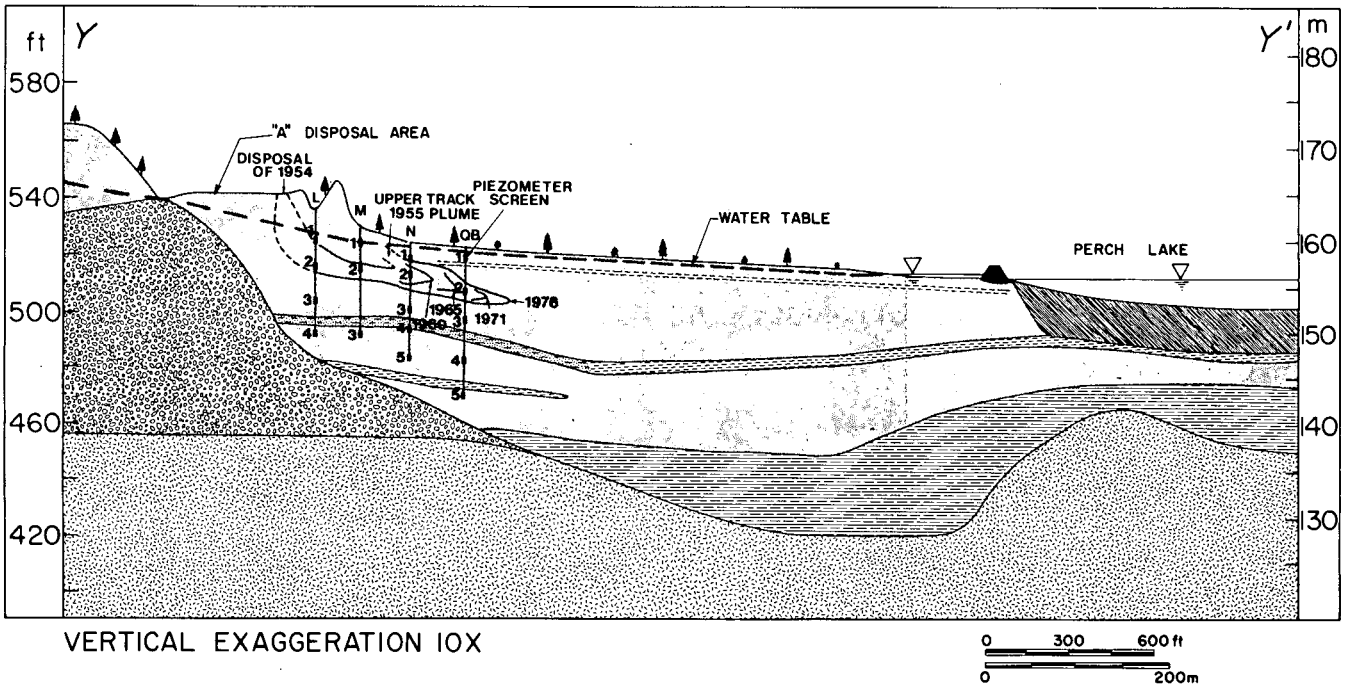

Figure 14

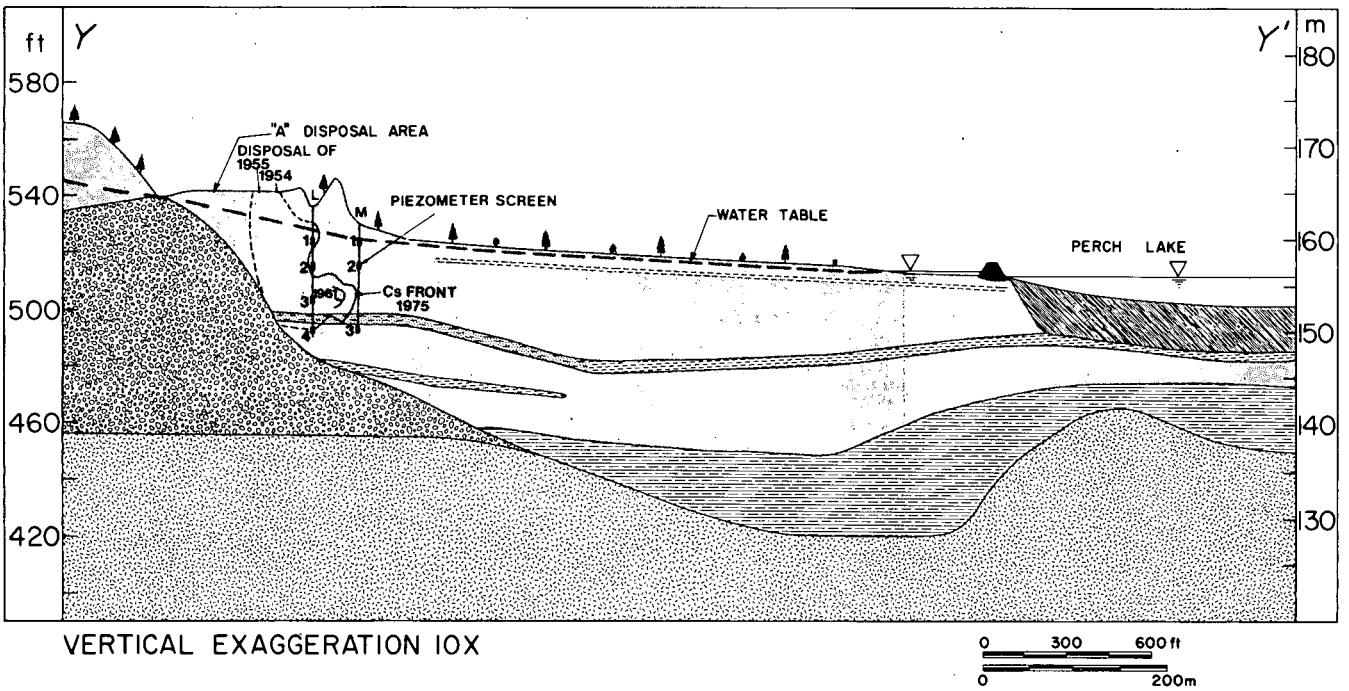

Figure 13. The 1954 ^{90}Sr migration path along the main profile.

Figure 14. The 1954 and 1955 ^{137}Cs migration path.

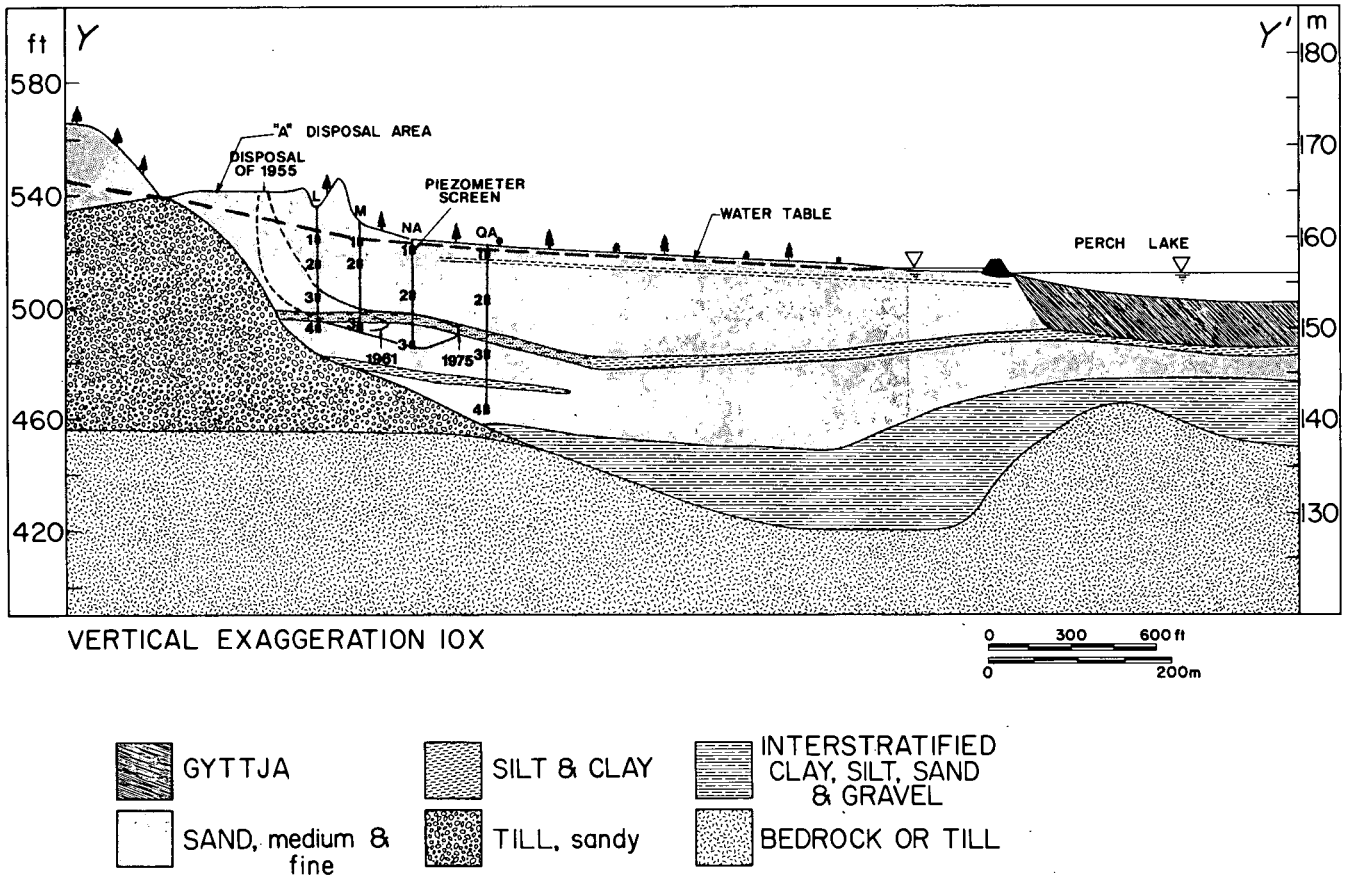

Figure 15. The 1955 ^{90}Sr migration path along the M-NA-QA profile.

velocity is approximately 3% of that of the groundwater; for ^{137}Cs, it is about 0.3%. Table 10 shows some early estimates of K_d by both field mapping using the retardation equation (Equation 67) and radiochemical analysis methods (Jackson *et al.*, 1977). The field mapping estimates are lower than the radiochemical estimates because only the fronts of the radioactive waste plumes have been mapped, yielding an estimate of the velocity of the fastest radionuclides, whereas the groundwater velocity is a mean value. On applying these velocities to Equation 67, V_A is overestimated and a conservative estimate of K_d is obtained.

Preliminary understanding of the adsorption of ^{90}Sr and ^{137}Cs in the groundwaters of the lower Perch Lake basin has come from the leaching experiments of Evans as reported in Mawson (1955). In these experiments, Evans (1954) subjected contaminated sediments to sequential washings with different eluting agents. The amounts shown in Table 11 are the radioactivity counts of the leachate solutions. In the first washing by hydrogen peroxide, most of the ^{90}Sr as well as some of the ^{137}Cs was released by the sediment. As Mawson (1955) pointed out, this would have destroyed all the organic matter

Table 10. Values of K_d by Field Mapping Using the Retardation Equation and Radiochemical Analysis (after Jackson *et al.*, 1977)

	K_d (mL/g)	
Radionuclide	Retardation equation	Radiochemical analysis
^{90}Sr	7	15
^{137}Cs	80	500

Table 11. Concentrations of Radionuclides in Elutants

	cpm/100 g of sediment	
Treatment	^{90}Sr	^{137}Cs
(1) H_2O_2	15.6×10^5	1.73×10^5
(2) $CaCl_2$	9.72×10^5	2.43×10^5
(3) Na_2CO_3	0	3.24×10^5

cpm—Counts per minute.

present in the sediments, which the data of Ophel *et al.* (1971) for Perch Lake bottom sediments suggest may be a sink for the ^{90}Sr, as well as releasing some exchangeable ^{90}Sr. It would, however, have also released ^{90}Sr and ^{137}Cs bound by hydrous iron and manganese oxides, as the hydrogen peroxide treatment causes their dissolution (Jenne, 1968, pp. 369-371). The second treatment involved washing with 1 *N* $CaCl_2$, causing the replacement of the rest of the adsorbed ^{90}Sr by Ca^{2+}. Nevertheless, much ^{137}Cs remained adsorbed. The sediment sample was then fractionated by the usual segregation procedures using Na_2CO_3 for dispersion and then the sediment fractions were dissolved in hydrofluoric acid. As the results in Table 12 show, most of the ^{137}Cs was still fixed to the sediment, although the sediments had been leached of ^{90}Sr.

Table 12. Concentrations of Radionuclides Remaining Sorbed

Sediment fraction	cpm/100 g of fraction	
	^{90}Sr	^{137}Cs
Sand	0	2.91×10^5
Coarse silt	0	3.13×10^5
Medium silt	0	1.20×10^5
Fine silt	0	1.93×10^5
Coarse clay	0	4.27×10^5
Medium and fine clay	0	2.64×10^5

The fixation of the radiocesium was explained by Evans (Mawson, 1955) as due to its irreversible adsorption when in solution in trace amounts by micaceous minerals. While Evans reported that no radiostrontium is fixed by the sediments, Ophel and his colleagues (1971) have published data which show that some strontium in the sands that form part of the bottom sediments of Perch Lake is fixed or is at least not desorbed by 1 *N* ammonium acetate. They further noticed that the amount fixed decreases as the organic matter content increases, suggesting an inorganic sink.

To account for the high levels of radioactivity fixed in the sand fraction, Evans separated the fraction into its three major mineralogical species and counted the radioactivity of each species. The results showed that most of the activity was adsorbed by the feldspar fraction (22 800 cpm/g), followed by the hornblende fraction (2535 cpm/g) and the quartz fraction (524 cpm/g). From this, Evans (1954) "postulated" that the radioactivity was being adsorbed by weathering products that had formed on the feldspar surfaces.

James and Rubin (1979) have shown that the attainment of local chemical equilibrium by calcium during transport through adsorbing porous media is only achieved "when the ratio of the hydrodynamic dispersion coefficient to the estimated molecular diffusion coefficient is near unity." In the aquifer sediments contaminated by the 1954 and 1955 disposals, a groundwater velocity of 47 cm/day was reported by Parsons (1961). Assuming a dispersivity value of $\alpha = 10$ cm (Pickens *et al.*, 1977), one obtains a hydrodynamic dispersion coefficient $D' = \alpha V \sim 5 \times 10^{-3}$ cm^2/s for the ^{90}Sr-contaminated groundwaters. Assuming a molecular diffusion coefficient for ^{90}Sr of approximately 5×10^{-6} cm^2/s (Lerman and Taniguchi, 1972), it is apparent that local chemical equilibrium is unlikely to have been attained during the migration of the radionuclides released in 1954 and 1955.

Groundwater Geochemistry

METHODS

The general procedure developed at Chalk River for obtaining groundwater samples is shown in Figure 16. The groundwaters are pumped from PVC piezometers, 25 mm I.D., with 60-cm Fiberglas-taped screens using Tygon tubing connected to a portable peristaltic pump and from multilevel samplers (Pickens *et al.*, 1978). After the measurement of the groundwater temperature and specific electrical conductance (YSI SCT meter), measurements of pH, E_H and S^{2-} were carried out in the field in airtight flow cells (Fig. 17) using combination glass, combination platinum and a sulphide ion-selective electrode, respectively (all from Orion Research Inc.). Electrode potentials and pH values were measured with Orion model 407A or 801A voltmeters; electrode potentials are quoted relative to the normal hydrogen electrode. An Orbisphere ppb Oxygen Analyzer was used to measure DO (dissolved oxygen) values.

All electrodes, pH buffer solutions, Zobell's solution and sulphide standards were equilibrated at groundwater temperature prior to use. The pH electrode was calibrated with two buffer solutions, and the Pt electrode was checked against Zobell's solution [0.003 *M* $Fe(CN)_6^{3-}/Fe(CN)_6^{4-}$ in 0.1 *M* KCl] or, preferably, 0.01 *M* $Fe(NH_4)_2(SO_4)_2/$

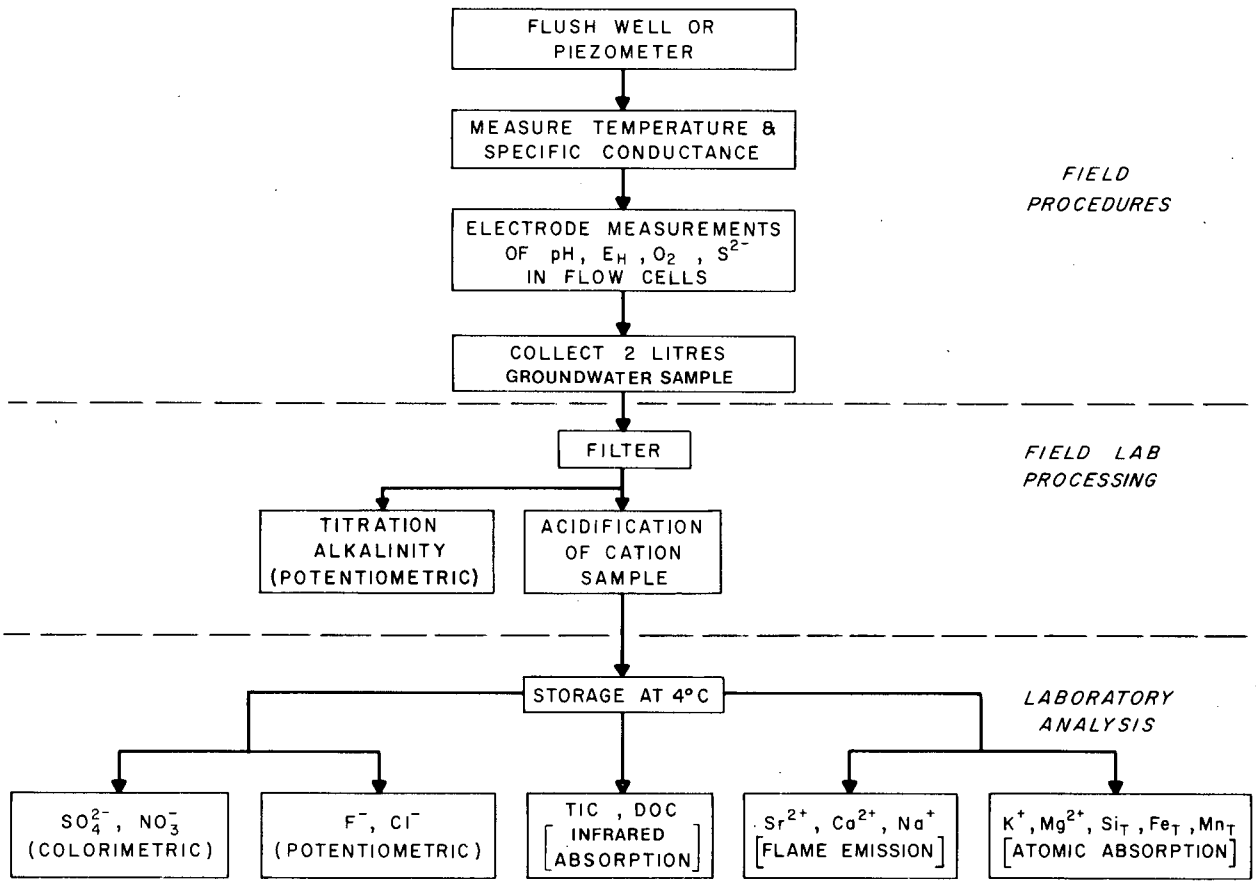

Figure 16. Flowchart of groundwater analyses.

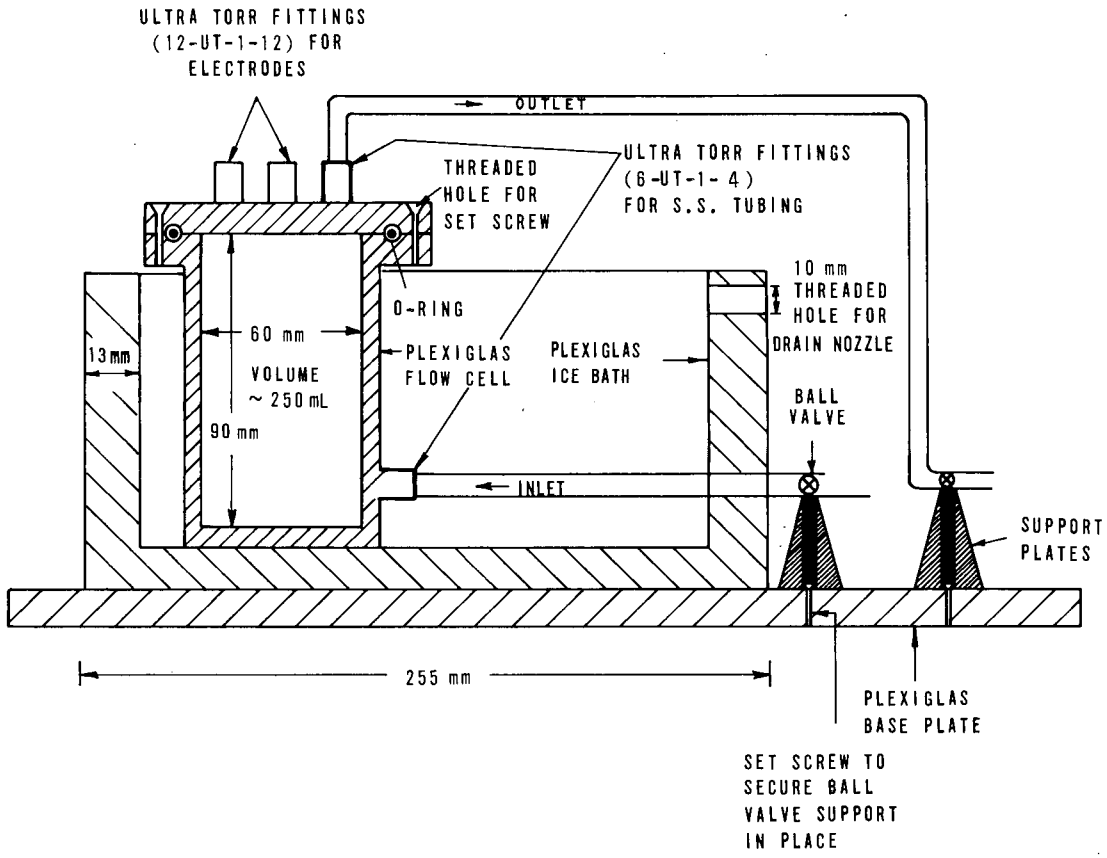

Figure 17. Airtight flow cell.

$FeNH_4(SO_4)_2$ in 1 *M* H_2SO_4. The sulphide electrode was calibrated with 0.1, 1.0 and 10 mg/L sulphide standards, prepared by dilution of a concentrated Na_2S solution with a 1 *M* NaOH – 1% (v/v) $N_2H_4 \cdot H_2O$ solution. For sulphide measurements, sufficient 10 *M* NaOH – 10% (v/v) $N_2H_4 \cdot H_2O$ was injected with a syringe into the flow cell containing the groundwater so that the resultant solution was 1 *M* NaOH – 1% $N_2H_4 \cdot H_2O$. The potential of the sulphide electrode was measured (against a double junction reference electrode) and the sulphide concentration was determined by interpolation from the calibration above (Champ *et al.*, 1979). While the addition of sufficient NaOH – $N_2H_4 \cdot H_2O$ to bring the sample solution to 1 *M* in NaOH may result in the supersaturation of metal sulphides in the sample, sulphide precipitation was not observed and stable, reproducible potentials were measured.

For chemical analysis, groundwater was collected in the field in a Millipore Plexiglas sampler and then forced under N_2 pressure through a 0.45-μm prerinsed in-line Swinnex filter (Millipore HA) into an acid-rinsed N_2-filled polyethylene bottle. A portion of the filtrate was acidified for cation analysis, the rest being kept for anion analysis; samples were stored at 4°C prior to analysis.

The methods used for the chemical analysis are generally those of Environment Canada (1974). Alkalinity was determined by potentiometric titration (Barnes, 1964) of the sample, immediately after its filtration. Colorimetric methods were used for the determination of SO_4^{2-} (Thorin) and NO_3^- (2,4 xylenol), and Cl^- was measured with an ion-selective electrode in a solution containing 50% sample and 50% zinc acetate to prevent sulphide interference (S. Rettig, U.S. Geol. Surv., Reston, VA, personal communication). A flame photometer (Beckman DU) was used to analyze Ca, Na and Sr (Judd and Coveart, 1965), and K, Mg, Fe and Mn were analyzed by atomic absorption spectroscopy using an air-acetylene flame (I.L. models 353 or 151). Total inorganic carbon (TIC) and dissolved organic carbon (DOC) were measured with an Oceanography International Total Carbon Analyzer.

The potential for sample contamination by sampling materials, such as PVC pipe and filter papers, was examined by placing known amounts of these materials in an acid-rinsed polyethylene bottle to which 0.4 L of distilled, demineralized water was added. The bottles were then permitted to sit for six months during which time they were occasionally shaken. A chemical analysis was then

performed on the waters. The results, which are shown in Table 13, represent a "worst case" condition, since the piezometers were emptied of standing water before sampling. All results except pH have been adjusted to that concentration in milligrams per litre in 0.4 L as a result of leaching 1 g of material. There are several sources of DOC contamination, and clearly glass-fibre filter papers are a source of Na^+ and TIC (i.e., alkalinity) contamination.

RESULTS

In addition to the groundwaters, precipitation, stemflow and throughfall waters falling on the lower Perch Lake basin have been collected in rain gauges and plastic buckets, and analyzed (Table 14). The groundwater quality data, shown in Table 15, have been analyzed using a computer program (WATEQF) for calculating chemical equilibria

Table 13. Chemical Analysis of Water Used to Leach Sampling Materials*

Material	pH	Alk. (meq/L)	DOC	Ca^{2+}	Mg^{2+}	Na^+	K^+	Fe^{2+}	Mn^{2+}	SO_4^{2-}	Cl^-
Fiberglas tape	6.1	<0.1	>0.9	0.3	0.06	0.02	0.01	<0.01	<0.01	<1	<1
PVC pipe coated with PVC cement	5.3	<0.1	>4	<0.2	<0.02	<0.02	<0.01	<0.01	<0.01	<1	<1
Tygon tubing	5.1	<0.1	>0.1	<0.2	<0.02	<0.02	<0.01	<0.01	<0.01	<1	<1
Nalgene polypropylene tubing	5.4	<0.1	>0.08	<0.2	<0.02	<0.02	<0.01	<0.01	<0.01	<1	<1
Filter paper											
Gelman GF	9.6	0.9	1.0	0.20	0.15	12.3	0.50	<0.01	<0.01	<1	<1
Millipore HA	5.3	<0.1	>4	<0.2	<0.02	0.13	0.09	<0.01	<0.01	<1	<1
Millipore VC	4.1	<0.1	>12	<0.2	<0.02	<0.02	0.06	<0.01	<0.01	<1	3.3
Blank	5.4	<0.1	0.17	<0.2	<0.02	<0.02	<0.01	<0.01	<0.01	<1	<1

*All data in milligrams per litre except where indicated. See text for explanation.

Table 14. Precipitation, Stemflow and Throughfall Water Quality Data, 1976 and 1977

Sample	Sample date (year, month)	pH	E_H (V)	SO_4^{2-} (mg/L)	NO_3^- (mg/L)	Cl^- (mg/L)	Comments
Rain	76-08	–	–	7.5	1.2	0.4	Analyzed by Atmospheric Environment Service, mean of 11 storms
Rain	77-07	4.1	0.6	–	–	–	Sample of P.C. Jay, CRNL
(1)	77-08	4.3	0.5	2.2	–	–	First rain, sample of L.K. Hendrie, University of Toronto
(2)	77-08	4.4	0.6	2.2	–	–	Second rain
Stemflow	77-08						Samples of L.K. Hendrie
Maple		4.5	0.5	5	–	–	
Large-toothed aspen		5	0.5	10	–	–	
Trembling aspen		7	0.4	10	–	–	
Birch		4	0.5	12	–	–	
Throughfall	77-08	6	0.4	6.1	–	–	

Table 15. Ground and Surface Water Quality Data*

Piezometer	Sample date (year, month)	Specific conductance†	pH	E_H (V)	DO	S_T^{2-}	Tit. alk.‡ (meq/L)	TIC	DOC	Ca^{2+}	Mg^{2+}	Sr^{2+}	Na^+	K^+	Fe_T§	Mn_T	Si_T	SO_4^{2-}	NO_3^-	Cl^-	F^-
HA1	76-10	390	5.4	0.58	2.4	N.D.	0.2	10.4	2.0	12.0	2.0		91	1.8	N.D.	0.03	4.9	15.1	3.5	170	
HA1	77-10	700	5.2	0.45	4.8	N.D.	0.1	17.7	1.6	20.0	3.2	0.20	170	4.8	N.D.	0.04	5.4	10.5	3.3	300	
MA10	78-08	40	6.0	0.55	5.0		0.2	2.5		4.2	1.3	N.D.	2.0	1.6	<0.1	0.01		7.5		4.8	
MA5	78-08	200	6.1	0.37	<0.4		0.4	4.7		12.0	4.8	0.06	17.2	2.4	3.6	0.56		11.5		62.0	
MA1	78-08	390	6.7	0.41	~2		0.7	9.1		24.4	13.8	0.11	44.0	3.5	0.2	0.18		18.0		108	
M2	75-10	70	6.0	0.43			0.4			12.8	1.3	0.05	4.2	1.9	0.1	0.04		15.2		10.9	0.07
M3	75-10	300	6.2	0.22			0.4			20.5	12.5	0.14	34.1	3.3	N.D.	N.D.		19.4		100	0.06
NA2	75-10	330	6.4	0.18			0.5			27.5	11.0	0.17	33.1	2.0	57	0.02	7.4	21.4		125	0.05
NA2	76-08	120	6.4	0.20	<0.4	0.04	0.8	10.2	4.2	10.8	5.3		21.5	1.8	4.6	0.10	7.4	12.8	1.5	31.0	
NA3	75-10	130	8.0	0.07			1.9			33.2	5.0	0.13	14.7	2.4	0.2	0.09	9.5	12.4		35.4	0.36
NA3	76-08	210	8.0	0.05	<0.4	0.01	1.9	23.2	2.4	36.8	8.2		13.6	3.2	0.8	0.13	9.5	12.8	1.7	37.0	
QA1	75-09		5.9	0.16			0.6			1.8	0.8	0.02	4.9	6.2	16.9	0.04	7.2	23.0		12.3	0.07
QA2	75-09		6.1	0.15			0.5			9.4	1.5	0.06	8.3	2.1	4.8	0.10	6.6	13.8		23.0	0.07
QA2	77-10	120	6.0	0.15	<0.4		0.4	19.4	3.5	9.4	3.3	0.05	15.2	2.0	6.1	0.12	8.4	12.7	N.D.	36.0	
QA3	75-09		8.3	0.09			1.5			22.3	3.3	0.08	6.8	1.6	0.2	0.24	10.8	14.4		2.2	0.38
QA3	77-10	120	8.1	0.10	<0.4		1.9	25.6	4.9	26.8	5.4	0.10	5.5	2.6	0.2	0.22	13.0	4.8	N.D.	<1.0	
QA4	75-09	130	8.3	0.10			1.5			28.2	4.5	0.10	5.1	1.3	0.1	0.14	10.6	7.6		21.3	0.53
QA4	77-10	150	8.4	0.12	<0.4		1.5		2.3	31.0	6.1	0.10	4.8	2.7	0.1	0.14	13.0	9.5	N.D.	23.0	
QB2	75-09		6.5	0.28			0.6			15.6	5.9	0.09	12.3	2.1	2.1	0.13	8.4	19.0		39.8	0.14
QB2	77-10	140	6.2	0.31	<0.4	N.D.	0.5	19.8	1.7	11.8	8.1	0.05	13.1	4.0	3.2	0.16	10.2	13.5	N.D.	45.0	
QB3	75-09		6.9	0.16			1.1			15.6	11.3	0.09	11.4	7.2	0.7	0.15	7.4	16.6		42.0	0.22
QB3	77-10	160	6.8	0.25	<0.4	N.D.	1.2	20.8	1.1	18.6	10.8	0.09	12.9	4.0	0.8	0.22	9.3	14.5	N.D.	38.4	
QB4	75-09		6.7	0.19			0.7			9.7	9.1	0.06	10.6	3.3	1.3	0.14	7.2	17.2		28.0	0.10
QB4	77-10	120	6.6	0.25	<0.4	N.D.	0.6	14.0	0.7	9.4	7.5	0.03	8.5	4.4	2.0	0.11	9.3	12.5	N.D.	25.6	
QB5	75-09		7.5	0.09			1.2			17.3	6.8	0.06	5.6	4.2	0.5	0.20	11.1	17.2		14.0	0.21
QB5	77-10	110	7.3	0.11			1.0	12.6	3.7	18.0	7.9	0.04	3.8	2.8	3.1	0.14	14.0	16.0	0.3	17.5	
O10	75-09		6.8	0.14			1.1			13.9	4.0	0.11	11.2	2.0	2.8	0.13	8.0	9.6		23.8	0.19
O7	75-09	150	6.9	0.17			1.0			14.4	8.9	0.10	11.8	3.0	1.1	0.14	7.3	18.0		28.0	0.23
O8	75-09	100	6.9	0.14			0.8			10.1	5.8	0.05	11.9	2.6	5.0	0.05	7.1	15.6		20.2	0.12
O8	76-11	120	6.9	0.19	<0.4	0.02	0.8	11.2	0.8	11.1	6.9		10.7	3.2	6.2	0.05	7.1	17.3	0.4	22.5	
KNEW2	76-11	100	7.8	0.07		0.06	1.4	17.4	1.8	16.4	5.5		3.5	1.4	0.2	0.06		5.7	0.5	<1.0	
KNEW2	77-11	90	8.2	0.07		0.06	1.4	18.4	1.4	19.0	4.7	0.06	3.8	1.5	0.1	0.07	13.0	5.7	N.D.	0.4	
KNEW4	77-11		8.6	0.06		0.01	2.0	25.4	2.3	15.8	3.1	0.32	20.0	3.1	0.1	0.02	5.6	2.0	0.3	0.4	
KO2	77-10	130	6.5	0.11	<0.4		1.6	32.9	11.7	14.2	7.0	0.10	4.0	1.2	16.6	0.22	13.0	3.0	0.7	15.0	
KO4	77-10	110	8.4	0.09	<0.4	0.12	1.1	15.4	1.7	19.5	4.6	0.05	4.6	2.2	0.1	0.09	11.2	5.8	N.D.	1.0	
KO5	77-10	110	8.1	0.11	<0.4	0.12	1.6	20.0	2.6	24.8	4.0	0.11	4.9	1.9	0.3	0.11	14.4	5.5	N.D.	3.3	
Main stream	77-10		5.5				0.1	3.2	39.6	2.7	2.5		5.1	1.2	0.8	0.03		9.7		11.5	
Inlet 2	77-10		6.2				0.1	4.2	35.2	2.7	2.5	0.04	4.3	0.8	0.8	0.04	5.6	9.7	0.9	11.0	

*All data in milligrams per litre except where indicated.
†Specific electrical conductance in micromhos per centimetre, groundwater temperatures 7°C to 10°C.
‡Titration alkalinity (using H_2SO_4).
§Subscript T indicates total concentration of all dissolved species.
N.D.—Not detected.

of natural waters [Truesdell and Jones (1974) as revised by N. Plummer, June 1975], the calculation procedures of which have been outlined in Chapter 2 of this report. From this program saturation indices for carbonate and sulphide minerals are reported in Table 16. Ion balance errors for the chemical analyses in Table 15 were 4% on the average.

DISCUSSION

The purpose of this discussion is to consider, in terms of the geochemical and biochemical processes introduced in Chapter 2, the *general* nature of the chemical evolution of groundwater in the aquifer system. In particular, those reactions that affect the mobility of contaminants will be discussed to the extent that the data available permit. No attempt will be made to develop a mass balance analysis of mineral weathering and dissolution reactions in the aquifer; such an analysis would require that detailed studies of the atmospheric chemistry, the geochemistry of carbon and the diagenesis of alumino-silicate minerals be conducted in order that a *unique* synthesis of the groundwater chemistry be obtained.

For this purpose the flow system may be considered as a giant chemical reactor composed largely of quartz and alumino-silicate minerals and alteration products,

Table 16. Saturation Indices for Groundwater Quality Data*

Piezometer	Sample date (year, month)	Mineral or precipitate				
		$CaCO_3$†	$SrCO_3$‡	SiO_2§	FeS‖	FeS_2¶
HA1	76-10	−4.6	–	−0.5	<0	<0
HA1	77-10	−4.7	−3.6	−0.5	<0	<0
MA10	78-08	−4.2	<0	–	–	–
MA5	78-08	−3.3	−2.6	–	–	–
MA1	78-08	−2.2	−1.5	–	–	–
M2	75-10	−3.3	−2.7	–	–	–
M3	75-10	−3.0	−2.1	–	–	–
NA2	75-10	−2.7	−1.8	−0.4	–	–
NA2	76-08	−2.8	–	−0.4	−0.5	+3.2
NA3	75-10	−0.4	+0.3	−0.3	–	–
NA3	76-08	−0.4	–	−0.2	+0.5	+0.6
QA1	75-09	−4.2	−3.0	−0.4	–	–
QA2	75-09	−3.4	−2.5	−0.4	–	–
QA2	77-10	−3.5	−2.7	−0.3	–	–
QA3	75-09	−0.4	+ 0.3	−0.2	–	–
QA3	77-10	−0.4	+0.3	−0.1	–	–
QA4	75-09	−0.3	+0.4	−0.2	–	–
QA4	77-10	−0.1	+0.5	−0.1	–	–
QB2	75-09	−2.7	−1.9	−0.3	–	–
QB2	77-10	−3.1	−2.4	−0.2	<0	<0
QB3	75-09	−2.1	−1.2	−0.4	–	–
QB3	77-10	−2.1	−1.3	−0.3	<0	<0
QB4	75-09	−2.6	−1.7	−0.4	–	–
QB4	77-10	−2.8	−2.2	−0.3	<0	<0
QB5	75-09	−1.4	−0.7	−0.2	–	–
QB5	77-10	−1.6	−1.2	−0.1	–	–
O10	75-09	−2.2	−1.2	−0.3	–	–
O7	75-09	−2.1	−1.2	−0.4	–	–
O8	75-09	−2.3	−1.5	−0.4	–	–
O8	76-11	−2.4	–	−0.4	+0.1	+4.1
KNEW2	76-11	−1.0	–	–	+0.3	+1.9
KNEW2	77-11	−0.6	0.0	−0.1	+0.4	+2.4
KNEW4	77-11	−0.4	+1.0	−0.5	−0.2	+0.7
KO2	77-10	−2.3	−1.3	−0.1	–	–
KO4	77-10	−0.4	+0.1	−0.2	+0.6	+3.8
KO5	77-10	−0.5	+0.3	−0.1	+1.1	+4.7

*All data are converted to $\log_{10}$SI where SI = IAP/K_{SO}.
†Aragonite, $pK_{SO} = -\log K_{SO} = 8.215$, T = 298°K.
‡Strontianite, $pK_{SO} = 11.41$.
§Silica gel, $pK_{SO} = 3.017$.
‖Mackinawite, $pK_{SO} = 17.566$.
¶Pyrite, $pK_{SO} = 27.6$.

with trace amounts (<1%) of organic matter, hydrous oxides of iron and manganese, and sulphide and carbonate minerals. The chemical reactions occurring within the flow system are observed in time and space by the withdrawal and analysis of samples from piezometers placed at strategic points in the flow system (Fig. 18). The system, as revealed by these (Table 15) and other data (Johnston *et al.*, 1978; Appendix, Table A-1), displays a steady-state condition except for seasonal road-salting effects.

It is possible to identify three chemical inputs to the flow system: (1) acid precipitation, (2) liquid radioactive waste and (3) road salt.

Acid precipitation falls on the basin (Table 14), is somewhat buffered by the hardwoods, undergoes 60% evapotranspiration (Barry, 1975) (i.e., concentration factor = 2.5), and is recharged ($\sim 10^8$ L/yr) to the flow system with approximately the following composition: pH ~ 4, E_H ~ 0.6 V, SO_4^{2-} ~ 10 mg/L, NO_3^- ~ 3 mg/L, Cl^- ~ 1 mg/L.

In addition to the liquid radioactive wastes released into pits in disposal area "A" in 1954 and 1955 (see Chapter 3), there is a continual release of about 1000 cubic metres per month of water containing tritium from the research reactors at CRNL into Reactor Pit No.2 (Fig. 6).

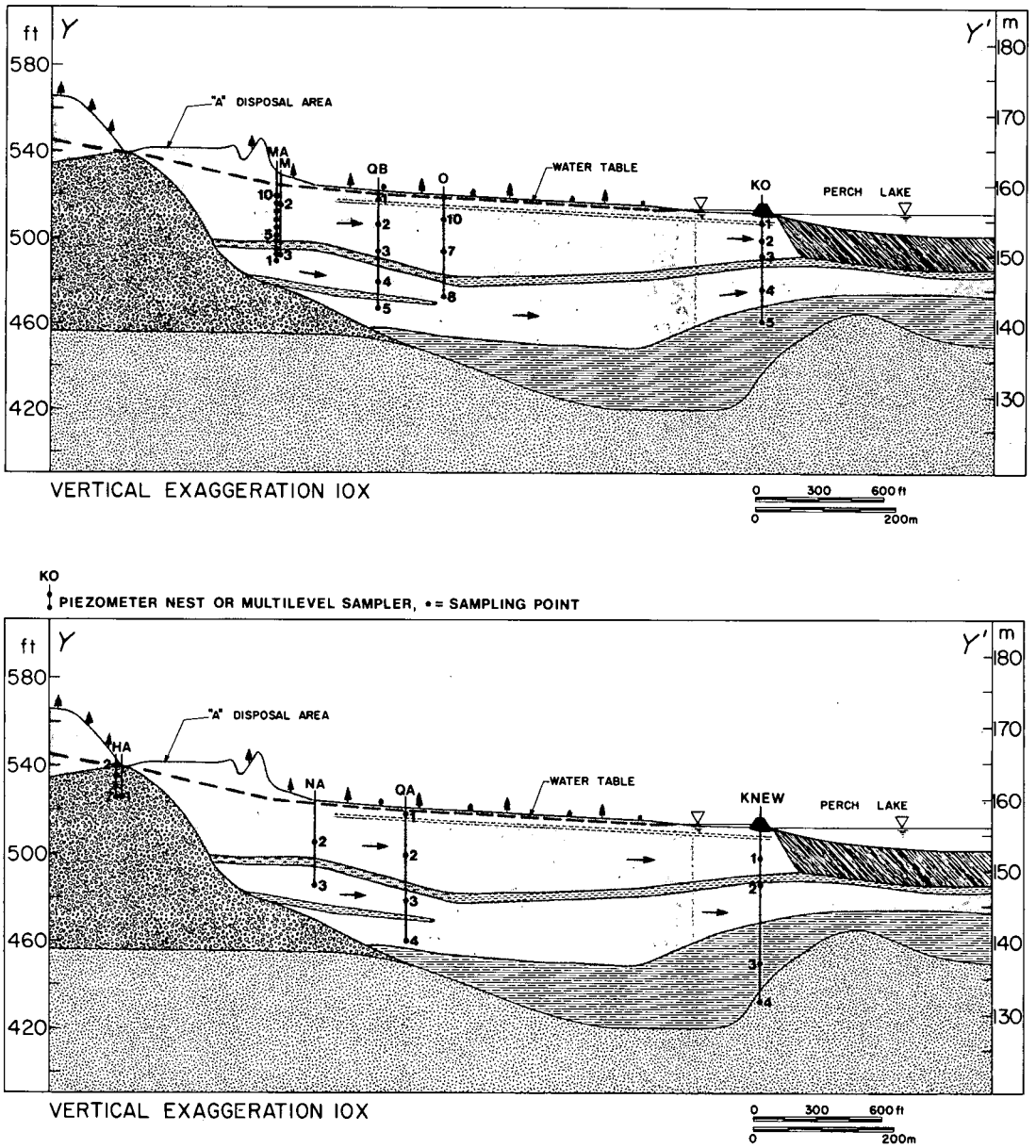

Figure 18. Location of piezometers. Those in the upper diagram are on the YY' profile; those below are adjacent to it.

This water is of low ionic strength [specific electrical conductance ~ 60 μmhos/cm, pH ~ 7 for October 1978 discharge waters (A. Voss, Chemical Operations Branch, CRNL)]. Assuming an annual precipitation total of 80 cm falling over a recharge area of 360 000 square metres resulting in 40% infiltration (60% evapotranspiration loss), the tritium disposals amount to approximately 10% (i.e., $\sim 10^7$ L/yr) of the groundwater recharge of acid precipitation.

Every year approximately ten tons (10^4 kg) of road salt (NaCl) is spread onto highways within the Perch Lake basin. A significant fraction of this total, following its dissolution, enters the groundwater flow system in the vicinity of HA piezometer nest and through recharge from the beaver dam ponds near HA piezometer nest (Fig. 6).

The output from the system is in the form of groundwater discharge to Perch Lake, although there is some leakage to bedrock and the Perch Swamp. This discharge to Perch Lake takes two forms: (1) shallow groundwater discharge through the middle sand aquifer which is diluted by swamp water infiltrating through this same aquifer due to locally high hydraulic heads created by the dyke at Inlet 2 (Fig. 6) and (2) deep groundwater discharge to Perch Lake through the lower sand aquifer. The deep discharge (piezometers KO4, KO5, KNEW2 and KNEW4) is, relative to the recharge, a basic, reduced aqueous solution with the following characteristics: pH $\geqslant$7.5, $E_H \leqslant 0.1$ V, alkalinity $\geqslant$ 1 meq/L, $Si_T \geqslant$ 10 mg/L, DOC $<$ 3 mg/L, Ca $\geqslant$ 15 mg/L and $\delta^{13}C$ = -15°/oo to -17°/oo. The shallow discharge (e.g., piezometer KO2) is slightly acidic (pH ~ 6.5) and high in DOC (>10 mg/L) due to dilution with surface water (see Appendix, Table A-2) but approaches the composition of the deep discharge with increasing depth.

Having outlined the input to and output from the system, it remains to describe the system itself with reference to those geochemical and biochemical concepts introduced in Chapter 2 that may affect the migration of radionuclides within the groundwater flow system.

Complexation

The percentage of complexed ions in these groundwaters relative to that of free ions is extremely low. For MA1($I = 5.5 \times 10^{-3}$) assuming $\gamma_{SrHCO_3^+} = \gamma_{SrSO_4^0} = 1.0$, the following approximations may be made from Equations 32 to 39:

$$pSr = -\log\{Sr^{2+}\} \sim 6$$

$$pSrHCO_3^+ \sim 10$$

$$pSrSO_4^0 \sim 13$$

Consequently only a minute fraction (<1%) of the total (analytical) dissolved strontium is in the form of the complex ions. The same point can be made for cesium and its complexes in these groundwaters. Therefore complexation should be of little importance in promoting the transport of ^{90}Sr and ^{137}Cs in this groundwater flow system; the point will be made that the adsorption of complexed ^{90}Sr must also be negligible.

Acid-Base Reactions

The solubility of various potential radionuclide precipitates (e.g., $^{90}SrCO_3$) and the surface charge of adsorbents are both strongly affected by acid-base reactions; pH and alkalinity measurements enable the hydrogeologist to attempt interpretations of such reactions.

Natural waters of low alkalinity and with pH levels of 5 to 7 may derive their H^+ ion assimilation capacity (i.e., buffer capacity) from mineral equilibria involving "$CaCO_3$, Fe_2O_3, alumino-silicates and MnO_2, adsorption minerals, colloids, and organic detritus, and from ion exchange with clay minerals and organic acids" (Kramer, 1978). From his study of several watersheds in northern Ontario, which are geochemically similar to the lower Perch Lake basin, Kramer (1978) concluded that the "buffering of a watershed can be approximated as a mixing of H_2O with a saturated H_2O - $CaCO_3$ system, and in most cases the H_2O - $CaCO_3$ component can be attributed to groundwater flow," i.e., due to the dissolution of trace amounts of carbonate minerals in the aquifer sediments of the watershed.

This conclusion is supported by the work of Fritz *et al.* (1978) in an aquifer immediately south of Perch Lake (Fig. 5); studies were begun in this area to provide information on the geochemistry of uncontaminated groundwaters in the Perch Lake basin. Fritz and others report that, despite the presence of only trace amounts (<1%) of carbonate minerals within the aquifer,

> ... the normal inorganic geochemical evolution of these waters also brings about an enrichment in ^{13}C from shallow ($\delta^{13}C \sim -24°/oo$) to deeper ($\delta^{13}C \sim -15°/oo$) groundwater and most of the changes towards more positive values with increasing depths ... can be explained by inorganic processes such as the dissolution of ^{13}C-rich carbonate minerals under closed system conditions.

Furthermore, they suggest the initial partial pressure of CO_2 in the soil zone is close to 10^{-2} atm and that "the initial pH's vary between 5 and 6."

The pH and alkalinity (alk.) variations in the lower Perch Lake basin are shown in Figure 19. Acid precipitation (pH ~ 4, alk. ~ 0 meq/L) is quickly buffered upon infiltration in the recharge area (e.g., HA1 and MA10); the resulting pH varies between 5 and 6 with alkalinities of 0.1 to 0.2 meq/L. Groundwaters in the transition zone between disposal area "A" and Perch Lake (e.g., QA, QB, O piezometer nests) have pH levels varying between 6 and 7 with alkalinities of up to 1 meq/L. Groundwaters in the discharge area (e.g., KNEW2, KNEW4, KO4 and KO5) and in certain deep sediments in the middle of the flow system (e.g., NA3, QA3, QA4 and QB5) show high pH levels (≥7.5) and high alkalinities (>1 meq/L), suggesting the presence of carbonate minerals in the aquifer sediments. The saturation indices of these waters (Table 16) indicate approximate equilibrium with respect to $CaCO_3$ and $SrCO_3$ mineral phases (i.e., log SI ~ 0.0 ± 0.1).

If indeed carbonate mineral dissolution is responsible for the buffer capacity of the aquifer, then the data from this flow system should be amenable to analysis by Langmuir's (1971) dissolution and precipitation models. The model chosen is generally known as the closed-system calcite model. The model assumes that groundwater unsaturated with respect to carbonate minerals becomes charged with CO_2 in the soil zone but is then isolated (closed) from fresh sources of CO_2. There follows a decline in P_{CO_2} (the partial pressure of CO_2) as the dissolved CO_2 is converted to bicarbonate by reaction with calcite:

$$CaCO_3 + CO_2 + H_2O = Ca^{2+} + 2\,HCO_3^- \qquad (69)$$

Figure 20 shows two theoretical calcite dissolution curves and a calcite saturation curve (Langmuir, 1971, Equations 14 and 16, respectively) with data plotted from the lower Perch Lake basin. The initial pH and bicarbonate molality chosen for the upper dissolution curve are those from piezometer nest HA (HA1-7): pH = 5.2, m HCO_3^- = $10^{-3.95}$ (HCO_3^- ~ 7 mg/L, P_{CO_2} ~ $10^{-1.5}$). According to the model, groundwaters migrating from HA toward Perch Lake should dissolve calcite and thereby produce pH and bicarbonate values according to the upper theoretical calcite dissolution curve. Only the HA points (not all plotted) fall on this curve; two groundwaters, both affected by surface water infiltration and therefore photosynthetic activity, fall above it. Most groundwaters are below the curve, suggesting that the average initial P_{CO_2} is somewhat less. The lower curve is drawn assuming the pH and bicarbonate at MA multilevel piezometer (e.g., MA10) are representative of initial conditions in the flow system: pH = 6.0, m HCO_3^- = $10^{-3.8}$ (HCO_3^- ~ 10 mg/L, P_{CO_2} ~$10^{-2.0}$). Since the data points fall between the two curves, we may conclude that the buffer capacity of the aquifer system is consistent with that derived from a model

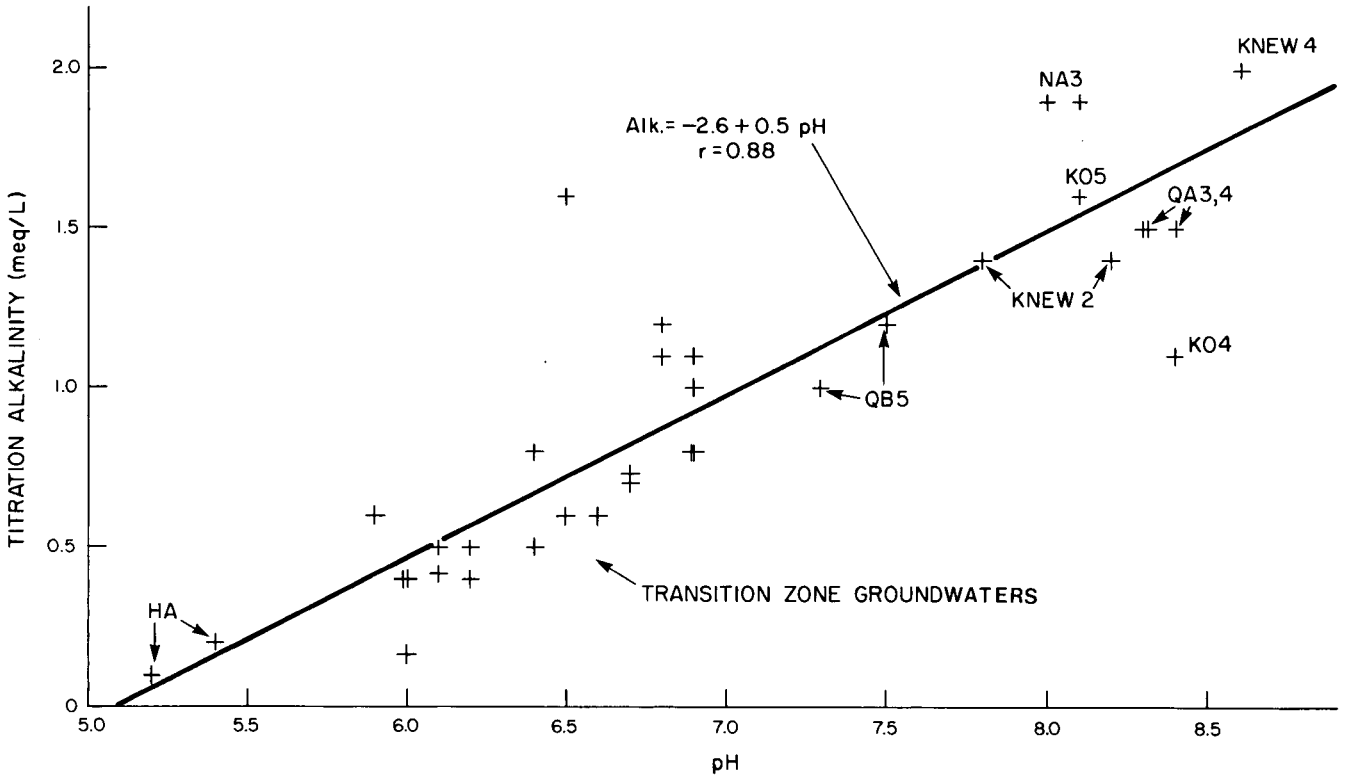

Figure 19. The pH and alkalinity (alk.) variations in the lower Perch Lake basin.

of closed-system calcite dissolution with the following initial (i.e., water table) conditions: pH = 5.2-6.0 and $P_{CO_2} = 10^{-1.5} - 10^{-2.0}$.

Given the small data base and the considerable uncertainties concerning the buffering effects of the other materials mentioned by Kramer (1978), it cannot be claimed that this model presents a unique solution to the problem of determining the origin of the buffer capacity of the system. For a groundwater whose pH and alkalinity are controlled by calcite dissociation via carbonic acid, the following electrical neutrality relation should be satisfied (Garrels and Christ, 1965, p. 88):

$$0 = (M_{HCO_3^-} + 2M_{CO_3^{2-}} + M_{OH^-}) - (2M_{Ca^{2+}} + M_{H^+}) \quad (70)$$

Values of the right-hand side of Equation 70 are presented in millimoles (mM) in Table 17. Positive values suggest a net alternative sink for Ca^{2+} and H^+; negative values suggest a net alternative source (E.J. Reardon, personal communication). The negative values may be attributed to sodium-for-calcium ion exchange following the dissolution of road salts in the groundwater recharge area. The positive values in the transition- and discharge-area groundwaters are probably due to a combination of Ca^{2+} adsorption and precipitation and the oxidation of DOC to TIC (Table 2).

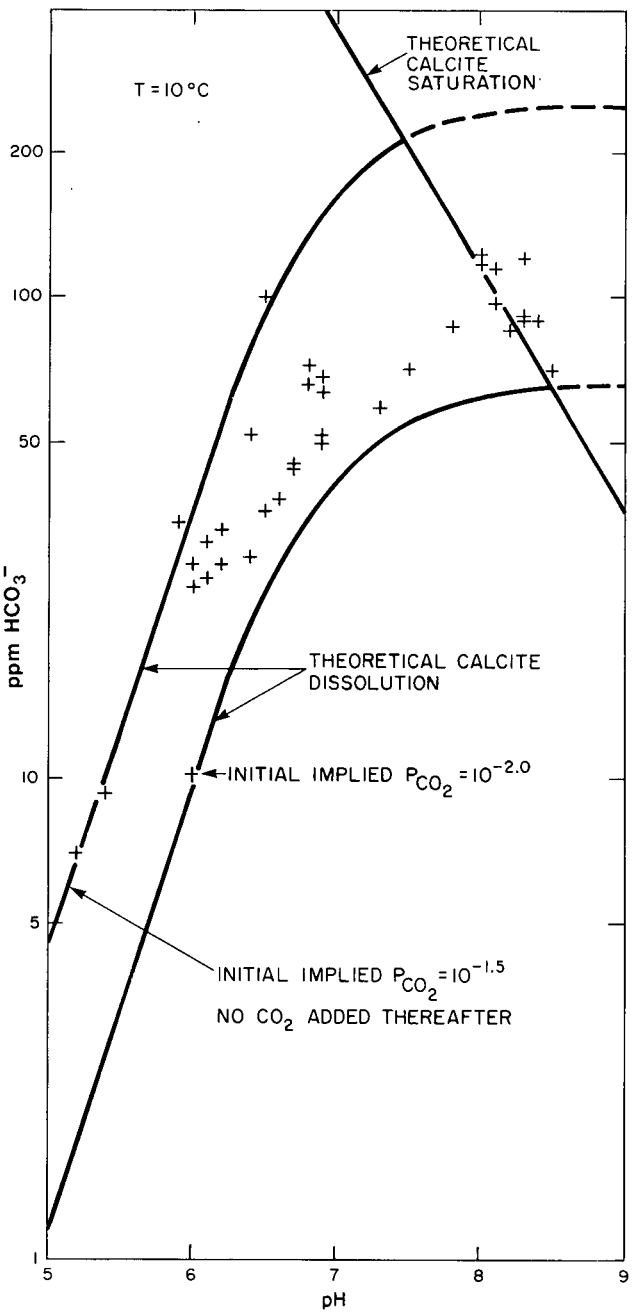

Figure 20. The closed-system calcite model.

Table 17. Values of Right-Hand Side of Equation 70 from WATEQF Calculations

Piezometer	Sample date (year, month)	Total (mM)*
HA1	76-10	−0.44
HA1	77-10	−0.87
MA10	78-08	−0.04
MA5	78-08	−0.17
MA1	78-08	−0.48
M2	75-10	−0.18
M3	75-10	−0.56
NA2	75-10	−0.87
NA2	76-08	+0.32
NA3	75-10	+0.25
NA3	76-08	+0.18
QA1	75-09	+0.47
QA2	75-09	+0.05
QA2	77-10	−0.05
QA3	75-09	+0.43
QA3	77-10	+0.56
QA4	75-09	+0.08
QA4	77-10	−0.08
QB2	75-09	−0.17
QB2	77-10	−0.04
QB3	75-09	+0.34
QB3	77-10	+0.26
QB4	75-09	+0.26
QB4	77-10	+0.17
QB5	75-09	+0.30
QB5	77-10	+0.08
O10	75-09	+0.39
O7	75-09	+0.31
O8	75-09	+0.34
O8	76-11	+0.27
KNEW2	76-11	+0.60
KNEW2	77-11	+0.41
KNEW4	77-11	+1.20
KO2	77-10	+0.93
KO4	77-10	+0.19
KO5	77-10	+0.36

*$(M_{HCO_3^-} + 2M_{CO_3^{2-}} + M_{OH^-}) - (2M_{Ca^{2+}} + M_{H^+})$

Consequently, it may be concluded that the primary acid-base buffering reactions in the aquifer sediments are those involving carbonate mineral dissolution in the presence of soil-zone derived CO_2; of secondary importance are organic matter oxidation and the weathering of aluminosilicates, neither of which may be quantitatively evaluated. X-Ray diffraction analyses, however, have indicated that the principal pH buffering reaction in the unsaturated zone is probably the weathering of biotite to vermiculite (R.J. Patterson, personal communication).

Redox Processes

Redox studies were undertaken in the lower Perch Lake basin to determine the thermodynamic stability of the hydrous Fe and Mn oxides in the aquifer, as these oxides may be important radionuclide adsorbents.

In Chapter 2, it was postulated on the basis of thermodynamic arguments that in a confined aquifer containing excess DOC and some solid phase Mn(IV) and Fe(III) minerals, the oxidized species present in the groundwater flow system would be reduced in the following order: dissolved oxygen (DO), nitrate, (solid) manganese oxides, (solid) ferric hydroxides, sulphate, dissolved CO_2 (e.g., HCO_3^-) and, finally, dissolved nitrogen. Figure 7 suggests that the Middle and Lower Sands units do indeed form a confined aquifer; solid phase organic carbon (~0.01%) and Mn(IV) (~0.001%) and ferric (~0.1%) oxides are present in the aquifer sediments. Consequently this groundwater flow system provides an opportunity to determine the extent to which a natural system approaches a conceptually defined system.

Variations in pH, E_H, DO and total dissolved sulphide (S_T^{2-}) along the main axis of groundwater flow (see cross-section line in Figure 6) are shown in Figure 21; the upper and lower graphs have the same abscissa, that being distance from the recharge area [measured from multilevel sampler LA (Fig. 6)]. The locations of several piezometer nests (MA, M, QB, O, KO) along this axis are noted; furthermore, comparable data from recharge area piezometer nest HA and discharge area piezometer nest KNEW are included. The upper graph shows the rise in pH that may be associated with calcite dissolution and a decay of E_H, which is a

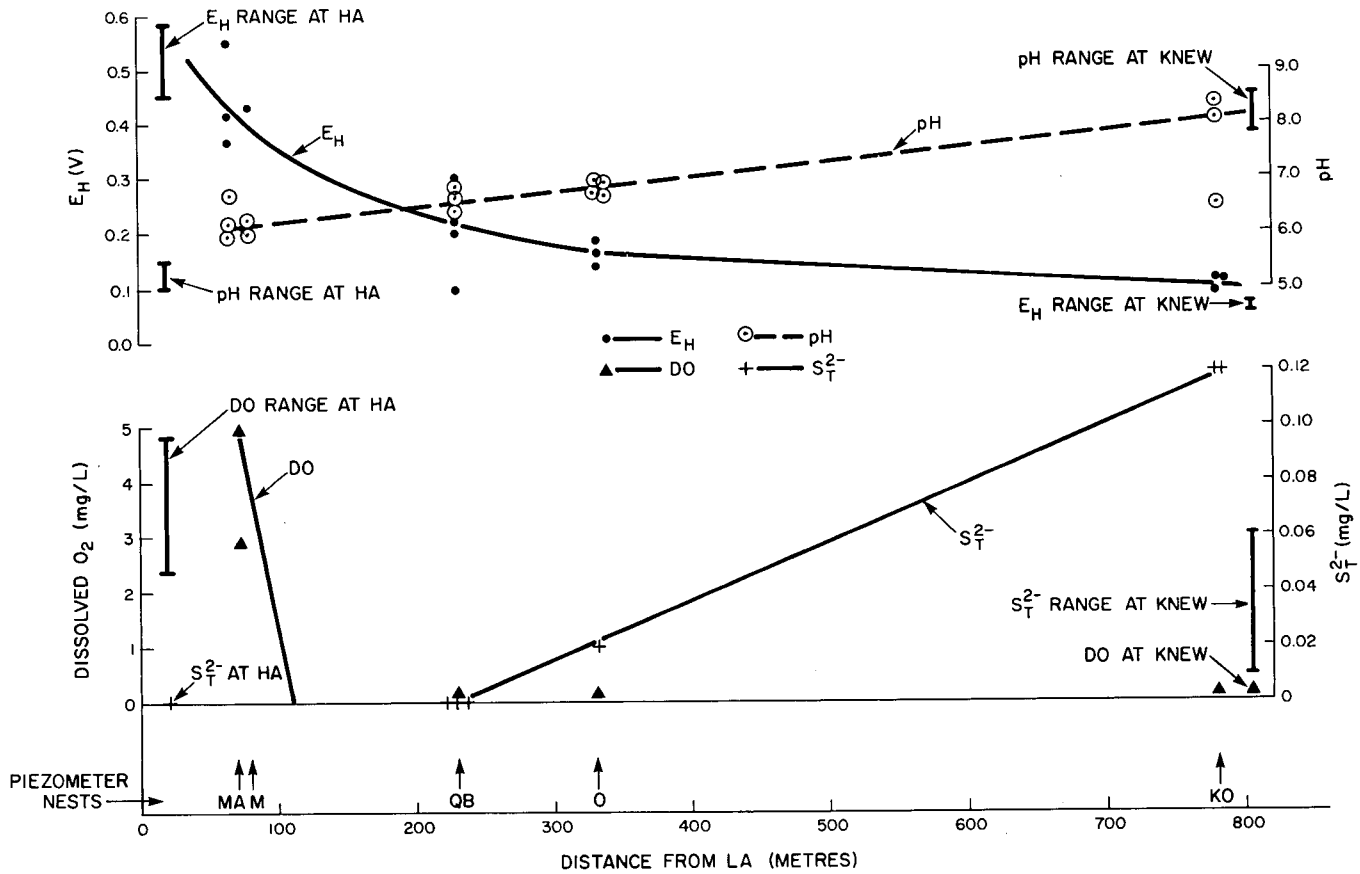

Figure 21. The pH, E_H, DO and S_T^{2-} variations along the flow system.

consequence of the lower free energy change of each of the subsequent reactions in Table 2 (Champ *et al.*, 1979); the pH and E_H values at HA and KNEW are similar to those at MA and KO, respectively. The lower graph shows that dissolved oxygen (DO) is present in the recharge area, whereas no sulphide is detectable until measured potentials of less than 200 mV are recorded (at O nest); thereafter sulphide concentrations increase to approximately 10^{-6} *M* beneath the dyke. Dissolved oxygen is not detectable in the discharge area piezometer above that level (~0.2 mg/L) which is attributable to oxygen diffusion through Tygon and polypropylene tubing.

In the transition zone of the groundwater flow system, several piezometers that are unaffected by surface water infiltration (e.g., QB and O piezometers) show high iron (>1 mg/L) and manganese concentrations (>0.1 mg/L), both of which become lower in the groundwaters beneath the dike (e.g., KO4, KO5, KNEW2 and KNEW4). The loss of approximately 0.1 mM of iron and sulphate between the transition and discharge areas (e.g., between O8 and KO4, KO5) is probably due to sulphate reduction and the subsequent precipitation of ferrous sulphides, which are supersaturated in the KO and KNEW groundwaters (Table 16).

Consequently it is observed, consistent with the thermodynamic closed-system redox model of Stumm (1967) modified by Champ *et al.* (1979) (see Table 2), that the oxidized species present in the groundwater flow system are reduced in the following order: DO, Mn(IV) and Fe(III) oxides and sulphate. There are insufficient data to assess the possible reduction of bicarbonate and nitrogen; nitrate values, however, decrease from HA1 to O8 to KO4 and KO5 in a manner consistent with the closed-system redox model.

The geochemistry of the iron-sulphur-water system may also be studied with the aid of E_H/pH diagrams such as the one shown in Figure 22. The ferric hydroxide-ferrous iron equilibrium line is drawn on the basis of (Stumm and Morgan, 1970, p. 317):

$$Fe(OH)_3 + 3H^+ + e^- = Fe^{2+} + 3H_2O, E^0 = 1.06\ V \quad (71)$$

The pyrite-ferrous iron equilibrium line is drawn on the basis of (Hem, 1960, p. 65):

$$FeS_2 + 8H_2O = Fe^{2+} + 2SO_4^{2-} + 16H^+ + 14e^-, E^0 = 0.37\ V \quad (72)$$

The dissolved iron and sulphate levels were chosen on the basis of the detection limit for dissolved iron using flame atomic absorption spectrophotometry (10^{-7} *M* = 5.5 μg Fe/L), the maximum observed concentration of ferrous iron in groundwaters unaffected by surface waters (10^{-4} *M* = 5.5 mg Fe/L) and the approximate level of dissolved sulphate in the groundwaters in question (10^{-4} *M* = 9.6 mg SO_4^{2-}/L).

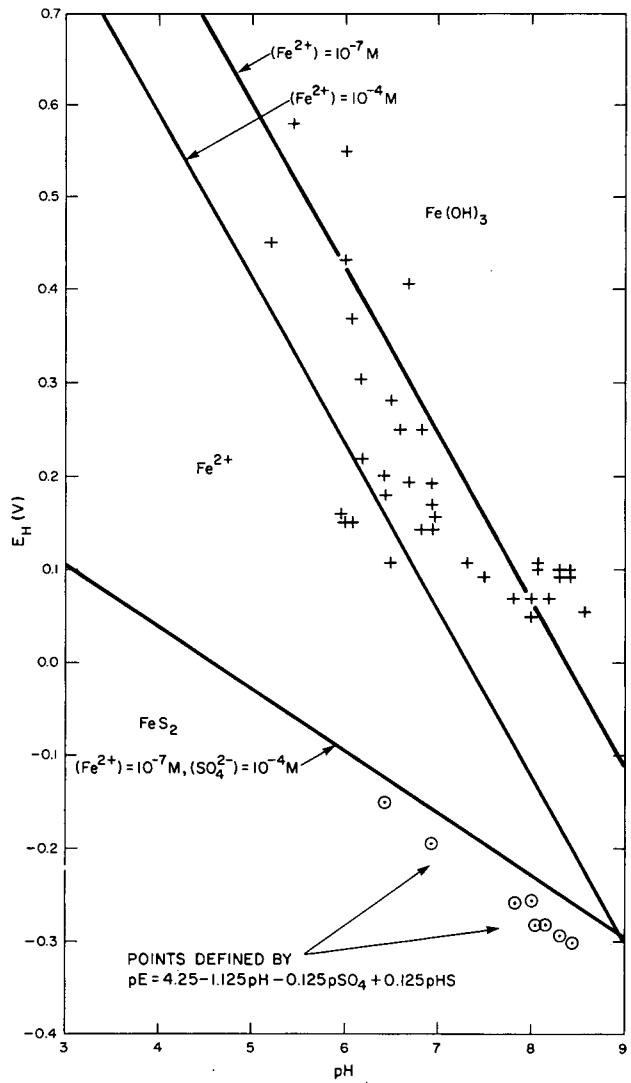

Figure 22. An E_H/pH diagram for Fe-S-H_2O at 25°C.

The E_H and pH data from Table 15 are plotted in Figure 22. In the oxygenated groundwaters of the recharge area, little or no dissolved iron is measured; in those groundwaters in which both DO and iron are measured it is likely that the iron is in the form of ferric-organic complexes. While the redox level of the groundwater, as measured by a platinum electrode, drops, dissolved iron concentrations increase to approximately 10^{-4} *M* in the transition zone piezometers unaffected by surface water infiltration (e.g.,

O8, QB2, QA2). According to Figure 22, however, the lowering of the dissolved iron levels in the discharge area is not due to ferrous sulphide precipitation as previously concluded but to ferric hydroxide precipitation at the higher pH levels of the discharge area groundwaters.

The explanation of this anomaly is that the platinum electrode is not recording the redox level of any particular iron couple but is responding to some other redox system which produces a higher exchange current at the Pt electrode (Stumm and Morgan, 1970, pp. 356-368). In order that the Pt electrode respond to a particular redox couple [e.g., Fe(III)-Fe(II)] the following conditions must be met (Champ *et al.*, 1979; Stumm and Morgan, 1970, pp. 360-362):

(1) The couple must be electroactive, i.e., electron transfer reactions are rapid and reversible.
(2) Both members of the couple must be present at concentrations greater than about 10^{-5} *M*.
(3) There are no species (e.g., O_2, S^{2-}, Cl^-, CN^-, S^0) adsorbed onto the electrode surface, thereby affecting the measured potential.

In the case in point, while the Fe(III)-Fe(II) couple is indeed electroactive, dissolved Fe(III) is not likely to be present in sufficient quantities to satisfy condition (2). Furthermore, sulphide and colloidal sulphur adsorption onto the Pt electrode can readily affect the measured potential (Whitfield, 1974; Boulegue, 1977). Consequently, the measured potential probably represents a mixed potential "not amenable to quantitative interpretation" (Stumm and Morgan, 1970, p. 362), as has been attempted in Figure 22.

Another estimation of the redox level of groundwaters in the discharge area may be obtained by computing an equilibrium or redox potential for the $SO_4^{2-} - HS^-$ system from the reaction (Stumm and Morgan, 1970, p. 310):

$$SO_4^{2-} + 9H^+ + 8e = HS^- + 4H_2O \qquad (47)$$

for which

$$pE = 4.25 - 1.125\ pH - 0.125\ pSO_4 + 0.125\ pHS \qquad (48)$$

Values of pE computed from Equation 48 were converted to equivalent E_H values using expression (42) and are presented in Table 18 as E_H (pE) together with the measured Pt electrode potential, E_H (Pt). Saturation indices for $Fe(OH)_3$ were determined for both values of E_H. The pE data points in Figure 22 indicate what the data of Table 18 confirm: if the sulphate-bisulphide couple accurately records the redox level of the groundwaters, then $Fe(OH)_3$ is undersaturated and must be dissolving in the transition and discharge areas of the aquifer. Therefore $Fe(OH)_3$ may only be a stable radionuclide sink in the groundwater recharge area. (N.B. If, as has been discussed, the method of sulphide measurement results in metal-sulphide precipitation, then S_T^{2-} will be underestimated. Therefore pHS and pE will be overestimated and the aqueous redox level will be more reducing. Consequently these conclusions are conservative.)

Although it is not necessarily the case that internal equilibrium between sulphate and sulphide is established in natural waters even with the aid of microbial catalysis (Champ *et al.*, 1979) or at the electrode surface, the points computed from expression (48) fall in the pyrite stability field of Figure 22, in qualitative agreement with the following empirical evidence:

(1) As previously mentioned, there is a loss from solution of approximately 0.1 mM of both dissolved iron and sulphate between the transition area and the discharge area.
(2) The groundwaters in the discharge area are supersaturated with respect to pyrite and, usually, mackinawite.
(3) Sulphate-reducing bacteria have been identified in these groundwaters (D.R. Champ, CRNL, personal communication).

Table 18. Comparison of the Saturation Indices for $Fe(OH)_3$ Based on Pt Electrode vs. SO_4^{2-}/S^{2-} Potentials*

Piezometer	Sample	E_H(Pt)	$\log_{10}$SI $Fe(OH)_3$	E_H(pE)	$\log_{10}$SI $Fe(OH)_3$
NA2	76-08	0.20	+0.2	-0.15	-6.0
NA3	76-08	0.05	+1.5	-0.26	-4.1
O8	76-11	0.19	+1.6	-0.19	-5.2
KNEW2	76-11	0.07	+0.7	-0.26	-5.3
KNEW2	77-11	0.07	+1.5	-0.28	-4.7
KO4	77-10	0.09	+2.0	-0.30	-4.3
KO5	77-10	0.11	+2.4	-0.28	-4.4

*Computation by WATEQF; $Fe(OH)_3 = Fe^{3+} + 3OH^-$, pK = 37.1 at 25°C.
E_H values in volts.

(4) Coupled scanning electron microscopy/X-ray elemental analysis (Davidson, 1978) of aquifer sediments has identified crystals composed of iron and sulphur.

At this point it is worth stating that Pt electrode measurements are of *qualitative* value in groundwater quality studies (Champ *et al.*, 1979) provided that

> the pretreatment of the electrode surface prior to measurement is reproduced; samples are measured in airtight flow cells; the electrode surface/solution interface has equilibrated. Under such conditions, meaningful E_H values can be obtained that provide a qualitative description of the redox state of ground waters; 'natural media that contain large quantities of oxidizing agents certainly give measurements of high E_H values and those containing large quantities of reducing agents have low potentials' (Stumm, 1967, p. 291).

In future groundwater quality studies it is recommended that E_H measurements be coupled with DO and S_T^{2-} measurements, as the latter measurements give an independent assessment of the redox level of a groundwater by their presence or absence as well as by their absolute concentrations. Furthermore, as is discussed in the following paragraphs, they are important as "immobilizing ligands" in their formation of metal oxides and sulphides.

These results and the closed-system redox model suggest that three distinct redox zones may exist in confined aquifers. The three zones shown in Figure 23 are identified as the oxygen, iron-manganese and sulphide zones. Upon recharge to the groundwater flow system oxygen is present in the groundwater but is rapidly reduced by organic carbon. Subsequently, the hydrous oxides of iron and manganese dissolve in the more reducing anoxic environment, and thus the iron and manganese become mobile in solution as Fe(II) and Mn(II). When the E_H drops sufficiently to permit the proliferation of sulphate-reducing bacteria, sulphide appears in solution, reducing the concentration of dissolved iron and manganese by their precipitation as insoluble sulphides.

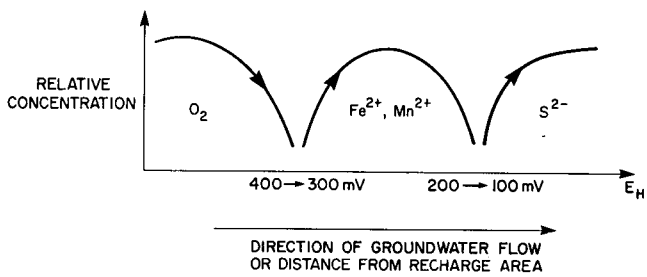

Figure 23. Redox zones in a confined aquifer.

The mobility in groundwater flow systems of the multivalent transition metals (e.g., Co, Ni, Cu, U as well as Fe and Mn) and the multivalent nonmetals (e.g., As, S and N) varies in each of these zones. In the oxygen zone, the mobile elements are those that form higher valent, soluble oxyanions (e.g., N, As, S and U), whereas the immobile elements are those that form higher valent, insoluble metal oxides (e.g., Fe and Mn). As the hydrous oxides of iron and manganese dissolve under more reducing conditions, it is conceivable that transition elements incorporated into these oxides, such as zinc, cobalt, nickel and copper, will appear in solution (Suarez and Langmuir, 1976). In the sulphide zone, the immobile elements are those forming lower valent, insoluble metal sulphides (e.g., Fe, Mn, Co, Ni, Cu and As).

Precipitation-Dissolution Reactions

Apart from ferrous sulphide precipitation, mineral precipitation-dissolution reactions involving carbonates and silicates are of interest in this study.

The data in Table 16 suggest that in its 10- to 20-year residence time in the flow system, the groundwater approaches equilibrium with respect to aragonite (and calcite) and becomes supersaturated with respect to $SrCO_3$. Whether this apparent supersaturation is real is uncertain; it may be due to analytical error or incorrect thermodynamic data. The important point to be drawn from these data, however, is that in certain zones of the aquifer system it is entirely possible that ^{90}Sr may be precipitated from solution as $^{90}SrCO_3$. Among these zones is that part of the lower sand aquifer in which the 1955 ^{90}Sr deep plume is migrating; this particular zone is shown in Figure 15 in the area of piezometers QA3, QA4 and NA3—all of which have groundwaters saturated with respect to $SrCO_3$.

There is no evidence of pronounced geochemical weathering occurring within the aquifer sediments. Scanning electron microscopy coupled with X-ray analysis permitted the identification of amorphous minerals on quartz grains (Davidson, 1978); yet their exact chemical composition is unknown. [N.B. Thermodynamic calculations (Table 16) indicate undersaturation of silica gel.] Since the silicate minerals, which compose the larger part of the aquifer sediments, have been in place for approximately 10 000 years, no fresh surfaces are developing. Consequently the dissolution rate of the feldspars should be low compared with that of the carbonate minerals present in the aquifer sediments; in the sequence of events of feldspar weathering recognized by Busenberg and Clemency (1976), these minerals should have reached the final or "steady-state stage characterized by the very slow release of cations and silicic acid."

Radionuclide Adsorption

In Chapter 4, the groundwater quality data were analyzed in terms of complexation, acid-base, redox and precipitation-dissolution processes in aqueous solutions. In this Chapter, the adsorption-desorption processes affecting ^{90}Sr and ^{137}Cs mobility in the lower Perch Lake basin are examined. It is shown that it is possible to obtain undisturbed core samples of contaminated, cohesionless aquifer sediments; these sediments may be processed to separate interstitial waters from the associated sediments; and simple chemical and mineralogical analyses of these two phases can yield information on the adsorption-desorption processes affecting radionuclide mobility in the aquifer.

METHODS

The procedure developed at CRNL to obtain undisturbed samples of contaminated aquifer materials is shown in Figure 24.

The core tube of a cohesionless sediment sampler [similar to that described by Parsons (1960)] was driven into the aquifer sediments exposed at the bottom of a borehole, 15 cm I.D. The core tube (Figs. 25 and 26), made of thin-walled aluminum, 5 cm I.D. and 1.5 m long, was then raised to the surface, capped, dried and monitored for alpha (α) and gamma (γ) radioactivity. In this manner at least 90% of the potential 1.5 m of cohesionless sediment was recovered with each core. The core tube was taken to a field laboratory where it was cut into sections (Fig. 27) within 20 min of coring to permit separation of the interstitial waters from the associated sediments. This subsequent step was conducted using immiscible fluid displacement (Patterson *et al.*, 1978) and centrifuge extraction (Edmunds and Bath, 1976) techniques.

Immiscible fluid displacement of a 30-cm core (Fig. 28) was conducted using a small mechanical press and a squeezer base into which the core tube was fitted.

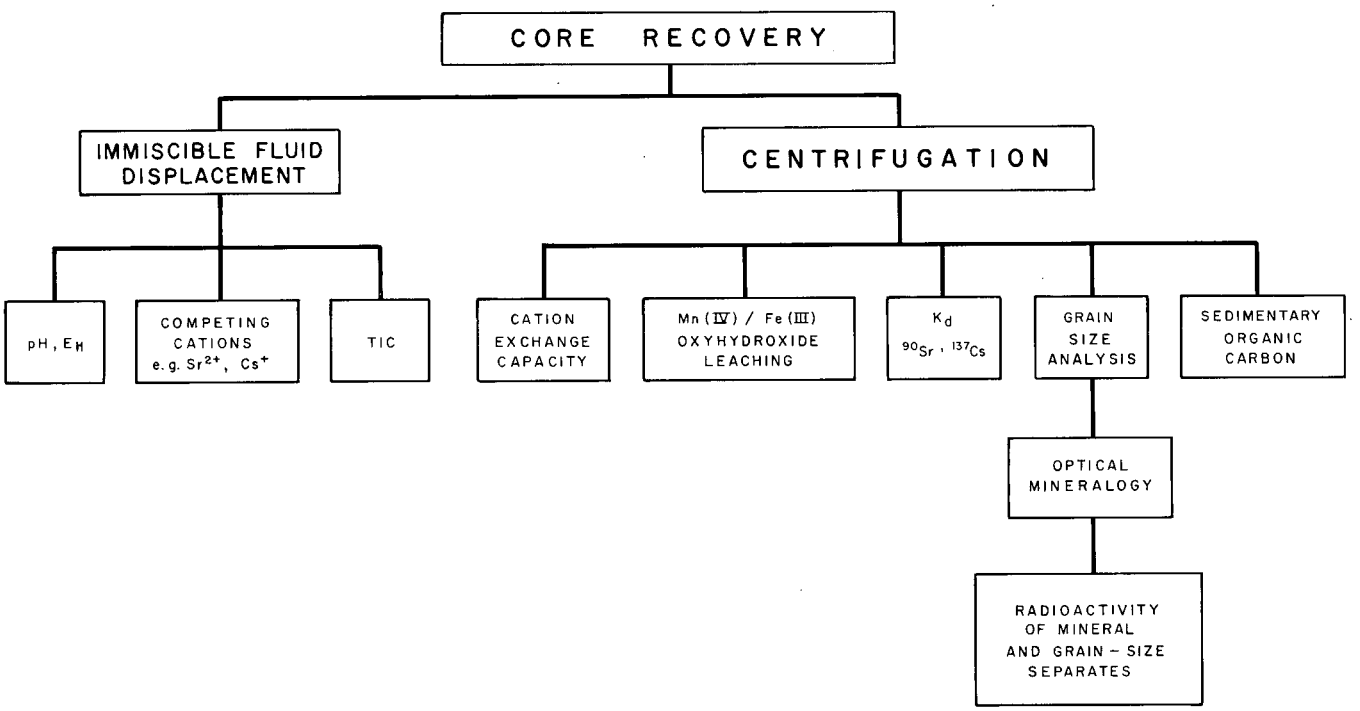

Figure 24. Flowchart of contaminated sediment analyses.

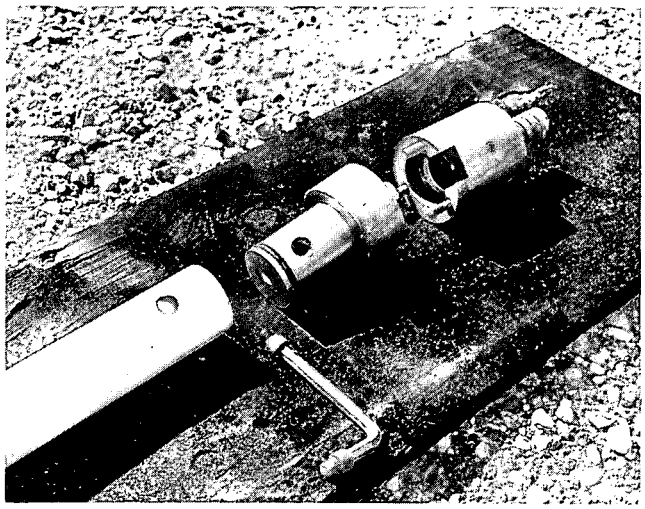

Figure 25. *Top right*, exploded view of cohesionless sediment sampler showing head with exposed rubber valve, which is forced with nitrogen gas pressure against the adjacent neck. The closing of this valve permits the withdrawal of the core tube, *lower left*, without loss of sediment. (Photo courtesy of AECL.)

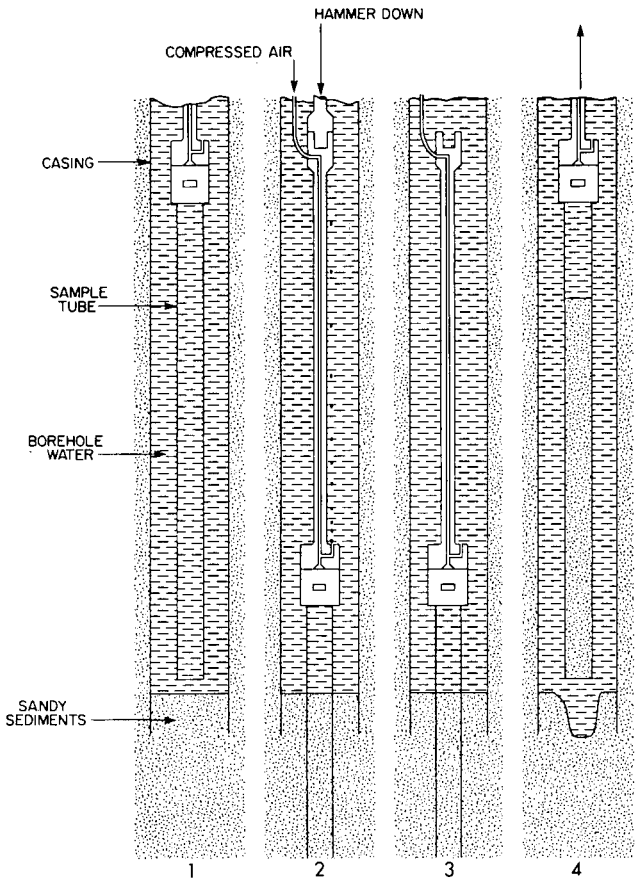

Figure 26. Operation of cohesionless sediment sampler. *1*–Sampler being lowered. *2*–Sampler driven beyond end of casing. Air pumped in to close valve above sample. *3*–Driving rods removed. *4*–Sample tube withdrawn and being lifted to surface.

The fluid used, Rohm and Haas Paraplex G-62, however, left the sediments in an oil-covered state, worthless for chemical or mineralogical analyses. Approximately 100 mL of filtered interstitial water was collected in several disposable syringes, which were then stored in water at 4°C prior to analysis. These samples were analyzed for (1) pH and E_H, using a flow cell and combination glass and Pt electrodes (from Orion Research Inc.) connected to an Orion model 801A voltmeter (Fig. 29); (2) competing cations, determined by neutron activation analysis (Merritt, 1971); and (3) total inorganic carbon (TIC), determined using an Oceanography International Total Carbon Analyzer.

Centrifuge extraction of interstitial waters in the core sections was conducted in the laboratories of the Environmental Research Branch at CRNL. The 6-cm core sections were fitted (Fig. 30) with polycarbonate cups and caps and centrifuged at 10 000 rpm (~8000 x g) three times for 20 min at 5°C. The centrifuge extraction technique complemented the immiscible fluid displacement technique in

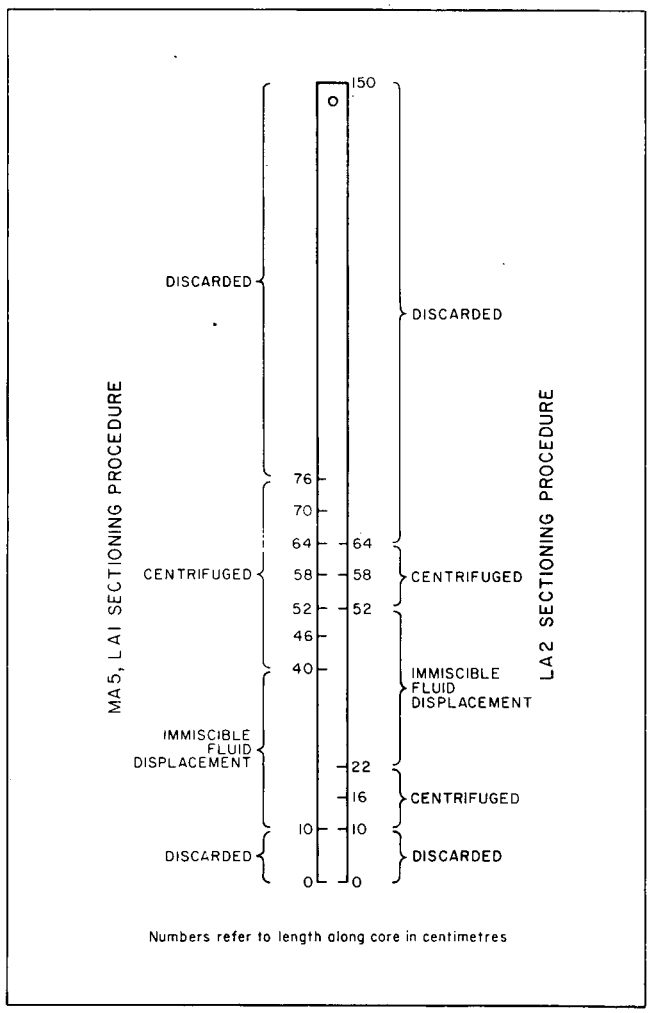

Figure 27. Sectioning procedures for MA5, LA1 and LA2 cores.

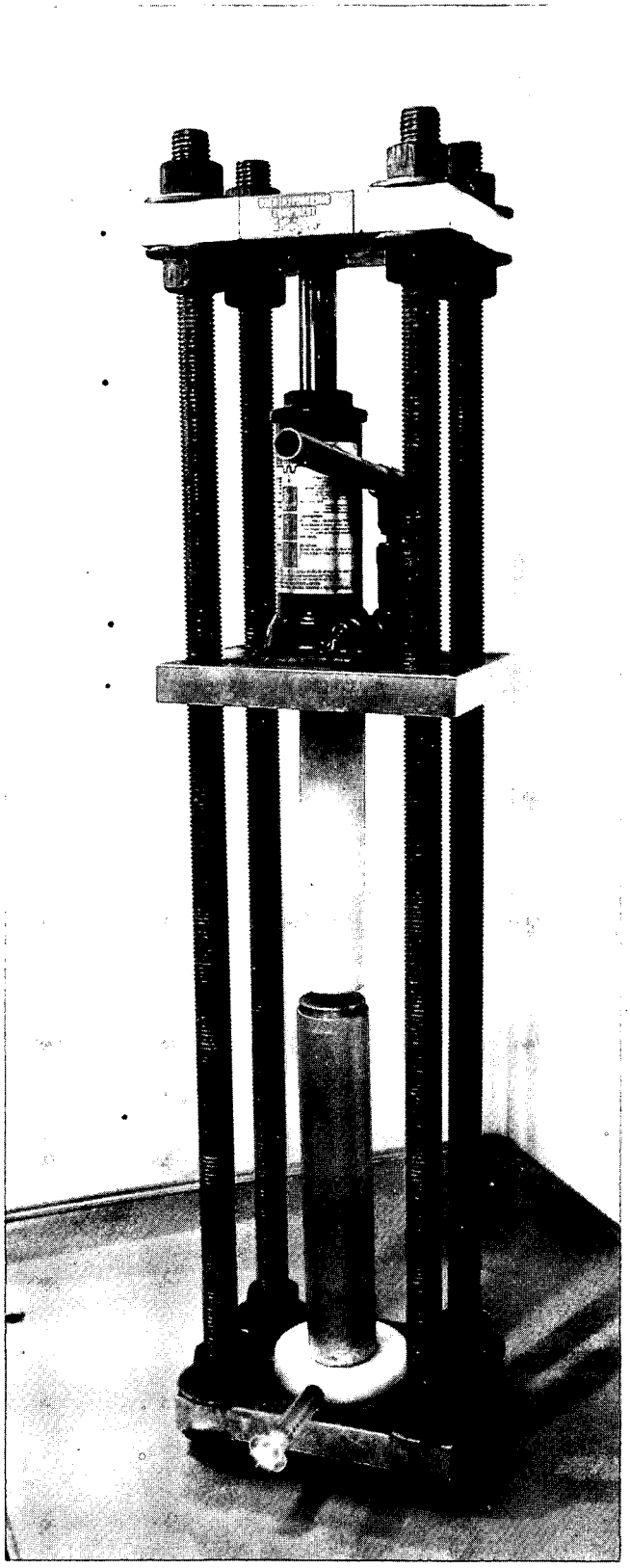

Figure 28. A 30-cm section of core prepared for the immiscible displacement of interstitial waters using Paraplex. (Photo courtesy of AECL.)

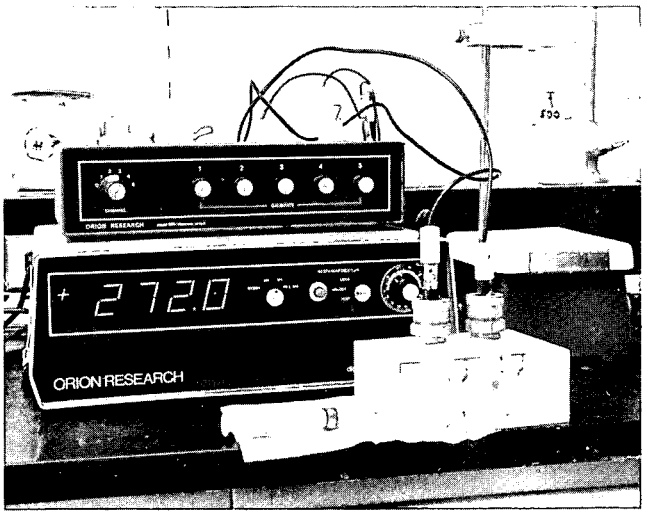

Figure 29. Measurement of pH and E_H of interstitial waters obtained from contaminated aquifer sediments by immiscible fluid displacement. (Photo courtesy of AECL.)

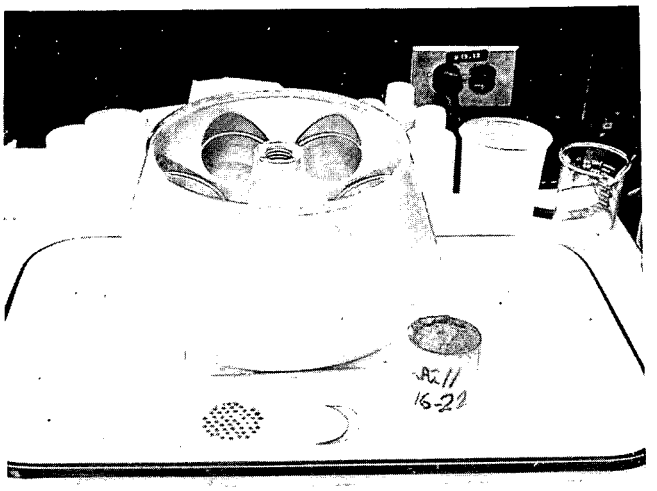

Figure 30. Apparatus for centrifuging contaminated aquifer sediments: *background*, centrifuge head with, *foreground*, *left to right*, centrifuge cup, aluminum support screen, filter paper and stainless steel support screen, 6-cm core and cap. (Photo courtesy of AECL.)

that the former provided dry sediment and the associated interstitial waters, which had, however, been exposed to the atmosphere during centrifugation and were therefore analyzed for only ^{90}Sr and ^{137}Cs; the latter technique provided an unexposed interstitial water sample which was analyzed for stable ions. Dry sediment and the associated interstitial waters obtained by centrifugation were used for subsequent chemical and mineralogical analyses, as shown in Figure 24. Groundwater and sediment aliquots from

adjacent 6-cm core sections were mixed in equal amounts following centrifugation. Mixed samples, made up from either two adjacent 6-cm core sections (LA1/3,4; LA2/1,2) or six adjacent core sections (MA5/1,2,3,4; LA/1,2), were analyzed using the following methods.

The total nonselective cation-adsorption capacity of the sediments was estimated by the cation-exchange capacity, which was measured using a modification of the U.S. Geol. Surv. method (Beetem *et al.*, 1962). Aquifer sediment (100 mg) was placed in a 20-mL plastic scintillation vial and saturated with 1 *N* $CoCl_2$ containing 0.1 mCi ^{60}Co/L. The vials were agitated gently overnight in such a manner as to avoid intergranular movement; the sediment was retained on a filter, washed with absolute alcohol and counted in a Packard Auto-Gamma Spectrometer.

Leaching experiments (Table 19) were conducted to determine the amount of adsorbed radioactivity that (1) was exchangeable with 0.5 *M* $CaCl_2$, (2) was adsorbed to Fe(III) and Mn(IV) oxyhydroxides (~0.1% and ~0.001% by weight of sediments, respectively), and (3) remained fixed following the desorption of the exchangeable and the oxyhydroxide-adsorbed activity. For these purposes the methods of Suarez and Langmuir (1976) were modified as follows.

A 30-g sample of contaminated sediment was counted (column A, Table 19) and placed in a 250-mL polycarbonate Erlenmeyer flask which had been washed with HCl and rinsed with distilled, deionized water. To determine amounts of exchangeable activity, 100 mL of 0.5 *M* $CaCl_2$ was added to each flask, which was agitated gently for three days; the supernatent (pH ~ 6) was decanted and counted (column B). The sediment was washed several times with distilled, deionized water and a 1-g portion was taken for counting (column C); the supernatent was discarded. Another 1-g portion of the washed sediment was dried overnight at 40°C. To determine amounts of oxyhydroxide-adsorbed activity, a 250-mg fraction of this dried sediment was placed in a scintillation vial with 15 mL of 0.1 *M* $NH_2OH \cdot HCl$ in 0.1 *M* $KOCOCOOH \cdot HCOCOOH \cdot 2H_2O$, which acts as a pH buffer (pH ~ 1.5) and as a reducing and complexing agent, and gently shaken overnight. The supernatent was extracted, counted (column D) and analyzed for dissolved iron and manganese by atomic absorption spectrophotometry; the sediment was counted to determine the fixed activity (column E).

Distribution coefficients for ^{90}Sr and ^{137}Cs were determined on the basis of Equation 31 using water and sediment samples obtained by centrifugation. Samples containing ^{137}Cs were counted directly using 20 g or 100 mL of sample inserted into a large, low background GeLi γ detector. A standard radiochemical procedure for ^{90}Sr isolation was used (Grummitt and Milton, 1957); Sr was determined by carbonate precipitation followed by fuming nitric acid separation employing 25 mL of interstitial water and 1 g of sediment (2 *N* HNO_3 extraction) and then counted in a low background β counter after 15 days to permit the growth of the yttrium daughter. All centrifuged waters were destructively analyzed in the course of this analysis.

Grain size and mineralogic separations and analyses of the contaminated aquifer sediments were conducted using dry sieving and optical methods, respectively. Sedimentary organic carbon was determined using an Oceanography International Total Carbon Analyzer.

RESULTS

Data from these methods of analysis are presented in Tables 19 to 24. The purpose of this section is to consider the reliability of the data whenever possible, using the range between duplicate samples as a measure.

The leaching experiments (Table 19) were conducted using six different cores. Samples from four cores (MA5/1, 2,3 and LA1/2) were mixed samples (see "Methods") which were analyzed in duplicate. These samples show only minor variability. Samples from two cores (LA1/4, LA2/2) contaminated with ^{137}Cs as well as ^{90}Sr were not mixed but were taken from adjacent 6-cm core sections and show considerable variability in adsorbed radioactivity between sections. An inspection of the ^{137}Cs data in Table 21 shows that differences in radioactivity between adjacent core sections may be as much as two or three orders of magnitude. It is not clear why B + C ≠ A and D + E ≠ C in Table 19; it may be due to different counting efficiencies for aqueous (B, D) and sediment (A, C, E) samples. Consequently, while the values in columns A, C and E are comparable as are those in B and D, it may not be meaningful to compare the absolute values of all five columns.

The reproducibility of data by analysis in duplicate of the aqueous and adsorbed ^{90}Sr radioactivities, which together yield the distribution coefficient (Table 20), was such that the standard deviations are generally 10% and 20% of the respective means. Because of constraints on the availability of the γ-counting equipment, ^{137}Cs was not analyzed in duplicate. The overall range in both ^{90}Sr and ^{137}Cs distribution coefficients is one order of magnitude or less. This is the same scale of variability that is found in other hydrogeological variables (e.g., dispersivity and velocity) appearing in solute transport equations; consequently this variability should not present a significant problem in the modeling of solute transport.

Table 19. Adsorbed Radioactivity (total β in counts per minute per gram, i.e. $^{90}Sr + ^{137}Cs$) Associated with Exchangeable, Oxyhydroxide and Fixed Phases

Core No.	A	B	C	D	E
(1) MA5/1 (1)	1 520 (0)	787	530	200	114
(2) MA5/1 (2)	1 510 (0)	693	370	195	85
(3) MA5/2 (1)	840 (0)	420	340	183	105
(4) MA5/2 (2)	820 (0)	357	320	125	112
(5) LA1/2 (1)	1 660 (0)	807	680	338	155
(6) LA1/2 (2)	1 640 (0)	870	610	333	126
(7) MA5/3 (1)	695 (0)	97	230	203	123
(8) MA5/3 (2)	810 (0)	97	210	195	114
(9) LA1/4 (64-70)	22 440 (57)	823	20 500 (59)	15 524	5030 (25)
(10) LA1/4 (70-76)	16 510 (42)	563	13 860 (34)	10 363	2683 (13)
(11) LA2/2 (52-58)	14 120 (38)	460	7 900 (26)	5 082	3940 (12)
(12) LA2/2 (58-64)	7 890 (17)	203	3 310 (10)	2 840	1160 (4)

A–Raw sediment containing exchangeable, oxyhydroxide and fixed activity.
B–Exchangeable activity.
C–Residual sediment activity, i.e., oxyhydroxide-adsorbed and fixed activity.
D–Oxyhydroxide-adsorbed activity.
E–Fixed activity.

Note: The γ activity (i.e., ^{137}Cs) is written in parentheses (units: nCi/g) in columns A to E.

Table 20. Distribution Coefficients for ^{90}Sr Obtained by Centrifugation of Cores from Sites MA and LA

Core No.	Core depth (m)	^{90}Sr (cpm/g) Mean	^{90}Sr (cpm/g) S.D.	^{90}Sr (cpm/mL) Mean	^{90}Sr (cpm/mL) S.D.	K_d^{Sr} (mL/g)
MA5/1	(5.3-5.6)	2816	20	655	18	4
MA5/2	(6.9-7.2)	1389	213	331	57	4
MA5/3	(8.3-8.6)	1682	1590	221	73	8
MA5/4	(10.0-10.3)	130	97	5	0	26*
LA1/1	(5.3-5.6)	19	11	0.6	0.5	32*
LA1/2	(6.9-7.2)	3757	442	264	16	14
LA1/3	(8.6-8.8)	1284	157	115	–	11
LA1/4	(9.9-10.0)	2551	1160	284	10	9
LA2/1a	(8.9-9.0)	946	390	70	–	14
LA2/1b	(8.5-8.6)	1599	94	86	–	19
LA2/2a	(10.4-10.6)	1160	185	210	16	6
LA2/2b	(10.0-10.2)	1617	250	234	23	7

*The low radioactivity values of these samples result in questionable K_d values.
S.D. = Standard deviation.

Table 21. Distribution Coefficients for ^{137}Cs Obtained by Centrifugation of Cores from Site LA

Core No.	Core depth	^{137}Cs (pCi/g)	^{137}Cs (pCi/mL)	K_d^{Cs} (mL/g)
LA1/4a	(9.9-10.0)	41 387	151	274
LA1/4b	(10.2-10.3)	28 490	122	234
LA1/4c	(10.2-10.3)	601	4	150
LA2/2a	(10.0-10.2)	38 146	73	523
LA2/2b	(10.5-10.6)	1 167	22	53

Table 22. Chemical Analysis of Interstitial Waters Derived by Immiscible Fluid Displacement *

Core No.	pH	E_H	TIC	Ca^{2+}	Sr^{2+}	Ba^{2+}	Cs^+ ($\times 10^6$)	Rb^+	Mean sample depth (m)
MA5/1	3.6	0.7	9.8	4.2	0.024	0.008	4	0.005	5.8
MA5/2	6.1	0.2	11.0	N.D.	0.039	0.028	15	0.005	7.3
MA5/3	6.3	0.1	15.2	15	0.064	0.054	106	0.009	8.8
MA5/4	6.5	0.3	18.4	18	0.073	0.062	134	0.009	10.4
LA1/1	6.9	0.2	4.6	6.8	0.015	0.007	4	0.002	5.8
LA1/2	6.2	0.4	8.4	12	0.050	0.025	9	0.008	7.3
LA1/3	6.4	0.3	6.4	7.0	0.031	0.026	15	0.012	8.8
LA1/4	6.3	0.3	18.6	N.D.	0.043	0.032	9	0.012	10.4
LA2/1	6.0	0.2	10.2	9.2	0.063	0.034	13	0.009	8.8
LA2/2	6.0	0.4	13.7	4.8	0.025	0.006	3	0.004	10.4
Blank HA†	5.5	–	N.D.	0.6	<0.001	<0.001	N.D.	0.0001	–
Blank GFA‡	8.9	–	0.7	0.4	<0.001	<0.001	N.D.	<0.0001	–

*All data in milligrams per litre except E_H in volts, $pH = -\log_{10}\{H^+\}$
†Blank using Millipore HA filter papers (LA2 samples).
‡Blank using Gelman filter papers (MA5 and LA1 samples).
N.D.—Not detected.

Table 23. Cation-Exchange Capacities of Contaminated Sediments (meq/100 g)

Core No.	Mean	Range*
MA5/1	0.92	0.84
MA5/2	1.16	1.06
MA5/3	1.05	0.90
MA5/4	1.74	1.20
LA1/1	0.76	0.18
LA1/2	1.18	0.10
LA1/3 (40-52)	0.95	1.04
LA1/3 (52-64)	0.46	0.02
LA1/3 (64-76)	1.50	1.36
LA1/4 (40-52)	0.81	0.46
LA1/4 (52-64)	0.74	0.40
LA1/4 (64-76)	0.56	0.10
LA2/1 (10-22)	1.00	0.68
LA2/1 (52-64)	0.44	0.06
LA2/2 (10-22)	0.86	0.60
LA2/2 (52-64)	0.34	0.02

*Range between duplicate values.

The chemical analysis of the interstitial waters (Table 22) was affected by the contamination of MA5 and LA1 samples by the dissolution of materials in the Gelman GFA glass-fibre filter papers. This strongly affected the first syringe sample taken which was used for pH and E_H measurements; the pH and E_H values reported are from the second or third syringe sample for which the pH was significantly less than the first. The GFA filters also affected TIC and Ca^{2+} values, as is shown by the values of the blanks run through the squeezer system. (Gelman GFA filter papers were used during the displacement of the MA5 and LA1 interstitial waters; Millipore HA filter papers were used for the LA2 cores.) The range between TIC duplicates was usually <1 mg/L. The low pH and high E_H of the MA5/1 sample cannot be explained. The cation data from neutron activation analysis were computed using an internal standard (Merritt, 1971).

Considerable variability was observed in the cation-exchange capacity data (Table 23). While this variability may be due to improper washing or to unsatisfactory sample mixing procedures which resulted in unequal amounts of mica being present in the duplicates, it would probably be advisable to increase the sample weight for low-exchange capacity sediments to 1 g from the 200-mg weight suggested by Beetem *et al.* (1962). Notwithstanding this variability, the absolute values (i.e., ~1 meq/100 g) measured are similar to those obtained using the ammonium-acetate method on sediments taken from the Middle and Lower Sands units at O piezometer nest (Jackson and Cherry, 1974).

Mineral abundance estimates on the grain size fractions (Table 24) employed several thousand grains per sample, giving a high degree of reliability. Therefore even the grain size separates with <1% of total weight (e.g., MA5/1, 1.25 ϕ fraction) contained 200 to 300 grains.

DISCUSSION

Interstitial Water Chemistry

Before the MA5 cores were taken, the initial hydrochemical conditions at the site (Fig. 31) were studied by sampling the ten MA multilevel piezometers (i.e., MA1-10) for temperature, pH, E_H, O_2 and conductance; chemical

Table 24. Radioactivity (total β) Associated with Various Grain Size Fractions and their Corresponding Mineral Quantities

Core No.	Grain size (ϕ)	% Weight	Radioactivity (cpm/100 mg)	% Mineral abundance*				
				Qtz.	Plag.	Ser.	Mica	Horn.
MA5/1 (5.5-m depth)	<1.25	<1	164	32	28	8	25	1
	1.25-2.0	12	50	52	27	11	8	<1
	2.0-2.5	37	38	43	36	8	10	2
	2.5-2.75	16	37	45	30	8	9	3
	2.75-3.0	12	41	39	30	4	14	4
	3.0-3.25	11	38	36	30	7	15	4
	3.25-3.5	5	54	32	23	6	15	8
	3.5-3.75	2	57	30	25	3	11	9
	3.75-4.0	1	84	29	33	2	17	5
	4.0-4.25	<1	86	23	33	2	15	11
	4.25-4.5	<1	147	28	29	6	22	7
MA5/3 (8.5-m depth)	<1.25	3	128	29	28	5	37	<1
	1.25-2.0	28	62	45	33	4	16	1
	2.0-2.5	34	26	47	35	5	10	<1
	2.5-2.75	13	29	50	30	5	6	2
	2.75-3.0	10	42	53	29	4	13	4
	3.0-3.25	7	48	42	30	5	12	6
	3.25-3.5	2	65	40	23	4	17	6
	3.5-3.75	1	132	40	21	4	16	8
LA1/4 (10.2-m depth)	<1.25	<1	978	13	15	9	63	<1
	1.25-2.0	16	140	45	30	11	10	<1
	2.0-2.5	40	91	52	29	10	5	1
	2.5-2.75	14	90	47	33	9	7	<1
	2.75-3.0	12	103	54	24	6	8	4
	3.0-3.25	9	109	50	25	5	10	5
	3.25-3.5	4	134	47	22	6	13	6
	3.5-3.75	2	197	46	19	6	15	7
	3.75-4.0	<1	215	48	19	4	14	7
	4.0-4.25	<1	276	40	24	2	20	7
	4.25-4.5	<1	821	42	23	4	18	7

*Abbreviations indicate quartz, plagioclase and sericitic feldspars, mica (muscovite + biotite) and hornblende, respectively.

analyses were conducted on samples from MA10, MA5 and MA1 (Table 15). These analyses showed that the interstitial waters associated with the contaminated sediments at MA are slightly acidic (pH 5.8-6.7) and, with the exceptions of MA5 and MA8, oxygenated (i.e., 0.4-5.0 mg O_2/L). Although TIC increases with depth, the sediments are undersaturated with respect to both aragonite and strontianite (Table 16); thus ^{90}Sr retardation owing to carbonate precipitation is unlikely in this part of the aquifer. With the exception of core MA5/1 the chemical data from immiscible fluid displacement (Table 22) are similar to those from sampling the piezometers. The hydrochemical conditions at LA are similar to those at MA.

Distribution Coefficients

The distribution coefficients for ^{90}Sr listed in Table 20 show no pattern of spatial variability. From the data, the mean $K_d^{Sr} \sim 10$ mL/g and the standard deviation (σ) ~ 5 mL/g. Data obtained in 1977 by a less reliable coring technique gave distribution coefficients of a similar value (see Table A-3 in Appendix). Furthermore, the mean plus one standard deviation values for K_d^{Sr} include within their range the early field-mapping and radiochemical analysis estimates (Table 10).

High γ radioactivity due to ^{137}Cs was only detected below 10 m at LA; analysis of cores LA1/4 and LA2/2 produced values ranging over one order of magnitude with mean $K_d^{Cs} \sim 250$ mL/g, $\sigma \sim 180$ mL/g. It is interesting to note that in the LA2/2 sample, which contained 100 pCi ^{137}Cs/L ($\sim 10^{-12}$ g/L), the radioion was present at concentrations four orders of magnitude less than the stable ion (Table 22).

The effect of variations in the stable Sr and Cs concentrations on the measured K_d's is not discernible in the data. Furthermore, it is not possible to compute selectivity quotients (Equation 58) because the competing cation (i.e., stable Sr^{2+} and Cs^{+}) data are obtained from a different part of the core than the K_d data (Fig. 27); significant

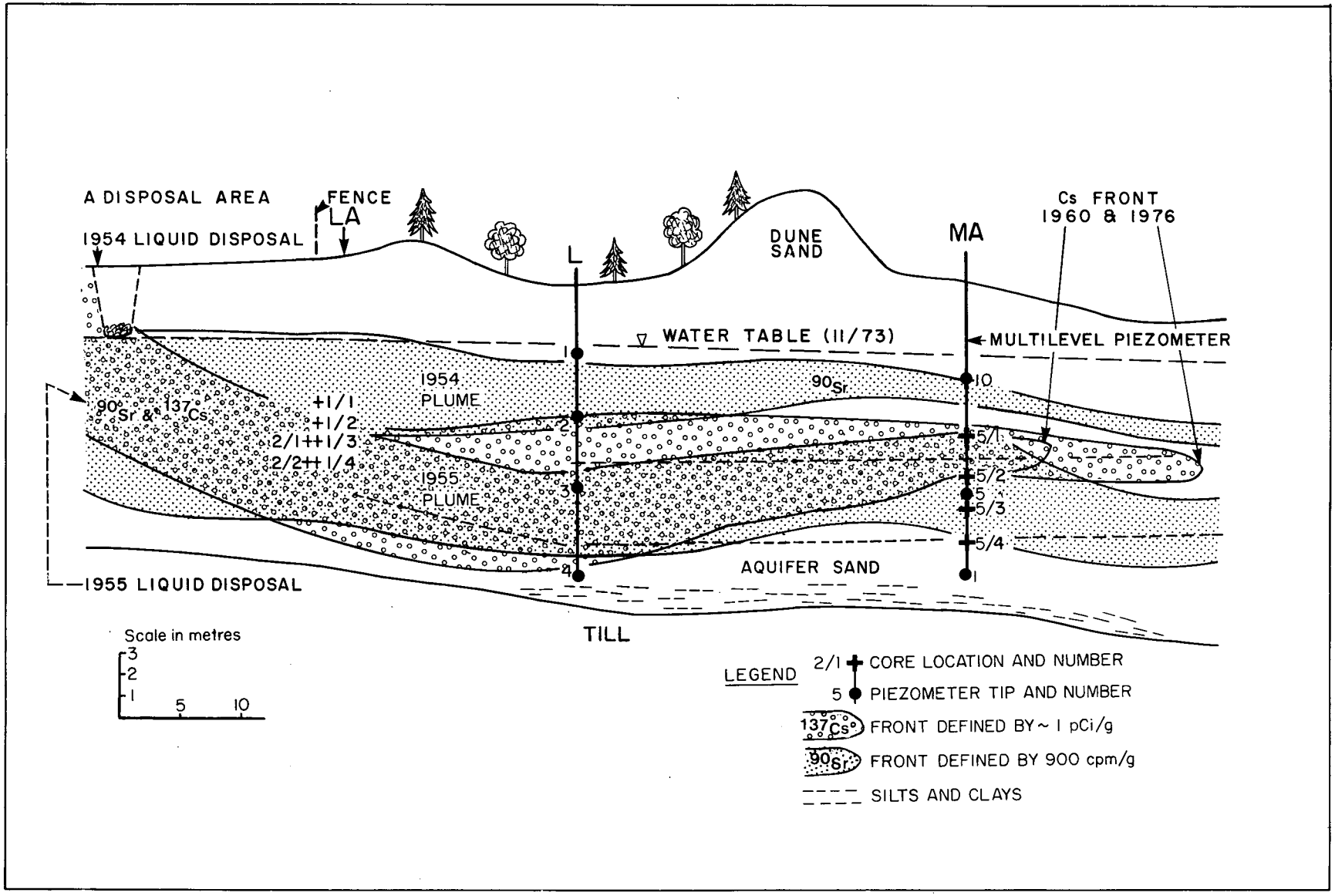

Figure 31. Location of LA and MA cores and configuration of ^{90}Sr and ^{137}Cs plumes.

longitudinal variations in adsorbed radioactivity (Tables 19, 20 and 21) indicate that it is inappropriate to use the two sets of data in the same equation. It is concluded that studies of this kind must be done in the finest possible detail in order that the geochemical controls are understood. Consequently, the hypothesis of Gillham *et al.* (1978) concerning competing cations could not be tested.

Mineralogical Controls on Adsorbed Radioactivity

Grain size analysis of contaminated aquifer sediments collected during the 1977 field season (Appendix, Table A-4) showed that the radioactivity tended to be preferentially adsorbed by the fine and coarse fractions on a basis of equal weight; taken together, however, these fractions ($\phi \leq 1.25$ and $\phi > 4.0$) comprise less than 3% of the total sediment weight. It was found that the high level of adsorbed radioactivity in the coarse fraction was due to relatively large amounts of mica, which was three times as radioactive per gram as the whole sediment.

These observations were confirmed during the 1978 field season (Table 24). Once again the coarse fraction proved to contain relatively high amounts of adsorbed radioactivity, which can be ascribed to correspondingly great abundances of micaceous minerals (muscovite and biotite). The preferential adsorption of radioactivity by the fine fraction may be expected on the basis of its relatively high surface area per unit weight. The micaceous minerals seem to be of importance in accounting for this high adsorption.

The radioactivity associated on a grain-for-grain basis with quartz, feldspar and mica is shown in Table 25; this demonstrates that each grain of biotite (and any interstratified vermiculite) adsorbed more radioactivity than each grain of similar size of feldspar (plagioclase, sericite and K-Fs). Quartz is a relatively poor adsorbent. Since the feldspars are several times as abundant in the aquifer sediments as biotite, however, most radioactivity, or at least most ^{90}Sr, is probably adsorbed by the feldspars.

Since samples MA5/1 and MA5/3 are contaminated with ^{90}Sr and not ^{137}Cs, the micas and feldspars are the important sinks for ^{90}Sr; this conclusion is in accord with Tamura's (1972) data which are reproduced in Table 8. The association of high ^{137}Cs adsorption by sediments (e.g., LA1/4) with abundant layer silicates has been well established (see Chapter 2). X-Ray diffraction analyses of contaminated sediments from this aquifer system have shown (Fig. 32) that vermiculite is interstratified with the mica; as such, the cation-exchange capacities and ^{137}Cs selectivity (Table 9) of mica-vermiculite probably would be enhanced over those of the unaltered mica.

Desorption Experiments

The desorption of the adsorbed radionuclides was conducted by the use of specific leaching agents. To recapitulate, the contaminated sediments were leached of exchangeably adsorbed radioactivity with 0.5 *M* $CaCl_2$ and then leached of radioactivity adsorbed to iron and manganese oxyhydroxides [e.g., FeOOH, $Fe(OH)_3$, $MnO(OH)_2$, MnO_2] by dissolving the oxyhydroxides with acidified (pH $\sim$ 1.5) hydroxylamine hydrochloride. In this manner it was possible to identify the relative amounts of adsorbed radioactivity that were exchangeable, adsorbed to Fe(III) and Mn(IV) oxyhydroxides or remained fixed. The results are shown in Table 19.

The data divide readily into two groups—the first (samples 1-8) contaminated with only ^{90}Sr and the second (samples 9-12) contaminated with both ^{90}Sr and ^{137}Cs. Whereas most of the ^{90}Sr is readily exchangeable (on the

Table 25. Radioactivity (total β in counts per minute per grain) Associated with Various Minerals of the 20- to 60-mesh (0.25-0.84 mm, 0.25-2.0 ϕ) Fraction

Core No.	Depth (m)	Quartz	Feldspar*	Mica
MA5/1	(5.3-5.6)	1.0	3.5	6.0 (mainly biotite)
MA5/3	(8.3-8.6)	0.2	1.4	1.6 (mainly biotite)
LA1/2	(6.9-7.2)	0.1	1.6	0.3 (muscovite) 1.4-2.6 (biotite)
LA1/4†	(10.2-10.3)	0.1	0.9	0.1 (muscovite) 1.9 (biotite)

*Includes sericitic plagioclase, plagioclase and K-feldspars.
†Sample LA1/4 contains significant quantities of ^{137}Cs; the other samples contain only ^{90}Sr.

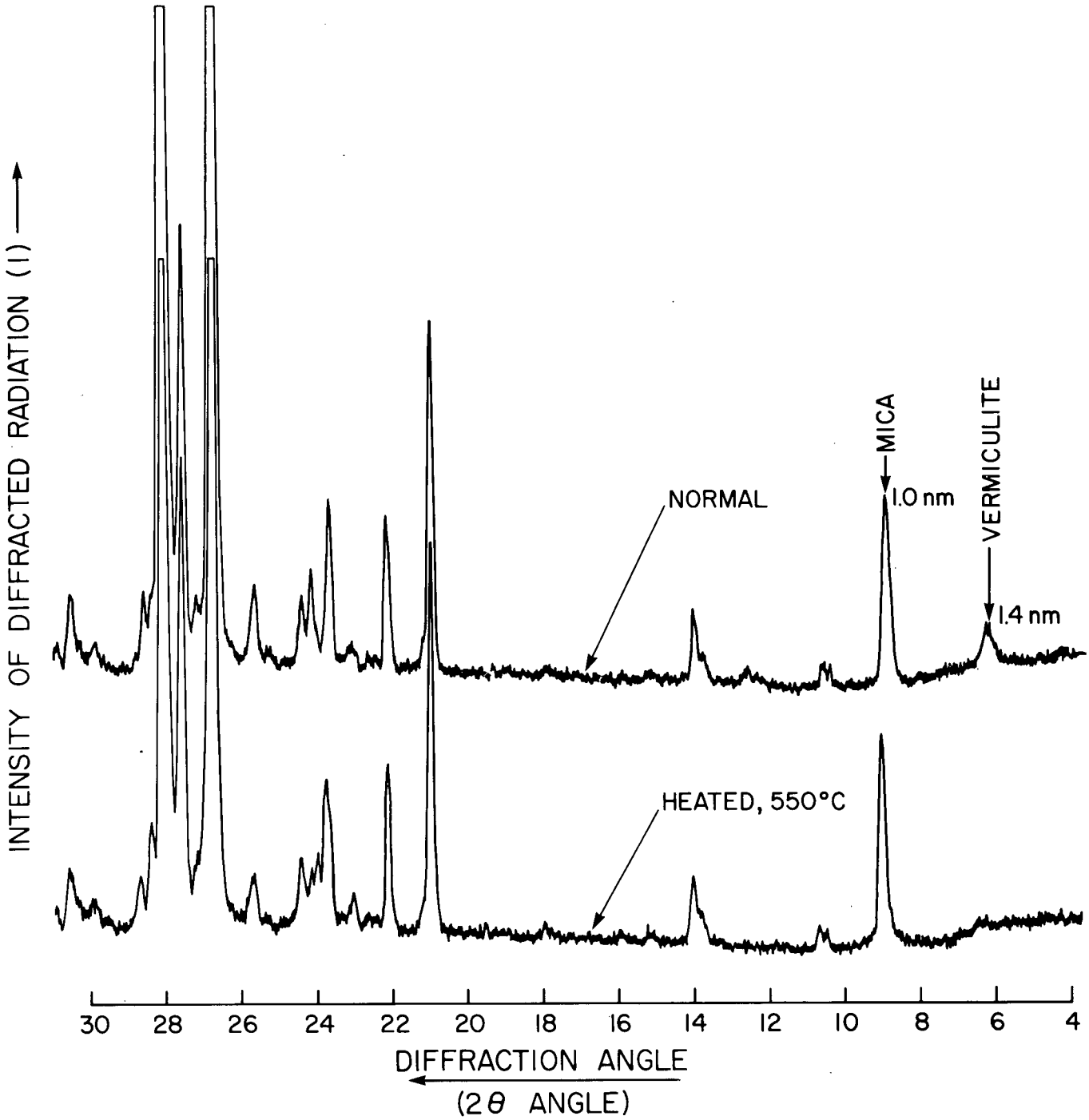

Figure 32. X-Ray diffractogram of sediment core MA5/1.

basis of columns A and C, samples 1-8), most ^{137}Cs is either adsorbed to oxyhydroxides or fixed (columns A and C, samples 9-12). Approximately twice as much ^{90}Sr appears to be adsorbed to oxyhydroxides as is fixed.

The fixed activity of the sediments contaminated with ^{137}Cs may be explained by the presence of vermiculite and the micas (Francis and Brinkley, 1976). Furthermore, the apparent adsorption of ^{137}Cs by Fe(III) and Mn(IV) oxyhydroxides is consistent with its documented adsorption by "hydrous $MnO(OH)_2$" (Amphlett, 1964, p. 87). The very large percentage of extracted ^{137}Cs (35% to 57%) released by this treatment, however, may be partially an experimental effect. It is probable that the

acidified hydroxylamine hydrochloride solution (pH ~ 1.5) is causing structural damage to the layer silicates (Suarez and Langmuir, 1976, p. 591), thereby releasing some of the fixed activity.

In the case of the sediments contaminated with ^{90}Sr, it is well established that ^{90}Sr may be specifically adsorbed by Fe(III) and Mn(IV) oxyhydroxides (e.g., Egorov and Lyubimov, 1969; Tamura, 1964; Kinniburgh *et al.*, 1975), although again structural damage releasing trapped ^{90}Sr may have occurred. The fixed activity may be due to some silicate interface (Frere and Champion, 1967) such as mica which was not present in the samples of ^{90}Sr that Evans leached (Table 12). The possibility that ^{90}Sr is associated with an oxyhydroxide surface by bonding with an adsorbed complexing ligand (Davis and Leckie, 1978) such as sulphate cannot be discounted; it has been shown in Chapter 4, however, that the concentration of such a complex is extremely low. Therefore, in conclusion, the largest fraction of adsorbed ^{90}Sr, that which was exchangeable, may be assumed to be electrostatically adsorbed to feldspars and layer silicates such as biotite and vermiculite.

Adsorption of Radionuclides in Fractured Granites

These sediments are the physical weathering products of granitic rocks; as such, these conclusions are of relevance to the adsorption of radionuclides in fractured granites. It would appear that oxides, sulphides, carbonates and chlorites, all of which have been observed on the fracture surfaces of granites, are potential sinks for radionuclides. Furthermore, this study suggests that *in situ* desorption experiments using specific agents may indicate the nature of adsorption of injected radionuclide tracers by the fracture surfaces.

Summary of Conclusions

The pH, alkalinity, calcium, E_H, oxygen, iron, manganese and sulphur values observed in the groundwater flow system of the lower Perch Lake basin are consistent with those derived from closed-system (i.e., oxidant and CO_2) models of organic matter oxidation and calcite dissolution. The alumino-silicate aquifer matrix of feldspar and quartz seems to be relatively insoluble on a basis of mineral abundance; this conclusion is in accord with results from studies of the kinetics of feldspar dissolution.

In studies of groundwater quality or pollution it is recommended that E_H measurements be complemented with measurements of dissolved oxygen and sulphide; the latter give an independent assessment of the redox level of a groundwater by their presence or absence as well as by their absolute concentrations. Furthermore, both species are important in affecting contaminant mobility owing to the formation of metal oxides and sulphides.

Three distinct redox zones may exist in confined aquifers: oxygen, iron-manganese and sulphide. The mobility of multivalent transition metals (e.g., Co, Ni, Cu, U, Fe, Mn) and the multivalent nonmetals (As, S, N) varies in these zones. Geochemical engineering of backfill or contaminant barriers could create immobilizing zones in waste management areas.

Chemical and mineralogical analysis of radioactively contaminated aquifer sediments shows that most of the ^{90}Sr ($K_d \sim 10$ mL/g) is exchangeably adsorbed, primarily to feldspars and layer silicates; the rest is either specifically adsorbed to Fe(III) [and perhaps Mn(IV)] oxyhydroxides or fixed to unknown sinks (Fig. 33). In some parts of the aquifer system geochemical retardation of ^{90}Sr may be occurring due to the precipitation of $SrCO_3$. Less than one half of adsorbed ^{137}Cs is exchangeable with 0.5 *M* $CaCl_2$; the high levels of Cs adsorption and fixation ($K_d \sim 10^2$ mL/g) may be ascribed to the presence of the layer silicates vermiculite and biotite. Complexation reactions appear to be unimportant in affecting ^{90}Sr and ^{137}Cs transport and adsorption. These conclusions may be relevant to adsorption of radionuclides in fractured granite.

The methods of centrifuge extraction and immiscible fluid displacement were found to be complementary; analysis of the work reported herein, however, was constrained by sectioning procedures which provided contaminated sediments on a rather large scale compared with the fine scale of the variations in adsorbed radioactivity. The mixing of samples in cores MA5 and LA1 was a mistake; the fine detail of important geochemical and mineralogical controls on radionuclide adsorption was thus lost.

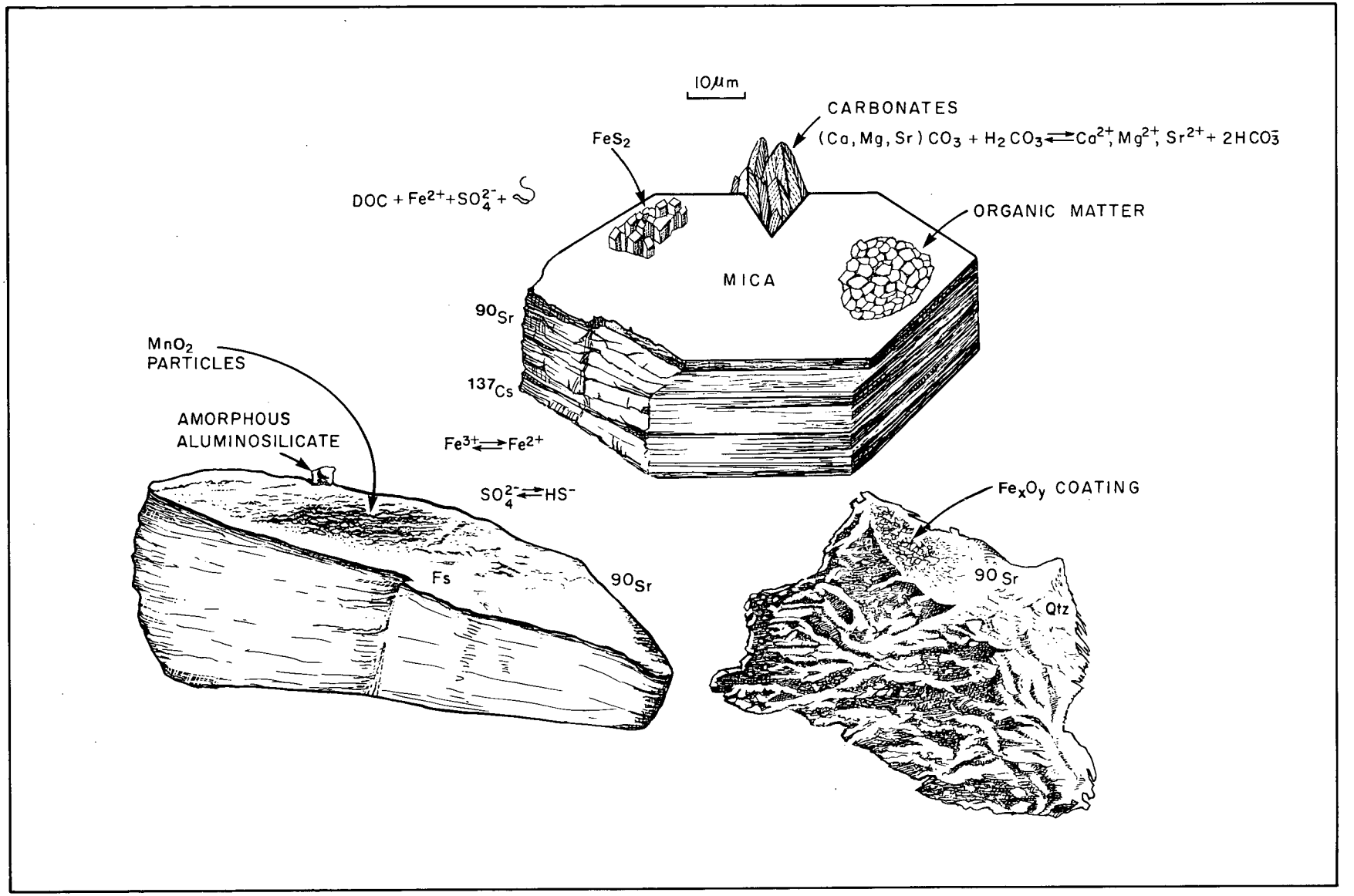

Figure 33. View of the inside of a pore as seen by a microbial observer.

References

Amphlett, C.B. 1964. *Inorganic Ion Exchangers.* Amsterdam: Elsevier Publishing Company.

Back, W. and B.B. Hanshaw. 1971. Rates of physical and chemical processes in a carbonate aquifer. *In* Non-equilibrium Systems in Natural Water Chemistry, edited by J.D. Hem, Am. Chem. Soc., Adv. Chem. Ser. 106, Washington, D.C., pp. 77-93.

Baetslé, L.H. 1969. Migration of radionuclides in porous media. Progress of Nuclear Energy, XII, Vol. 2, Part 1, edited by T. Duhamel, pp. 707-730.

Barnes, I. 1964. Field measurement of alkalinity and pH. U.S. Geol. Surv. Water-Supply Pap. 1535-H.

Barry, P.J. 1975. Perch Lake. *In* Hydrological Studies on a Small Basin on the Canadian Shield. Edited by P.J. Barry. At. Energy Can. Ltd. AECL Rep. 5041/I, pp. 93-130.

Barry, P.J. and F. Entwistle. 1975. Tritium in lower Perch Lake basin. At. Energy Can. Ltd. AECL Rep. 5039.

Beetem, W.A., V.J. Janzer and J.S. Wahlberg. 1962. Use of cesium-137 in the determination of cation exchange capacity. U.S. Geol. Surv. Bull. 1140-B.

Berner, R.A., J.T. Westrich, R. Graber, J. Smith and C.S. Martens. 1978. Inhibition of aragonite precipitation from supersaturated seawater: a laboratory and field study. Am. J. Sci. 278: 816-837.

Boulegue, J. 1977. Equilibria in a sulfide rich water from Enghien-les-Bains, France. Geochim. Cosmochim. Acta, 41: 1751-1758.

Buchanan, R.M. 1958. Mineralogical examination of six soil fractions submitted by AECL, Chalk River, Ontario. Department of Mines and Technical Surveys, Mines Branch Investigation Report IR 58-221.

Busenberg, E. and C.V. Clemency. 1976. The dissolution kinetics of feldspar at 25°C and 1 atm. CO_2 partial pressure. Geochim. Cosmochim. Acta, 40: 41-49.

Carroll, D. 1959. Ion exchange in clays and other minerals. Geol. Soc. Am. Bull. 70: 749-780.

Catto, N.R. 1978. The Late Quaternary geology of the Chalk River region, Ontario and Québec. B.Sc. Thesis, Department of Geological Sciences, Queen's University, Kingston, Ontario.

Champ, D.R., J. Gulens and R.E. Jackson. 1979. Oxidation-reduction sequences in ground water flow systems. Can. J. Earth Sci. 16: 12-23.

Cherry, J.A., R.W. Gillham and J.F. Pickens. 1975a. Contaminant hydrogeology. Part 1. Physical processes. Geosci. Can. 2 (2).

Cherry, J.A., R.E. Jackson, D. McNaughton, J.F. Pickens and H. Woldetensae. 1975b. Physical hydrogeology of the lower Perch Lake basin. *In* Hydrological Studies on a Small Basin on the Canadian Shield. Edited by P.J. Barry. At. Energy Can. Ltd. AECL Rep. 5041/II, pp. 625-680.

Davidson, R.D. 1978. SEMS/EDS examination of Perch Lake basin sand grains. Memorandum, System Materials Branch, Fuels and Materials Division, AECL, Chalk River, Ontario, August 11, 1978.

Davis, S.N. and R.J.M. Dewiest. 1966. *Hydrogeology.* New York: J.W. Wiley & Sons.

Davis, J.A. and J.O. Leckie. 1978. Effect of complexing ligands on trace metal uptake by hydrous oxides. Environ. Sci. Technol. 12: 1309-1315.

Edmunds, W.M. 1977. Groundwater geochemistry—controls and process. *In* Papers and Proceedings, Groundwater Quality, Measurement, Prediction and Protection. Water Research Centre, Medmenham, England, pp. 115-147.

Edmunds, W.M. and A.H. Bath. 1976. Centrifuge extraction and chemical analysis of interstitial waters. Environ. Sci. Technol. 10: 467-472.

Egorov, Yu., V. and A.S. Lyubimov. 1969. Hydrate oxide collectors in radiochemistry. III. Nature of the heterogeneity of sorption centers of some preparations of active manganese dioxide. Sov. Radiochem. 11: 206-211.

Environment Canada. 1974. *Analytical Methods Manual.* Inland Waters Directorate, Ottawa, Canada.

Evans, E.J. December 1954. Properties of disposal area soil. Typed MS, unpublished. Environmental Research Branch, AECL, CRNL, Chalk River, Ontario.

Evans, E.J. 1958. Chemical investigations of the movement of fission products in soil. At. Energy Can. Ltd. AECL Rep. 667.

Evans, E.J. and A.J. Dekker. 1966. Fixation and release of Cs-137 in soils and soil separates. Can. J. Soil Sci. 46: 217-222.

Ewing, B.B. 1959. Field test of the movement of radioactive cations. Proc. Am. Soc. Civ. Eng. SA1, pp. 39-59.

Francis, C.W. and F.S. Brinkley. 1976. Preferential adsorption of ^{137}Cs to micaceous minerals in contaminated freshwater sediment. Nature, 260: 511-513.

Freeze, R.A. 1972. Subsurface hydrology at waste disposal sites. IBM J. Res. Dev. 16: 117-129.

Frere, M.H. and D.F. Champion. 1967. Characterization of fixed strontium in sesquioxide gel-kaolinite clay systems. Soil Sci. Soc. Am. Proc. 31: 188-191.

Fritz, P., E.J. Reardon, J. Barker, R.M. Brown, J.A. Cherry, D. Killey and D. McNaughton. 1978. The carbon-isotope geochemistry of a small groundwater system in northeastern Ontario. Water Resour. Res. 14: 1059-1067.

Gadd, N.R. 1958. Geologic aspects of radioactive waste disposal, Chalk River, Ontario. Unpublished. Geol. Surv. Can. Rep.

Gadd, N.R. 1959. Surficial geology of waste disposal areas, AECL project, Chalk River, Ontario. Topical Report No. 6, Geol. Surv. Can.

Gadd, N.R. 1962. Descriptive notes, surficial geology, Chalk River, Ontario-Québec. Geol. Surv. Can., Ottawa, Ontario, Map 1132A.

Garrels, R.M. and C.L. Christ. 1965. *Solutions, Minerals and Equilibria.* New York: Harper & Row.

Garrels, R.M. and M.E. Thompson. 1962. A chemical model for sea water at 25°C and one atmosphere total pressure. Am. J. Sci. 260: 57-66.

Gillham, R.W., L.E. Lindsay and J.A. Cherry. 1978. Laboratory studies of distribution coefficients for cesium and strontium in glacial deposits. Abstracts with Programs, Geological Association of Canada/Mineralogical Association of Canada, Vol. 3, p. 408.

Grisak, G.E. and R.E. Jackson. 1978. An appraisal of the hydrogeological processes involved in shallow subsurface radioactive waste management in Canadian terrain. Scientific Series No. 84, Inland Waters Directorate, Environment Canada, Ottawa.

Grummitt, W.E. and G.M. Milton. 1957. Radiochemical procedures for strontium and yttrium. Atomic Energy of Canada Ltd., Chalk River, Ontario, CRC-688, AECL-934.

Halevy, E. and V. Tzur. 1964. Precipitation of Sr by $CaCO_3$ in calcareous soils and measurement of cation exchange capacity. Soil Sci. 98: 66-67.

Hem, J.D. 1960. Some chemical relationships among sulfur species and dissolved ferrous iron. U.S. Geol. Surv. Water-Supply Pap. 1459-C, pp. 57-73.

Hutchinson, M. 1974. Microbiological aspects of groundwater pollution. *In* Groundwater Pollution in Europe, edited by J.A. Cole, Water Information Center, Inc., Port Washington, N.Y., pp. 167-202.

Jackson, R.E. and J.A. Cherry. 1974. A progress report on hydrogeological studies in the lower Perch Lake basin, CRNL. Department of Earth Sciences, University of Waterloo, Waterloo, Ontario.

Jackson, R.E., W.F. Merritt, D.R. Champ, J. Gulens and K.J. Inch. 1977. The distribution coefficient as a geochemical measure of the mobility of contaminants in a groundwater flow system. *In* The Use of Nuclear Techniques in Water Pollution Studies, IAEA, Vienna. Still in press.

James, R.V. and J. Rubin. 1979. Applicability of the local equilibrium assumption to transport through soils of solutes affected by ion exchange. *In* Chemical Modeling in Aqueous Systems, edited by E.A. Jenne, Am. Chem. Soc., Symp. Ser. 93, Washington, D.C., pp. 225-235.

Jenne, E.A. 1968. Control of Mn, Fe, Ni, Cu, and Zn concentration in soils and waters: significant role of hydrous Mn and Fe oxides. *In* Trace Inorganics in Water, Am. Chem. Soc., Adv. Chem. Ser. 73, Washington, D.C., pp. 337-387.

Jenne, E.A. 1977. Trace element sorption by sediments and soils—sites and processes. *In* Symposium on Molybdenum in the Environment, edited by W. Chappel and K. Petersen, Vol. 2, Chap. 5, M. Dekker Inc., New York, N.Y., pp. 425-523.

Jenne, E.A. and J.S. Wahlberg. 1968. Role of certain stream-sediment components in radio ion sorption. U.S. Geol. Surv. Prof. Pap. 433-F.

Johnston, L.M., K. Inch and R.E. Jackson. 1978. Seasonal variations in chemical properties of ground water in the lower Perch Lake basin. Perch Lake Workshop Proceedings. At. Energy Can. Ltd. AECL Rep. 6404.

Judd, J.M. and A.S. Coveart. 1965. Flame emission spectrophotometric method for the determination of stable strontium and calcium in fish. At. Energy Can. Ltd. AECL Rep. 2518.

Kielland, J. 1937. Individual activity coefficients of ions in aqueous solutions. J. Am. Chem. Soc. 59: 1675-1678.

Kinniburgh, D.G., J.K. Syers and M.L. Jackson. 1975. Specific adsorption of trace amounts of calcium and strontium by hydrous oxides of iron and aluminum. Soil Sci. Soc. Am. Proc. 39: 464-470.

Kramer, J.R. 1978. Alkalinity of soft waters and acid rain. Abstracts with Programs, Geological Association of Canada/Mineralogical Association of Canada, Vol. 3, p. 438.

Krauskopf, K. 1967. *Introduction to Geochemistry.* Toronto: McGraw-Hill.

Lai, S.H. and J.J. Jurinak. 1972. Cation adsorption in one-dimensional flow through soils: a numerical solution. Water Resour. Res. 8: 99-107.

Langmuir, D. 1971. The geochemistry of some carbonate groundwaters in central Pennsylvania. Geochim. Cosmochim. Acta, 35: 1023-1045.

Langmuir, D. 1972. Controls on the amounts of pollutants in subsurface waters. Earth Miner. Sci. 42: 9-13.

Langmuir, D. 1979. Techniques of estimating thermodynamic properties for some aqueous complexes of

geochemical interest. *In* Chemical Modeling in Aqueous Systems, edited by E.A. Jenne, Am. Chem. Soc., Symp. Ser. 93, Washington, D.C., pp. 353-387.

Lennox, D.H. and M.L. Parsons. 1975. Subsurface hydrology in Canada during the International Hydrological Decade. Proc. Can. Hydrol. Symp.

Lerman, A. and H. Taniguchi. 1972. Strontium-90—diffusional transport in sediments of the Great Lakes. J. Geophys. Res. 77:474-481.

Lozej, G.P. and F.W. Beales. 1975. The unmetamorphosed sedimentary fill of the Brent meteorite crater, southeastern Ontario. Can. J. Earth Sci. 12: 606-628.

Marshall, C.E. 1964. *The Physical Chemistry and Mineralogy of Soils.* New York: J.W. Wiley & Sons.

Matthess, G. 1972. Hydrogeologic criteria for the self-purification of groundwater. Int. Geol. Congr., Montreal, Section 11, pp. 295-304.

Mawson, C.A. 1955. Waste disposal into the ground. *In* Proc. Int. Conf. Peaceful Uses of Atomic Energy, Geneva, Vol. 9, pp. 676-678.

Merritt, W.F. 1971. Identification and measurement of trace elements in fresh water by neutron activation. *In* Int. Symp. on Identification and Measurement of Environmental Pollutants, June 1971, Ottawa. Published by National Research Council of Canada, pp. 358-362.

Merritt, W.F. and C.A. Mawson. 1967. Experiences with ground disposal at Chalk River. *In* Disposal of Radioactive Wastes into the Ground, IAEA, Vienna, pp. 79-93.

Meyboom, P. 1968. Hydrogeology: a decennial appraisal and forecast. *In* The Earth Sciences in Canada, edited by E.R.W. Neale, R. Soc. Can. Spec. Pub. No. 11, pp. 203-221.

Moore, W.J. 1964. *Physical Chemistry.* 3rd ed. Englewood Cliffs, N.J.: Prentice-Hall.

Murray, D.S., T.W. Healy and D.W. Fuerstenau. 1968. The adsorption of aqueous metal on colloidal hydrous manganese oxide. *In* Adsorption from Aqueous Solution, Am. Chem. Soc., Adv. Chem. Ser. 79, Washington, D.C., pp. 74-81.

Nightingale, E.R., Jr. 1959. Phenomenological theory of ion solvation. Effective radii of hydrated ions. J. Phys. Chem. 63: 1381-1387.

Ogata, A. 1970. Theory of dispersion in a granular medium. U.S. Geol. Surv. Prof. Pap. 411-I.

Ophel, I.L., C.D. Fraser and J.M. Judd. 1971. Strontium concentration factors in biota and bottom sediments of freshwater lake. Proc. Int. Symp. on Radioecology Applied to the Protection of Man and His Environment, Rome, pp. 509-527.

Parks, G.A. 1975. Adsorption in the marine environment. *In* Chemical Oceanography, Vol. 1. 2nd ed. Edited by J.P. Riley and G. Skirrow, Academic Press, New York, pp. 241-308.

Parsons, P.J. 1960. Movement of radioactive wastes through soil. Part I. Soil and ground-water investigations in lower Perch Lake basin. At. Energy Can. Ltd. AECL Rep. 1038.

Parsons, P.J. 1961. Movement of radioactive wastes through soil. Part III. Investigating the migration of fission products from high-ionic liquids deposited in soil. At. Energy Can. Ltd. AECL Rep. 1525.

Patterson, R.J., S.K. Frape, L.S. Dykes and R.A. McLeod. 1978. A coring and squeezing technique for the detailed studies of subsurface water chemistry. Can. J. Earth Sci. 15: 162-169.

Pickens, J.F., W.F. Merritt and J.A. Cherry. 1977. Field determination of the physical transport parameters in a sandy aquifer. *In* The Use of Nuclear Techniques in Water Pollution Studies, IAEA, Vienna. Still in press.

Pickens, J.F., J.A. Cherry, G.E. Grisak, W.F. Merritt, and B.A. Risto. 1978. A multilevel device for groundwater sampling and piezometric monitoring. Ground Water, 16: 322-327.

Plummer, L.N. and T.M.L. Wigley. 1976. The dissolution of calcite in CO_2-saturated solutions at 25°C and 1 atmosphere total pressure. Geochim. Cosmochim. Acta, 40: 191-202.

Ragone, S.E., J. Vecchioli and H.F. Ku. 1973. Short-term effect of tertiary-treated sewage on iron concentration in Magothy aquifer, Bay Park, New York. *In* Underground Waste Management and Artificial Recharge, Vol. 1, AAPG/USGS/IAHS.

Routson, R.C. 1973. Review of studies on soil-waste relationships on the Hanford reservation from 1944-1967. Battelle Pacific Northwest Labs., Richland, Washington, BNWL-1464.

Schulz, R.K., R. Overstreet and I. Barshad. 1960. On the soil chemistry of cesium 137. Soil Sci. 89: 16-27.

Schwille, F. 1976. Anthropogenically reduced groundwaters. Hydrol. Sci. Bull. XXI (4): 629-645.

Seelmann-Eggebert, W., F. Pfennig and H. Munzel. 1974. Chart of the nuclides. Institute for Radiochemistry, Nuclear Research Centre, Karlsruhe, West Germany.

Sennett, P. and J.P. Olivier. 1965. Colloidal dispersions, electrokinetic effects and the concept of zeta potential. *In* Chemistry and Physics of Interfaces, Am. Chem. Soc., Washington, D.C., pp. 75-92.

Stumm, W. 1967. Redox potential as an environmental parameter; conceptual significance and operational limitation. Adv. Water Poll. Res. 1: 283-307.

Stumm, W. and J.J. Morgan. 1970. *Aquatic Chemistry.* New York: Wiley-Interscience.

Suarez, D.L. and D. Langmuir. 1976. Heavy metal relationships in a Pennsylvania soil. Geochim. Cosmochim. Acta, 40: 589-598.

Tamura, T. 1964. Reactions of cesium-137 and strontium-90 with soil minerals and sesquioxides. 8th Int.

Congr. Soil Sci. Trans. 3: 465-478.

Tamura, T. 1972. Sorption phenomena significant in radioactive-waste disposal. *In* Underground Waste Management and Environment Implications, edited by T.D. Cook, AAPG Memoir 18, Tulsa, Oklahoma, pp. 318-329.

Truesdell, A.H. and B.F. Jones. 1974. WATEQ, a computer program for calculating chemical equilibria of natural waters. J. Res. U.S. Geol. Surv. 2: 233-248.

Wahlberg, J.S. and R.S. Dewar. 1965. Comparison of distribution coefficients for strontium exchange from solutions containing one and two competing cations. U.S. Geol. Surv. Bull. 1140-D.

Wahlberg, J.S. and M.J. Fishman. 1962. Adsorption of cesium on clay minerals. U.S. Geol. Surv. Bull. 1140-A.

Wahlberg, J.S., J.H. Baker, R.W. Vernon and R.S. Dewar. 1965. Exchange adsorption of strontium on clay minerals. U.S. Geol. Surv. Bull. 1140-C.

Whitfield, M. 1974. Thermodynamic limitations on the use of the platinum electrode in E_H measurements. Limnol. Oceanogr. 19: 857-865.

APPENDIX

Table A-1. Groundwater Quality Data from along the Dyke, October 1973*

Piezometer (depth in feet)	δC^{13} (‰)	pH	HCO_3^-	DOC	Si_T	Ca^{2+}	Fe_T	Mg^{2+}	Mn_T	K^+	Na^+
D3(10)	−15.8	6.57	154.2	17.10	12.3	21.1	22.7	6.90	0.26	2.28	3.45
D2(26)	−16.7	7.34	98.1	13.49	10.1	19.1	4.42	4.40	0.25	1.92	3.10
KNEW1(15)	−8.3	5.83	42.0	30.19	8.34	8.80	7.3	3.12	0.09	0.81	2.80
KNEW2(27)	−15.0	7.60	84.1	6.32	10.9	17.3	1.19	4.19	0.10	1.58	3.65
KNEW3(58)	−16.8	8.01	119.1	7.55	10.3	21.8	0.13	3.97	0.08	3.48	4.86
KNEW4(80)	−15.6	7.55	128.5	10.92	5.49	16.8	0.96	3.35	0.29	2.95	20.9
F3(10)	−14.5	6.56	119.1	6.29	6.85	12.3	25.0	3.86	0.48	1.71	4.62
F2(30)	−16.4	7.92	91.1	8.88	9.18	20.2	0.39	4.90	0.10	2.05	3.11
F1(50)	−4.7	6.78	327.0	16.42	6.74	76.5	4.32	8.40	1.07	4.37	5.68
H3(10)	−8.0	7.35	144.8	22.24	8.14	31.3	2.12	6.32	0.20	2.94	3.53
H2(32)	−11.3	7.48	79.4	15.50	8.58	14.0	4.84	2.79	0.14	1.77	2.81
H1(44.5)	−10.0	7.32	114.5	10.40	7.46	21.4	11.1	2.60	0.50	3.67	6.2
14-73(55)	−10.4	9.20	84.1	8.89	6.67	12.7	0.22	1.74	0.13	5.74	16.0

*All data in milligrams per litre except where noted.

Table A-2. Groundwater Quality Data along the YY Profile, August 1973*

Piezometer (depth in feet)	pH	HCO_3^-	Si_T	Ca^{2+}	Fe_T	Mg^{2+}	Mn_T	Sr^{2+}	K^+	Na^+	Cl^-	PO_4^{3-}
02(15)	6.45	56.1	8.7	13.2	4.8	6.6	0.09	0.137	8.40	14.0	24.3	0.13
03(30)	7.00	72.4	7.5	15.2	1.9	12.0	0.13	0.126	9.50	11.0	26.3	0.03
P2(10)	6.49	44.4	12.9	13.6	15.0	7.5	0.09	0.137	4.95	5.5	10.0	0.05
P3(20)	6.38	46.7	12.0	7.3	7.5	4.1	0.05	0.081	4.40	4.6	26.5	0.04
KNEW1(16)	5.92	45.6	7.7	5.9	4.8	2.9	0.02	0.046	1.75	3.0	4.2	0.20
KNEW2(28)	7.98	86.4	12.9	13.6	2.4	6.5	0.08	0.061	6.90	5.0	4.2	0.27
Inlet 2	6.52	25.7	6.9	5.3	2.2	3.0	0.13	0.052	3.75	7.9	12.3	0.43

*All data in milligrams per litre except where noted.

Table A-3. Distribution Coefficients for ^{90}Sr and ^{137}Cs from 1977 Field Season

Core No.	Depth (m)	cpm/g	^{90}Sr (cpm/mL)	K_d^{Sr} (mL/g)	K_d^{Cs} (mL/g)
MA1/2	4.0	8	<1	–	–
MA2/2	5.5	2733	341	8	–
MA3/1	7.9	898	22	41	292
MA3/2	9.1	11	<1	–	–
MA1/9	9.4	67	18	4	–
MA1/10	9.8	40	8	5	–

Table A-4. Variation of Radioactivity (total β in counts per minute per milligram) with Grain Size for 1977 Field Season Data

Grain size (ϕ)	MA2/1 depth: 4.5 m	MA2/1 depth: 5.1 m
1.25	13	4
2.0	3	1
2.5	2	1
2.75	2	1
3.0	2	1
3.25	2	1
3.5	2	2
3.75	3	2
4.0	13	9